AD-A142 013 SCIENTIFIC ANALYSIS OF EXISTING DATA ON AEROSOL DISPERSION AND TRANSPORT I..(U) FRAUNHOFER-INST FUER ATMOSPHAERISCHE UMWELTFORSCHUNG GARMISCH.. 1/1

UNCLASSIFIED R REITER ET AL. APR 84 DAJA45-83-C-0037 F/G 13/2 NL

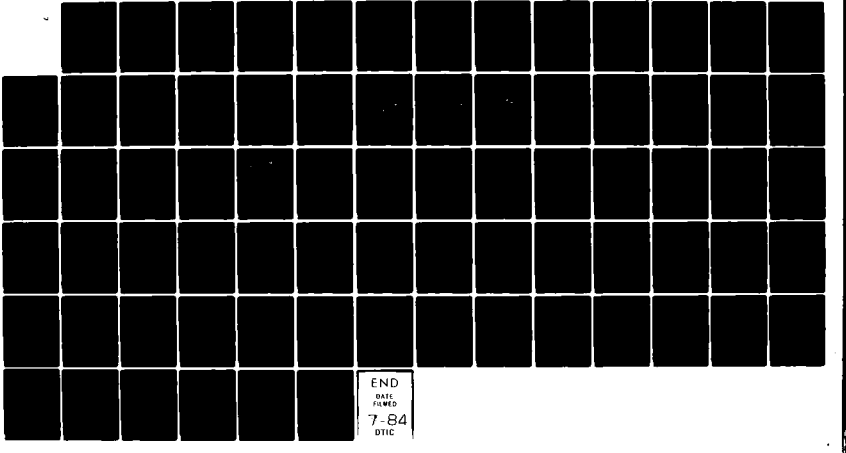

END
DATE FILMED
7-84
DTIC

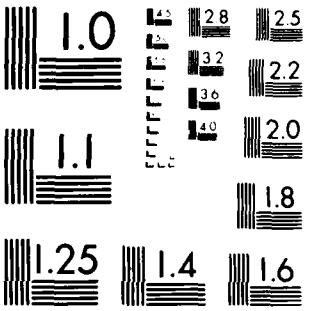

AD

# SCIENTIFIC ANALYSIS OF EXISTING DATA ON AEROSOL DISPERSION AND TRANSPORT IN A MOUNTAIN VALLEY

Final Scientific Report

by

REINHOLD REITER
HANS MÜLLER
RUDOLF SLADKOVIC

April 1984

European Research Office
United States Army
London, England

Contract Number DAJA-45-83-C-0037

Fraunhofer-Institut für Atmosphärische
Umweltforschung
Kreuzeckbahnstraße 19
D-8100 Garmisch-Partenkirchen



Approved for Public Release; distribution unlimited

SECURITY CLASSIFICATION OF THIS PAGE (When Data Entered)

| REPORT DOCUMENTATION PAGE | READ INSTRUCTIONS BEFORE COMPLETING FORM |
|---|---|
| 1. REPORT NUMBER | 2. GOVT ACCESSION NO. A142 013 — 3. RECIPIENT'S CATALOG NUMBER |
| 4. TITLE (and Subtitle) SCIENTIFIC ANALYSIS OF EXISTING DATA ON AEROSOL DISPERSION AND TRANSPORT IN A MOUNTAIN VALLEY | 5. TYPE OF REPORT & PERIOD COVERED Final Technical Report February 83 - May 1984 |
| | 6. PERFORMING ORG. REPORT NUMBER |
| 7. AUTHOR(s) Reinhold Reiter, Hans Müller, Rudolf Sladkovic | 8. CONTRACT OR GRANT NUMBER(s) DAJA45-83-C-0037 |
| 9. PERFORMING ORGANIZATION NAME AND ADDRESS Fraunhofer Institut für Atmosphärische Umweltforschung, Kreuzeckbahnstrasse 19 D-8100 Garmisch-Partenkirchen, West Germany | 10. PROGRAM ELEMENT, PROJECT, TASK AREA & WORK UNIT NUMBERS |
| 11. CONTROLLING OFFICE NAME AND ADDRESS USARDSG-UK Box 65, FPO New York, NY 09510 | 12. REPORT DATE May 1984 |
| | 13. NUMBER OF PAGES 69 |
| 14. MONITORING AGENCY NAME & ADDRESS(if different from Controlling Office) | 15. SECURITY CLASS. (of this report) Unclassified |
| | 15a. DECLASSIFICATION/DOWNGRADING SCHEDULE |

16. DISTRIBUTION STATEMENT (of this Report)

Approved for public release; distribution unlimited

17. DISTRIBUTION STATEMENT (of the abstract entered in Block 20, if different from Report)

SUPPLEMENTARY NOTES

19. KEY WORDS (Continue on reverse side if necessary and identify by block number)

Aerosols, fluorescent particles, atmospheric tracers, rotorod samplers, pollutant transport, dispersion, up-valley wind, capping inversion, Gaussian plume model.

20. ABSTRACT (Continue on reverse side if necessary and identify by block number)

Fluorescent particle tracer experiments were conducted to investigate the pollutant transport and dispersion in the north-alpine Loisach river valley. Experimental procedures are outlined. Analysis of data for a variety of meteorological conditions including inversion cases is presented. In all cases the dilution rates were greater than those obtained by the Gaussian plume model with a sigma scheme applying to flat terrain. Highest tracer concentrations were observed with a capping inversion layer. In the theoretical part the straight channel model developed by Gotaas is reviewed.

DD FORM 1 JAN 73 1473 EDITION OF 1 NOV 65 IS OBSOLETE

UNCLASSIFIED

SECURITY CLASSIFICATION OF THIS PAGE (When Data Entered)

AD _____

# SCIENTIFIC ANALYSIS OF EXISTING DATA ON AEROSOL DISPERSION AND TRANSPORT IN A MOUNTAIN VALLEY

Final Scientific Report

by

REINHOLD REITER
HANS MÜLLER
RUDOLF SLADKOVIC

April 1984

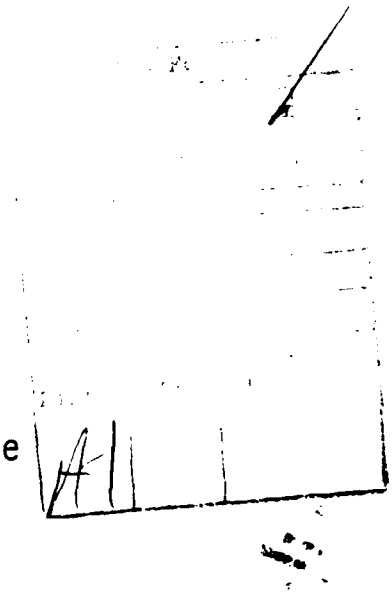

European Research Office
United States Army
London, England

Contract Number DAJA-45-83-C-0037

Fraunhofer-Institut für Atmosphärische
Umweltforschung
Kreuzeckbahnstraße 19
D-8100 Garmisch-Partenkirchen

TABLE OF CONTENTS

## ABSTRACT

Existing data of fourteen tracer experiments are analysed to specify the pollutant transport and dispersion in the north-alpine Loisach river valley for a variety of meteorological conditions including inversion cases. In the experiments zinc sulfide particles (MMD = 3.6 µm) were used as tracers. Particles were released from an isolated hill (300 m abg) at the valley entrance and sampled by H-shaped Rotorod devices (located along the valley floor and, in a few cases, at some mountain sites above the Garmisch basin). Duration of release was typical about one hour. These experimental specifics are briefly outlined.

For unstable lapse-rate conditions with well-developed up-valley wind (U) the normalized axial concentration of the tracer along the valley (SU/Q) agrees within a factor of 2 with the Gaussian plume model (and with a sigma scheme applying to open terrain conditions). The highest centerline concentrations of SU/Q were observed with a capping inversion layer. In this case the measured concentration pattern was found in good agreement with a Gaussian plume model assuming perfect reflection from the inversion, but none from the ground.

Tracers were also detected at the mountain sites, in one case the concentrations were considerably higher than those in the Garmisch basin. The transport to the mountain stations depends on the manner in which the valley wind enters the Garmisch basin and on the interaction between the valley wind and the synoptic flow at upper levels.

In the first part of this report the "straight channel" model developed by Gotaas [7] is reviewed. The model has been designed to estimate the effect of vertical sidewalls and a capping inversion layer on the diffusion from a continuous point source. The model valley is thought to be useful in case of reanalyzing existing data or in planning future experiments.

## 1. INTRODUCTION

Although considerable progress in understanding the fundamentals of transport and dispersion of air pollutants in complex terrain has been achieved in recent years - in particular by means of tracer field studies at various topographical settings such as steep-walled canyons [1, 9, 20], deep fjord valleys [19] or broad basins [11] - there is still an urgent need for more observational data pertinent to terrain-related diffusion processes [2]. This is most evident from the fact that appropriate models for impact assessment in areas of complex terrain are not yet available [19]. This shortcoming demonstrates that "adequate models for such conditions will not be developed until the effective processes have been better quantified" [15].

The transport of airborne particles in a mountain valley differs in several aspects from that in flat terrain. The most striking difference is, of course, that the windfield in mountain valleys is governed to a high degree by thermally driven local flows which are often completely decoupled from the large scale flow. Well known are mountain valley wind circulations and slope wind regimes. In those flows other dispersion mechanisms than small scale turbulence may be effective, Fosberg et al. [4], e.g., point to the effects of organized divergence fields associated with the valley wind and propose a "divergence correction" to be applied to the conventional Gaussian plume model. Reid [15] emphasizes the "generally higher

mechanical turbulence levels" leading to greater dilution rates near the source, but also points to the "topographic constraints on the horizontal dispersion and higher frequency of capping inversions" which may lead to higher pollutant concentrations further away.

The present report details the analysis of tracer experiments which were conducted in the north-alpine Loisach river valley to investigate the relevant dispersion processes for a variety of meteorological conditions including inversion cases. The basic data are summarized in a Data Report [17]. Since terrain-channelling effects are important in mountain valleys, the "straight channel dispersion model" developed by Gotaas [7] has been adopted to provide a theoretical frame. This model has been designed "to investigate diffusion in a valley taking into account reflection and absorption from hillsides, at the ground and at an inversion layer" [7]. Since it was felt that this model could be of more general interest - e.g. in case of reanalyzing existing data or in planning future experiments - the model is reviewed in the first part of this report in detail. A method is proposed how the concentration pattern at every cross-section of the valley-channel can be obtained without any cumbersome calculation.

## 2. THE MODEL

### 2.1. Basic Equations

The model developed by Gotaas [7] is an extended Gaussian plume model. It has been designed to estimate the effect

of side walls and an inversion layer on the diffusion in a valley from a continuous point source. The reflection at the barriers is considered by optical reflection factors (using the well known multi mirror reflecting technique).

Adopting a x, y, z - coordinate system with the source at P = (O, O, H), the vertical walls at y = - a and y = b, respectively, and the horizontal inversion lid at z = h (Fig. 1a), the diffusive functions $S_y$ and $S_z$ in the general relationship for the concentration S (x, y, z)

$$S = (Q/U)\ S_y\ S_z \qquad (1)$$

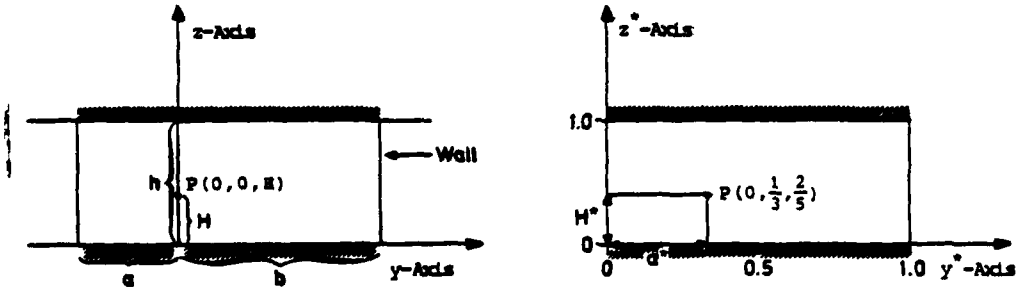


Fig. 1: a) Rectangular channel in the y, z-plane (after Gotaas [7]).

b) The same, but for the y*, z*-plane.

become [7]:

$$S_y = \frac{1}{\sqrt{2\pi}\,\sigma_y}\left[e^{-\frac{y^2}{2\sigma_y^2}} + \sum_{n=1}^{\infty}\left\{\gamma^{2n}\left(e^{-\frac{[y+2n(a+b)]^2}{2\sigma_y^2}} + e^{-\frac{[y-2n(a+b)]^2}{2\sigma_y^2}}\right)\right.\right. \tag{1a}$$
$$\left.\left. + \gamma^{2n-1}\left(e^{-\frac{[y+2a-2n(a+b)]^2}{2\sigma_y^2}} + e^{-\frac{[y-2b+2n(a+b)]^2}{2\sigma_y^2}}\right)\right\}\right]$$

$$S_z = \frac{1}{\sqrt{2\pi}\,\sigma_z}\left[e^{-\frac{(z-H)^2}{2\sigma_z^2}} + \alpha\, e^{-\frac{(z+H)^2}{2\sigma_z^2}} + \beta\, e^{-\frac{(z-2h+H)^2}{2\sigma_z^2}}\right.$$
$$+ \sum_{n=1}^{\infty}\left\{\alpha^n\beta^n\left(e^{-\frac{(z-H-2nh)^2}{2\sigma_z^2}} + e^{-\frac{(z-H+2nh)^2}{2\sigma_z^2}}\right)\right. \tag{1b}$$
$$\left.\left. + \alpha^{n+1}\beta^n e^{-\frac{(z+H+2nh)^2}{2\sigma_z^2}} + \alpha^n\beta^{n+1} e^{-\frac{[z+H-2(n+1)h]^2}{2\sigma_z^2}}\right\}\right]$$

Q emission rate of the source.

H effective source height above the ground surface.

$\alpha$, $\beta$, $\gamma$ reflection factors of the ground, the inversion lid and the sidewalls, respectively.

U mean windspeed.

$\sigma_y$ lateral dispersion coefficient (standard deviation of the crosswind concentration distribution).

$\sigma_z$ vertical dispersion coefficient (standard deviation in the vertical of the concentration distribution).

The x-dependence enters functionally since $\sigma_y$ and $\sigma_z$ are both increasing functions of x (see chapter 3).

## 2.2. Simplifications

The Eqs. (1) are somewhat lengthy formulas and are not well suited for an easy treatment. As the reflection factors vary between 0 and 1, however, a great deal of insight may already be gained by only considering these limiting cases.

Table 1 contains the simplified formulas for the horizontal and vertical diffusive functions for different combinations of the $\alpha$, $\beta$, $\gamma$-factors. Case I describes the trapping between totally reflecting barriers; trapping occurs between the ground ($\alpha = 1$) and the inversion lid ($\beta = 1$) - see Eqn. (2 a) for the $S_z$-term-, and between the sidewalls ($\gamma = 1$) - see Eqn. (2 b) for the $S_y$-term. Eqn. (2 a) is well known in diffusion meteorology (e.g. Csanady [3]). In case II there is no reflection from the ground ($\alpha = 0$) but total reflection from the stable layer ($\beta = 1$), see Eqn. (3 a). Case III is the widely used Gaussian plume model (e.g. Stern et al. [21]), with total reflection

Table 1: Simplified formulas for the diffusive functions $S_y$ and $S_z$ for different combinations of the reflection factors $\alpha$, $\beta$, $\gamma$. For details see text.

| | $\alpha$ | $\beta$ | $S_z\sqrt{2\pi}\,\sigma_z$ | |
|---|---|---|---|---|
| I | 1 | 1 | $\sum_{n=-\infty}^{\infty}\left\{e^{-\frac{(z-H+2nh)^2}{2\sigma_z^2}}+e^{-\frac{(z+H+2nh)^2}{2\sigma_z^2}}\right\}$ | (2a) |
| II | 0 | 1 | $e^{-\frac{(z-H)^2}{2\sigma_z^2}}+e^{-\frac{(z-2h+H)^2}{2\sigma_z^2}}$ | (3a) |
| III | 1 | 0 | $e^{-\frac{(z-H)^2}{2\sigma_z^2}}+e^{-\frac{(z+H)^2}{2\sigma_z^2}}$ | (4a) |
| IV | 0 | 0 | $e^{-\frac{(z-H)^2}{2\sigma_z^2}}$ | (5a) |

| | $\delta$ | $S_y\sqrt{2\pi}\,\sigma_y$ | |
|---|---|---|---|
| I | 1 | $\sum_{n=-\infty}^{\infty}\left\{e^{-\frac{[y+2n(a+b)]^2}{2\sigma_y^2}}+e^{-\frac{[y+2a+2n(a+b)]^2}{2\sigma_y^2}}\right\}$ | (2b) |
| IV | 0 | $e^{-\frac{y^2}{2\sigma_y^2}}$ | (4b) |

from the ground ($\alpha = 1$) and no reflection from the stable layer (equivalent to case of absent diffusion lid), see Eqn. (4a). In case IV all reflection factors are zero, and thus, no reflection takes place, see Eqs. (5a) and (4b), respectively.

### 2.2.1. Some Often Used Formulas

For many practical purposes the ground level concentration is of special interest. A convenient measure is the wind-speed-normalized relative concentration SU/Q which is simply given by $SU/Q = S_y S_z$ (Eqn. 1).

When the Eqs. (3a, 4a, 5a) for the $S_z$-term are combined with the Eqn. (4b) for the $S_y$-term (Table 1) one gets in case of the axial ($y = 0$) concentration for the ground level ($z = 0$) the following relations:

a) Total reflection at the inversion lid ($\beta = 1$), no reflection at the ground ($\alpha = 0$):

$$SU/Q = (2\pi \sigma_y \sigma_z)^{-1} \left[ e^{-\frac{H^2}{2\sigma_z^2}} + e^{-\frac{(H-2h)^2}{2\sigma_z^2}} \right] \qquad (6)$$

b) Total reflection at the ground ($\alpha = 1$), absence of an inversion lid (Gaussian plume model):

$$SU/Q = (\pi \sigma_y \sigma_z)^{-1} \, e^{-\frac{H^2}{2\sigma_z^2}} \qquad (7a)$$

c) No reflection at the ground ($\alpha = 0$), absence of an inversion lid (Gaussian absorption formula):

$$SU/Q = (2\pi \sigma_y \sigma_z)^{-1} e^{-\frac{H^2}{2\sigma_z^2}} \qquad (7b)$$

## 2.3. Dimensionless Equations

The Eqs. (2a) and (2b) in Table 1 describe the vertical and horizontal variation of the plume concentration in a straight channel with totally reflecting barriers ($\alpha = \beta = \gamma = 1$); the dependence on the x-direction enters through the semi-empirical relationships $\sigma_y(x)$ and $\sigma_z(x)$, see chapter 3. A few steps are needed to bring this set in a more tractable form. In order to derive a general non-dimensional relationship the vertical and horizontal diffusive functions are treated separately.

### 2.3.1. Vertical Diffusive Function

Using the height of the inversion layer h as scaling height the following dimensionless quantities are obtained:

$$z^* = z/h, \quad H^* = H/h, \quad \sigma_z^* = \sigma_z/h. \qquad (8)$$

Note that both the height coordinate $z^*$ and the source position parameter $H^*$ vary between 0 and 1 (see also Fig. 1b). With this the dimensionless vertical diffusive

function $S_z^*$ is related to

$S_z$ by

$$S_z^* = h\, S_z, \tag{9}$$

where

$$S_z^* = \frac{1}{\sqrt{2\pi}\,\sigma_z^*} \sum_{n=-\infty}^{\infty} \left\{ e^{-\frac{(z^* - H^* + 2n)^2}{2\sigma_z^{*2}}} + e^{-\frac{(z^* + H^* + 2n)^2}{2\sigma_z^{*2}}} \right\} \tag{10}$$

The case of no reflection at the inversion lid ($\beta = 0$) leads to the Gasussian plume model:

$$\hat{S}_z^* = \frac{1}{\sqrt{2\pi}\,\sigma_z^*} \left[ e^{-\frac{(z^* - H^*)^2}{2\sigma_z^{*2}}} + e^{-\frac{(z^* + H^*)^2}{2\sigma_z^{*2}}} \right] \tag{11}$$

## 2.3.2. Horizontal Diffusive Function

In an analogous way the width of the valley B (= a + b) is used to get the other dimensionless quantities:

$$y^* = (y + a)/B,\ a^* = a/B,\ \sigma_y^* = \sigma_y/B \tag{12}$$

It follows, that $y^* = 0$ for $y = -a$ and $y^* = 1$ for $y = b$, and, therefore, the lateral dimensionless coordinate $y^*$ varies in the range $0 \leq y^* \leq 1$ (see also Fig.1b). The source position parameter $a^*$ varies also between 0

and 1, in case of the source position at the center of the valley (a = b = B/2) it follows a* = 0.5.

The dimensionless horizontal diffusive function $S_y^*$ is related to $S_y$ by

$$S_y^* = B\, S_y, \tag{13}$$

where

$$S_y^* = \frac{1}{\sqrt{2\pi}\,\sigma_y^*} \sum_{n=-\infty}^{\infty} \left\{ e^{-\frac{(y^*-a^*+2n)^2}{2\sigma_y^{*2}}} + e^{-\frac{(y^*+a^*+2n)^2}{2\sigma_y^{*2}}} \right\} \tag{14}$$

The case of no reflection at the sidewalls ($\gamma = 0$) leads to the Gaussian plume model:

$$\hat{S}_y^* = \frac{1}{\sqrt{2\pi}\,\sigma_y^*}\, e^{-\frac{(y^*-a^*)^2}{2\sigma_y^{*2}}} \tag{15}$$

### 2.3.3. General Relationship

With the aid of the Eqs. (10) and (14) for $S_z^*$ and $S_y^*$ the concentration S can be expressed as

$$\boxed{S/S_{Lim} = S_y^* \cdot S_z^*}\ , \tag{16}$$

wher

$$S_{Li} \qquad \cdot B \cdot h). \tag{17}$$

$S_{Lim}$ is the far field concentration in the channel, the concentration at great distance will not fall below this limiting value.

Since $S_y^*$ and $S_z^*$ show the same functional dependence, i.e., $S_y^* = F^*(\sigma_y^*, y^*, a^*)$ and $S_z^* = F^*(\sigma_z^*, z^*, H^*)$, a general non-dimensional diffusive function $F^*$ may be expressed as:

$$F^*(\sigma^*; l^*; \zeta^*) = \frac{1}{\sqrt{2\pi}\,\sigma^*} \sum_{n=-\infty}^{\infty} \left\{ e^{-\frac{(l^* - \zeta^* + 2n)^2}{2\sigma^{*2}}} + e^{-\frac{(l^* + \zeta^* + 2n)^2}{2\sigma^{*2}}} \right\} \quad (18)$$

In case of $F^* = S_y^*$ the general parameters are identified as $\sigma^* = \sigma_y^*$, $l^* = y^*$, $\zeta^* = a^*$, and in case of $F^* = S_z^*$ as $\sigma^* = \sigma_z^*$, $l^* = z^*$, $\zeta^* = H^*$. Thus, the concentration ratio $S/S_{Lim}$ can be written:

$$S/S_{Lim} = F^*(\sigma_y^*, y^*, a^*) \cdot F^*(\sigma_z^*, z^*, H^*) \quad (19)$$

In order to enable a quick estimate of $S/S_{Lim}$ according to Eqn. (19), the functional dependence of $F^*$ on the general parameters $\sigma^*$, $l^*$ and $\zeta^*$ (Eqn. 18) has been tabulated (see Table B1 in appendix B). The repeated application of the tabulated set - both for the parameters $\sigma_z^*$, $z^*$, $H^*$ and for $\sigma_y^*$, $y^*$, $a^*$ - gives $S/S_{Lim}$ at any desired location of the channel in a very easy way (an example is given in chapter 4). Of course, this method presupposes that the functional dependence of the dispersion coefficients ($\sigma_y$, $\sigma_z$ or $\sigma_y^*$, $\sigma_z^*$) on stability and distance is known. This problem is postponed to chapter 3, the next step is a short discussion on the characteristics of the diffusive functions.

## 2.3.4. Characteristics of the Diffusive Functions

The functional behaviour of $F^*(\sigma^*, l^*, \zeta^*)$ for a variety of specified conditions is to be seen from the Figures 2 - 4. Note that $F^* \equiv S_y^*$ in case of $\sigma^* = \sigma_y^*$, $l^* = y^*$, $\zeta^* = a^*$ or $F^* \equiv S_z^*$ for $\sigma^* = \sigma_z^*$, $l^* = z^*$, $\zeta^* = H^*$, respectively.

Fig. 2 shows the variation of $F^*$ with distance $\sigma^*$ at various locations $l^*$ (parameter), the source position is fixed at $\zeta^* = 0.5$. Hence, in case of $F^* \equiv S_y^*$ the diagram depicts the cross-section distribution ($0 \leq y^* \leq 1$) at the distance $\sigma_y^*$ for a source located at the centre of the valley ($a^* = 0.5$). For $F^* \equiv S_z^*$ it shows the vertical distribution ($0 \leq z^* \leq 1$) at the distance $\sigma_z^*$ for a source located midway between the ground and the inversion lid ($H^* = 0.5$). In either case it is seen that $F^* = 1$ for $\sigma^* \geq 0.5$.

Fig. 3 shows the variation of $F^*$ with distance $\sigma^*$ at the location $l^* = 0$ for different source positions $\zeta^*$ (parameter). Hence, this diagram depicts the variations along the wall ($y^* = 0$) and at the ground ($z^* = 0$), respectively. It is seen that $F^* = 1$ for $\sigma^* \geq 1$.

Fig. 4 reflects the case $l^* = \zeta^*$ for different source positions (parameter). In case of $F^* \equiv S_z^*$ the variation refers to the source height ($z^* = H^*$); the curve $z^* = 0$, e.g., describes the variation of $S_z^*$ at ground level for a ground level source. It is seen that $F^*$ approaches the limit 1 in the range $0.5 < \sigma^* \leq 1$.

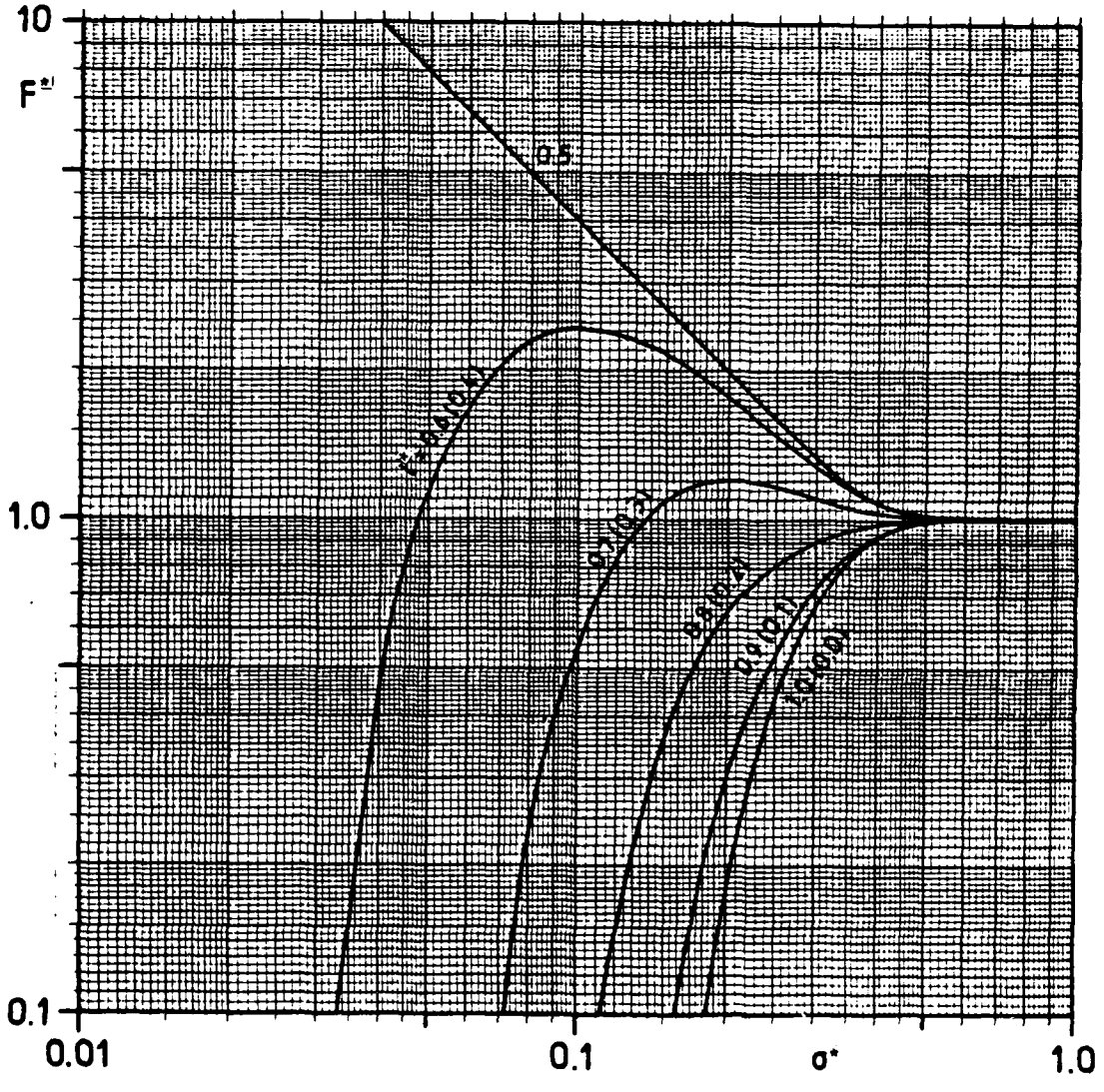


Fig. 2: Variation of diffusive function F* with non-dimensional distance σ* at different locations l* (parameter) according to Eqn. (18). The source position is fixed at ζ* = 0.5.

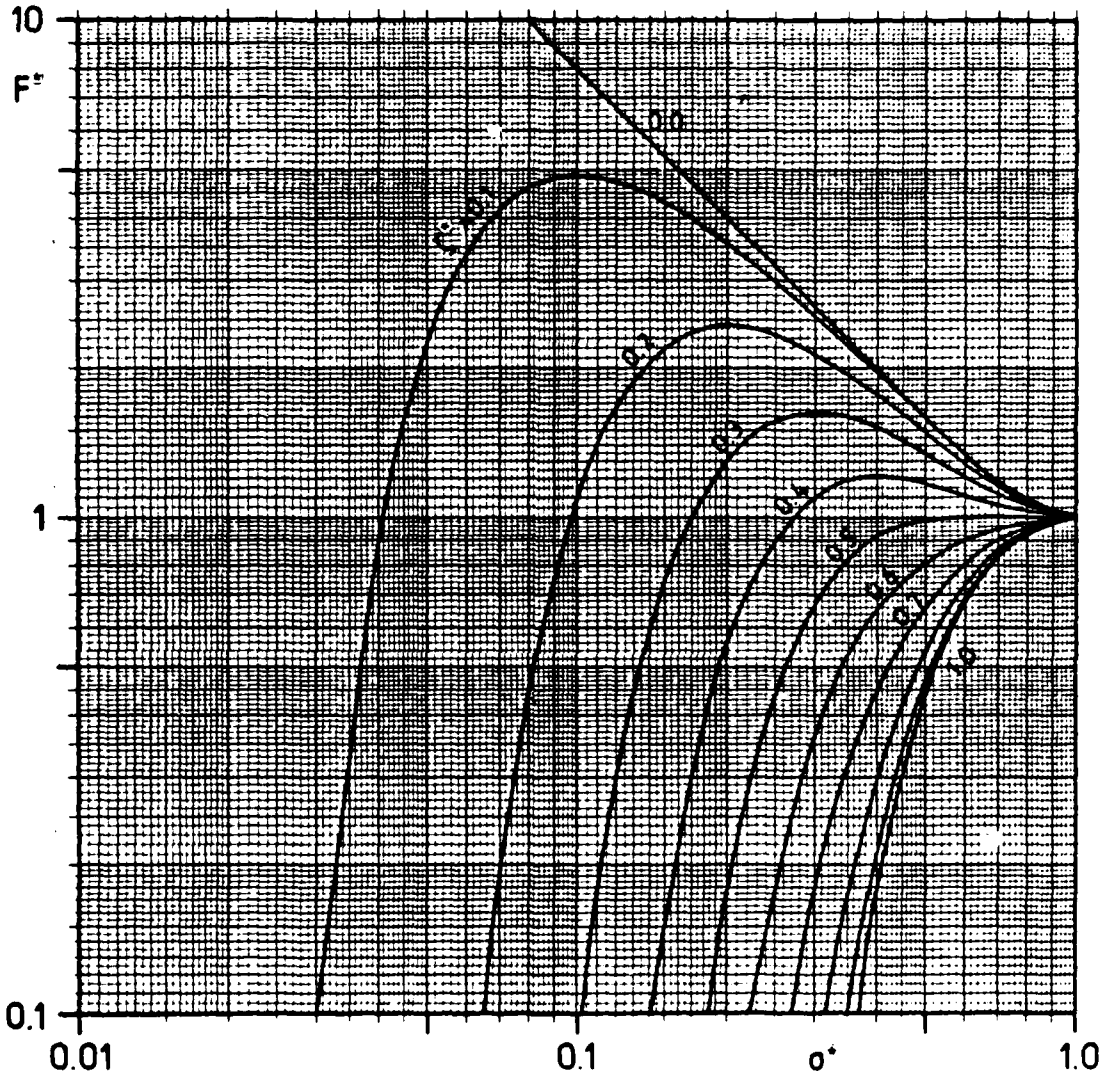


Fig. 3: Variation of diffusive function F* with non-dimensional distance σ* at the boundaries of the channel (l* = 0) according to Eqn. (18). Parameter is the source position ζ*.

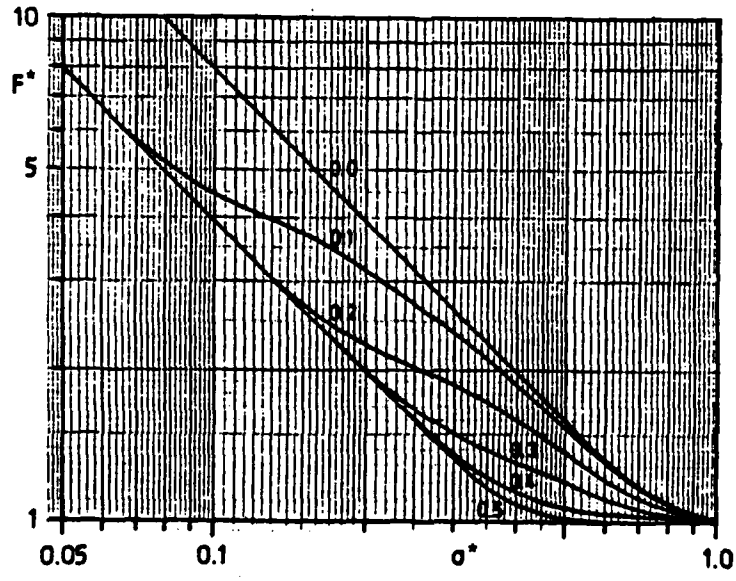


Fig. 4: Variation of diffusive function F* with non-dimensional distance σ* at the location l* = ζ* according to Eqn. (18). Parameter is the source position ζ*.

A comparison was also made between the multi reflection formula $S_z^*$ (Eqn. 10) and the respective formula for the Gaussian plume model $\hat{S}_z^*$ (Eqn. 11) for the ground level $z^* = 0$. Fig. 5 shows the result, i.e. the ratio $S_z^*/\hat{S}_z^*$ as a function of $\sigma_z^*$ for different source positions H* (parameter). Since $S_z^* = 1$ for $\sigma_z^* \geq 1$ (Fig. 3), the curves for $\sigma_z^* \geq 1$ simply reflect the relationship $1/S_z^* = \sqrt{\Pi/2}\,\sigma_z^* \exp(H^{*2}/2\sigma_z^{*2})$. For $\sigma_z^* < 1$ the ratio varies between 1 and 2. The factor 2 is found for H* = 1, i.e. with the source at the height of the upper lid, in this case the ground level concentration is doubled everywhere. Similar diagrams may be obtained for $S_y^*/\hat{S}_y^*$.

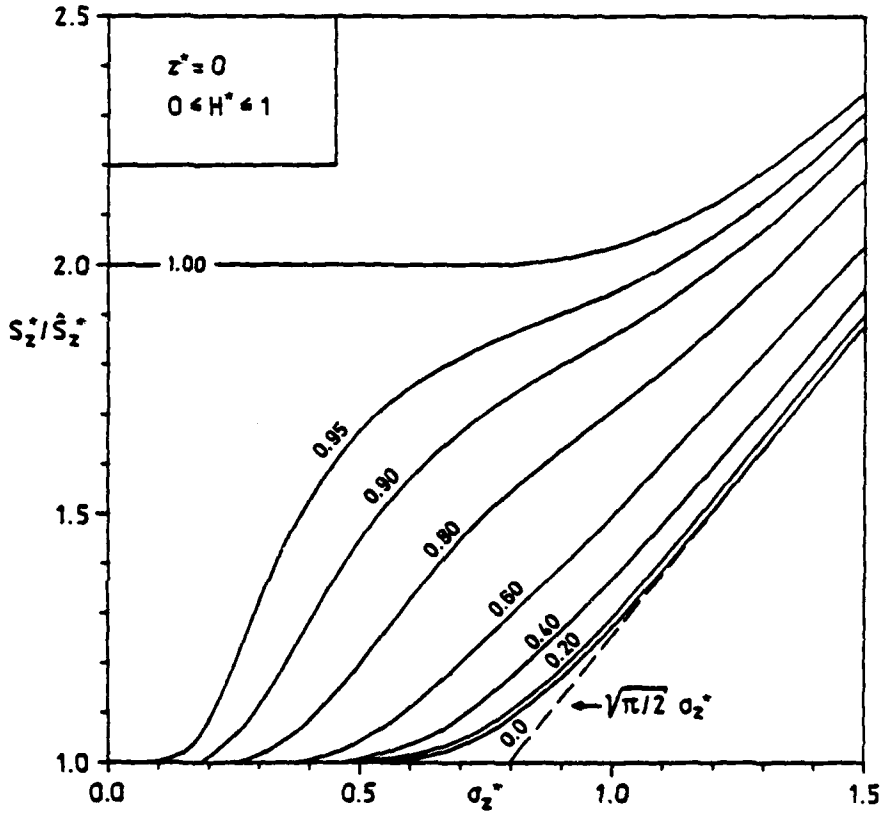


Fig. 5: The ratio $S_z^*/\hat{S}_z^*$ at ground level ($z^* = 0$) as a function of $\sigma_z^*$. Parameter is the source position $H^*$.

## 3. FORMULAS FOR THE DISPERSION COEFFICIENTS

In order to treat specific problems, the dependence of $\sigma_y$, $\sigma_z$ (or $\sigma_y^*$, $\sigma_z^*$) on stability and distance must be known. Since there are several sigma schemes in use (see [5, 6, 19]), the reader may apply a scheme of his own choice. In the following we rely on the scheme proposed by Nowicki [13], which is based on a comprehensive analysis of numerous diffusion measurements. The "universal" relationships for $\sigma_y$ and $\sigma_z$ not only consider the dependence on atmospheric stability and distance x but also on height and aerodynamic roughness $z_o$. The classification of stability is done via the exponent m in the power law of the vertical wind profile. For the mean values between $z_o$ and H, i.e. for the coefficients to be used directly in the diffusion formulas, Nowicki suggests the following relationships:

$$\sigma_y = 0.08(6m^{-0.3} + 1 - \ln H/z_o)x^{0.367(2.5-m)} \qquad (20)$$

$$\sigma_z = 0.38m^{1.3}(8.7 - \ln H/z_o)x^{1.55 \exp(-2.35m)} \qquad (21)$$

With a "roughness function" R defined by

$$R = 0.08(8.7 - \ln H/z_o), \qquad (22)$$

the power laws for $\sigma_y$ and $\sigma_z$ may be expressed as

$$\sigma_y = Fx^f \qquad (23)$$

with

$$F = F_o + R, \tag{23a}$$

$$F_o = 0.08(6m^{-0.3} - 7.7), \tag{23b}$$

$$f = 0.367(2.5 - m), \tag{23c}$$

or,

$$\sigma_z = Gx^g, \tag{24}$$

with

$$G = G_o \cdot R, \tag{24a}$$

$$G_o = 4.75m^{1.3}, \tag{24b}$$

$$g = 1.55 \exp(-2.35). \tag{24c}$$

Table 2: Dependence of the parameters in the power laws for $\sigma_y$ and $\sigma_z$ on the diffusion stability class.

| | A | B | C | D | E | F |
|---|---|---|---|---|---|---|
| m | 0.079 | 0.143 | 0.196 | 0.270 | 0.363 | 0.440 |
| f | 0.889 | 0.865 | 0.846 | 0.818 | 0.784 | 0.756 |
| $F_o$ | 0.4119 | 0.2442 | 0.1666 | 0.0949 | 0.0345 | - 0.0019 |
| g | 1.287 | 1.108 | 0.978 | 0.822 | 0.660 | 0.551 |
| $G_o$ | 0.1752 | 0.3790 | 0.5710 | 0.8659 | 1.2722 | 1.6337 |

Table 2 shows how the stability parameter m and the m-dependent functions $F_o$, f, $G_o$, g vary within the widely used diffusion categorization scheme discussed by Pasquill [14] and Turner [22].

With this frame the σ-power laws (Eqs. 23, 24) are readily obtained: for a special problem - with known H and $z_o$ - it is only necessary to calculate the roughness function R (Eqn. 22) to get F (Eqn. 23a) and G (Eqn. 24a) in a very easy way; the exponents f and g in the power laws may directly be taken from Table 2 for the respective stability class (an example is given in the next chapter).

## 4. EXAMPLE OF DIFFUSION SPREAD IN THE STRAIGHT CHANNEL MODEL

With the availability of the $\sigma_y(x)$ and $\sigma_z(x)$ power laws an estimate of the concentration pattern $S/S_{Lim}$ (Eqn. 19) may be obtained for any given channel configuration. For practical purposes it often is sufficient to have some knowledge of the concentration distribution at a few selected cross-sections. This can be accomplished very rapidly and without any cumbersome calculations. How to proceed in this case will be outlined in this section with an example.

Starting point is the ground level concentration pattern for a channel of width B = 2000 m and height h = 500 m, the point source is at H = 100 m and its distance from

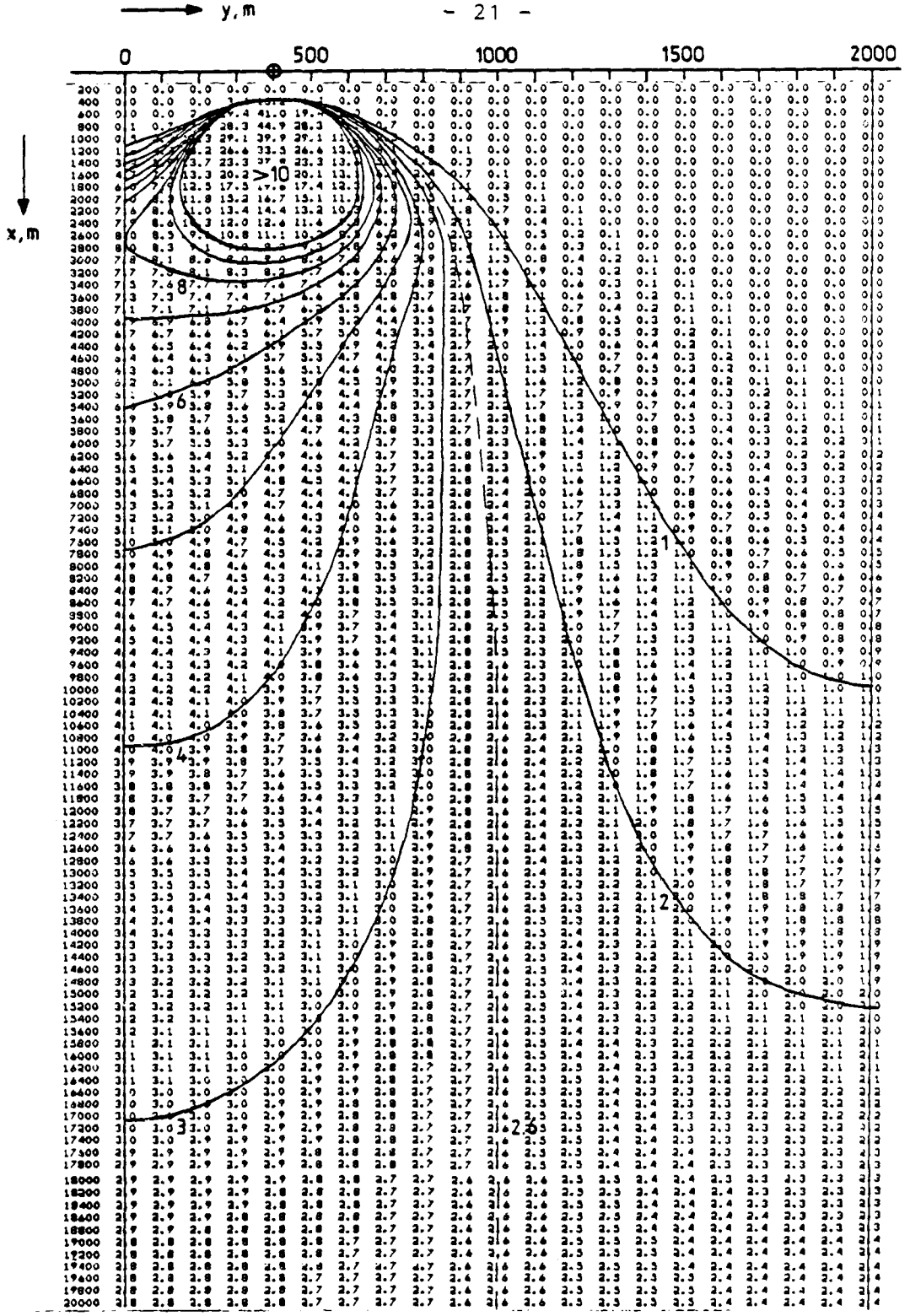


Fig. 6: Ground level concentrations S(x, y, 0) within the 'straight channel' downwind of a continuous point source at height H = 100 m and with a = 400 m (lateral distance from the wall). Numbers at the grid points denote S in $10^3$ particles/$m^3$. For model input parameters see Table 3.

the wall is a = 400 m (see Fig. 6). Numbers at the grid points (mesh widths in lateral (y) and longitudinal (x) directions are 100 m and 200 m, respectively) denote the concentration S in $10^3$ particles/$m^3$. For $S \leq 10^4$ particles/$m^3$ isolines are drawn also. With an emission rate $Q = 1.3 * 10^{10}$ particles/s, a mean windspeed of U = 5 m/s and the channel dimensions, the far field concentration $S_{Lim}$ (Eqn. 17) amounts to $2.6 * 10^3$ particles/$m^3$. Fig. 6 shows how this limiting value is approached from both channel sides with growing distance (change from inhomogeneous to homogeneous conditions).

A scheme has been prepared to allow the estimate of the concentration at any desired distance x (Table 3). The model input includes the specification of the diffusion meteorology, the channel configuration and the source parameters; no further comment is necessary on the determination of $S_{Lim}$, the dimensionless parameters (z*, H*, a*) and the specification of the factors in the power laws for $\sigma_y$, $\sigma_z$. For illustration the parameters of the chosen example (Fig. 6) are listed in the scheme.

The lower half of the table shows the cross-section distribution of $S/S_{Lim}$ and S at the distance x = 3000 m (example). Since $S/S_{Lim} = S_y^* \cdot S_z^*$, it is only necessary to use Table B1, to pick out the respective values for $S_y^*$ and $S_z^*$, and to do some little desk calculator multiplication (in case of $S_y^*$ it holds: $F^* \equiv S_y^*$, $\zeta^* \equiv a^* = 0.2$, $\sigma^* \equiv \sigma_y^* = 0.16$ (Table B1). The cross-section distribution of $S_y^*$ is tabulated for $l^* \equiv y^*$ ("upper scale") in the range $0 \leq y^* \leq 1$, these values are listed in Table 3).

Table 3: Scheme of input parameters for the straight channel model with an example. For details see text.

| | | |
|---|---|---|
| Stability class | A-F | C |
| Mean wind speed | U | 5 m/s |
| Height of the stable layer | h | 500 m |
| Width of the valley | B | 2000 m |
| Aerodynamic roughness | $z_0$ | 0.20 m |
| SOURCE PARAMETERS | | |
| a) Strength | Q | $1.3 \cdot 10^{10}$ particles/s |
| b) Height | H | 100 m |
| c) Lateral distance from the wall | a | 400 m |
| Farfield concentration $S_{Lim} = Q/(U \cdot B \cdot h)$ | $S_{Lim}$ | $2.6 \cdot 10^3$ particles/$m^3$ |
| Immission level (z = 0: ground) | z | 0 m |
| $z^* = z/h$ | $z^*$ | 0 |
| $H^* = H/h$ | $H^*$ | 0.20 |
| $a^* = a/B$ | $a^*$ | 0.20 |
| Specification of the power laws for the dispersion coefficients ($\sigma_y = Fx^f$, $\sigma_z = Gx^g$) | | |
| $H/z_0$ | $H/z_0$ | 500 |
| $R = 0.08\ (8.7 - \ln H/z_0)$ | R | 0.1988 |
| $F_0$ (Table 2) | $F_0$ | 0.1666 |
| $G_0$ (Table 2) | $G_0$ | 0.5710 |
| $F = F_0 + R$ | F | 0.365 |
| $G = G_0 \cdot R$ | G | 0.114 |
| f (Table 2) | f | 0.846 |
| g (Table 2) | g | 0.978 |

EXAMPLE

| DISTANCE X (m) | $\sigma_y^*$ | $\sigma_z^*$ | $S_z^*$ |
|---|---|---|---|
| 3000 | 0.16 | 0.57 | 1.32 |

CROSS - SECTION $0 \leq y^* \leq 1$

| | 0.0 | 0.1 | 0.2 | 0.3 | 0.4 | 0.5 | 0.6 | 0.7 | 0.8 | 0.9 | 1.0 |
|---|---|---|---|---|---|---|---|---|---|---|---|
| $S_y^*$ | 2.28 | 2.48 | 2.60 | 2.07 | 1.14 | 0.43 | 0.11 | 0.02 | 0 | 0 | 0 |
| $S/S_{Lim}$ | 3.0 | 3.3 | 3.4 | 2.7 | 1.5 | 0.6 | 0.2 | 0 | 0 | 0 | 0 |
| ($10^3$ particles/$m^3$ | 7.8 | 8.5 | 8.9 | 7.1 | 3.9 | 1.5 | 0.4 | 0.1 | 0 | 0 | 0 |

Any other configuration may be treated in an analogous manner. This procedure may be very useful in case of a reanalysis of existing data or in case of planning strategies for future experiments.

## 5. DIFFUSION IN A REAL VALLEY

### 5.1. General Remarks

The fluorescent particle (FP) tracer experiments in the Loisach river valley area were conducted to gain basic insights into the mountain diffusion meteorology and to test the applicability of the conventional model framework to the complex conditions in a deep mountain valley. The details of the fourteen experiments, which took place from May 1975 to July 1976 under a variety of meteorological conditions including inversion cases, are summarized in a Data Report (prepared for the European Research Office, United States Army, London, see Reiter et al. [17]).

Since the subsequent analysis relies on these data some background information on the topography and the experimental procedures will be repeated here for the reader's convenience.

### 5.2. Site Description and Measuring Facilities

The Loisach river valley, which is well-known for its distinct diurnal wind system [16, 18] - with daytime

north-eastern (NE) up-valley winds and nighttime south-western (SW) down-valley winds -, is about 20 km long, 2 km wide and, in its northern part, 1 km deep (Fig. 7). The northern part of the valley is SSW - NNE oriented and enters the 'Murnauer Moos' fen or the Bavarian pre-alpine region in a funnel-shaped way.

The other section of the valley, the Garmisch basin, runs from WSW to ENE and thus shows a considerably deviating direction. In the south it is surmounted by several ranges of the Wetterstein massif with the Zugspitze (≈3000 m a.s.l.) being its highest peak. Since the main ridge raises to 2600 m height or almost 2000 m above the valley floor, the southern ranges are by far the highest of all surrounding mountain chains including those of the Kramer complex in the northwest.

The walls of the main valley are forested up to the timberline at about 1700 m a.s.l.; the sloping, however, varies considerably from place to place, only the eastern flank (Estergebirge) of the northern part shows a fairly homogeneous structure with an inclination of approximately $30^{\circ}$ to a height of 1300 m above the river.

The nature of the valley floor is characterized by meadows, small forests and urban districts marking this area as one of considerable inhomogeneous aerodynamic roughness.

The plan to accomplish diffusion measurements in this area has been considerably promoted by the existence

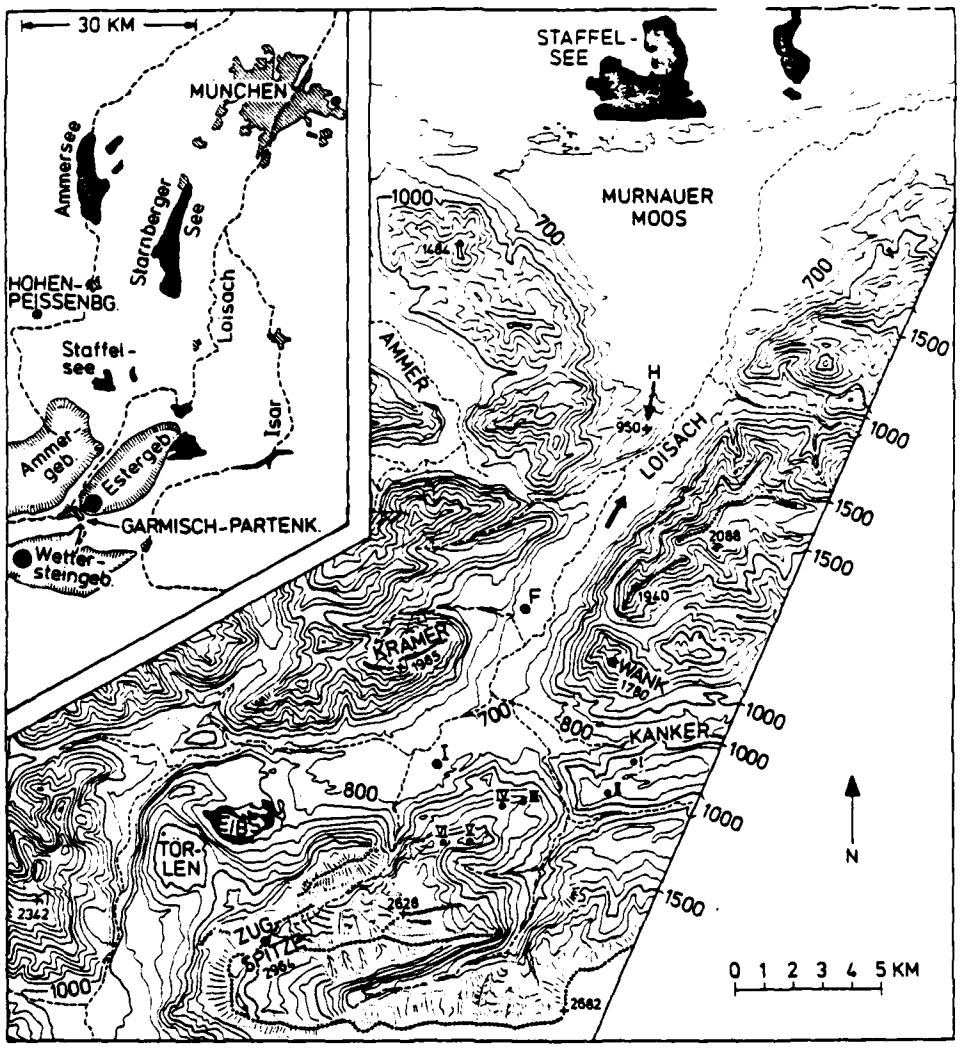


Fig. 7: Map of the Loisach River area with contour-lines (m) drawn in 100 m intervals. Tracer was released at the Höhenberg mountain 'H'. Samplers were located at the valley floor and at mountain sites (Wank peak and sites numbered I - VI). The Institute is indicated by the letter 'I'. Dashed lines: Rivers or creeks. Dotted: ridge lines.

of an isolated hill (300 m abg) in the immediate vicinity of the valley entrance. This hill, being a unique topographical feature, invites to release the tracer from its top (the 'release' mountain is indicated by an 'H' in Fig. 7). With the tracer released at the valley entrance our primary objective has been to investigate the aerosol transport along and across the valley under a variety of characteristic, but different meteorological up-valley wind conditions.

Generally, most samplers were installed at various downwind locations at the valley floor, in several cases, however, some few devices were also run at selected mountain sites (Wank peak and sites labeled by roman numbers (I - VI) in Fig. 7).

For each experiment comprehensive meteorological information was provided: i) by the permanent meteorological measuring facilities at the Institute (indicated by an "I" in Fig. 7) and the surrounding high mountain observatories Wank and Zugspitze; ii) by special pibal tracking (windfield) and radiosonde ascents (temperature) at several locations in the valley prior to, during and after each experiment. Cloud cover, radiation conditions and other relevant parameters were also included to gain further insight into the diffusion meteorology.

## 5.3. Experimental Techniques

The tracers were zinc sulfide fluorescent particles (FP) from the United States Radium Corporation (USCR). The

mass median diameter MMD was 3.6µm and the particle density PPG (particles per gram) was $0.91 * 10^{10}$.

The dissemination of the aerosol was accomplished by a Metronics Model 8 Blower Generator of the series widely used in the field (Leighton et al. [12]). For all experiments an emission rate $Q \approx 1.3*10^{10}$ particles/s was used, the duration of emission varied between 40 and 60 min. This mode of acting assured sufficient coverage in all cases to apply the FP-technique successfully.

Tracer samples were collected by H-shaped Rotorod samplers. These were, however, no Metronics fabricated devices, but in fact the Metronics standard type (as described by Grinell et al. [8], or Leighton et al. [12]) was reproduced by our laboratory, with a total of 20 devices. Considering the Rotorod efficiency of about 65% (for the particle size range used in the experiments and for rods coated according to the standard procedure [8]), the true sampling rate turned out to be 26.9 l/min.

Before each experiment the collector arms of the Rotorods were "manually coated" with special silicone grease according to the recommended standard procedure [8].

During the experiment all samplers were fixed to metal posts at approximately one meter above the ground, as is common practice in comparable field trials (e.g. Archuleta et al. [1]).

The samplers were operated on specially designed 9-volt d.c. battery systems providing constant rotation speeds (with a constancy better than that of the standard version (±2%) during a several hours run).

The samplers were energized just prior to a release. After cloud passage the period of operation was 'held to a minimum in order to avoid obscuration of FP by atmospheric particulates deposited after cloud passage' (as has been recommended by Leighton et al. [12]).

After each experiment the particles on the collector rods were counted by means of a Zeiss microscope of magnification 160 x (10 x eyepiece and 16 x objective of 0.35 N.A.) with incident UV light (to excite the fluorescence).

With the particle counts denoted by $D_\tau$ - where the sampling time $\tau$ (min) is indicated by the index - the mean particle concentration $S_\tau$ was determined by

$$S_\tau = \frac{D\tau}{F_r \cdot \tau} \qquad (25)$$

with $F_r$ = 26.9 $\mathrm{lmin}^{-1}$ being the true sampling rate.

The $S_\tau$ concentration was converted to a $S_{10}$ 10 min average by the power law recommended by Turner [23]:

$$S_{10} = S_\tau (\tau/10)^{0.2}. \qquad (26)$$

In case of $\tau$ = 60 min, the $S_{60}$ values were multiplied by 1.43, a conversion factor well known in diffusion meteorology.

## 5.4. Survey on the Experimental Specifics

A survey on the experimental specifics - release data, meteorological conditions, number of samplers at different areas of interest - is given in Table 4.

Table 4: Survey on the experimental specifics of the Loisach river valley diffusion experiments.

| EXPERIMENT | | | | Meteorological conditions | | Number of samplers at | | |
|---|---|---|---|---|---|---|---|---|
| Number | Date | Time (CET) | Duration (min) | Stability class | Wind speed ($ms^{-1}$) | Northern part of the valley | Garmisch basin | Mountain sites |
| 1 | 13 May 75 | 12:35 | 60 | D | 3.0 | 18 | 1 | 1 |
| 2 | 26 Jun 75 | 11:00 | 60 | C(B) | 6.0 | 18 | 1 | 1 |
| 3 | 7 Jul 75 | 11:10 | 60 | B | 5.5 | 18 | 1 | 1 |
| 4 | 9 Jul 75 | 11:30 | 60 | C(D) | 4.5 | 13 | 5 | - |
| 5 | 23 Jul 75 | 12:04 | 60 | B | 6.0 | 19 | - | 1 |
| 6 | 28 Jul 75 | 12:00 | 40 | C(B) | 6.5 | 7 | 7 | 5 |
| 7 | 6 Aug 75 | 11:30 | 40 | C(D) | 6.0 | 4 | 10 | 6 |
| 8 | 13 Aug 75 | 12:00 | 40 | C | 5.0 | 4 | 10 | 6 |
| 9 | 11 Nov 75 | 12:45 | 40 | D | 5.5 | 20 | - | - |
| 10 | 16 Dez 75 | 13:00 | 40 | - | - | 20 | - | - |
| 11 | 8 Mar 76 | 11:30 | 60 | D | 5.0 | 20 | - | - |
| 12 | 14 Apr 76 | 10:15 | 45 | C | - | 20 | - | - |
| 13 | 28 Jun 76 | 11:00 | 45 | B(C) | 6.0 | 6 | 9 | 5 |
| 14 | 7 Jul 76 | 10:30 | 60 | B | 7.0 | 8 | 9 | 3 |

The stability class was determined by the most widely used diffusion categorization scheme discussed by Pasquill [14] and Turner [22], and the mean flow was specified by an average wind speed between ground level and 300 m height (source level) deduced from the pibal measurements. According to this, the stability ranged between B and D categories, and the wind speed varied between 3 and 7 m/s. Most (10) experiments were conducted during the summertime with well-developed up-valley winds, whereas the remaining four experiments represent winter/spring cases with partly complex meteorological conditions (inversion structures and in one case (No. 12) unsteady winds).

## 5.5. Analysis

The results of the FP tracer sampling program are discussed in terms of the wind-speed-normalized relative concentration SU/Q which appears to be the most convenient entry when comparing dilution rates of different experiments. A comparison with theory was also made whenever it seemed appropriate. Special aspects, e.g. the release of the tracer material above a persistent, lifted ground based inversion, are treated in a separate section (5.5.3.).

### 5.5.1. Inversion Lid Conditions

A fairly good example for the diffusion during an inversion with the source below the inversion base is the Experiment No. 12 (8 March 1976). In this case the highest

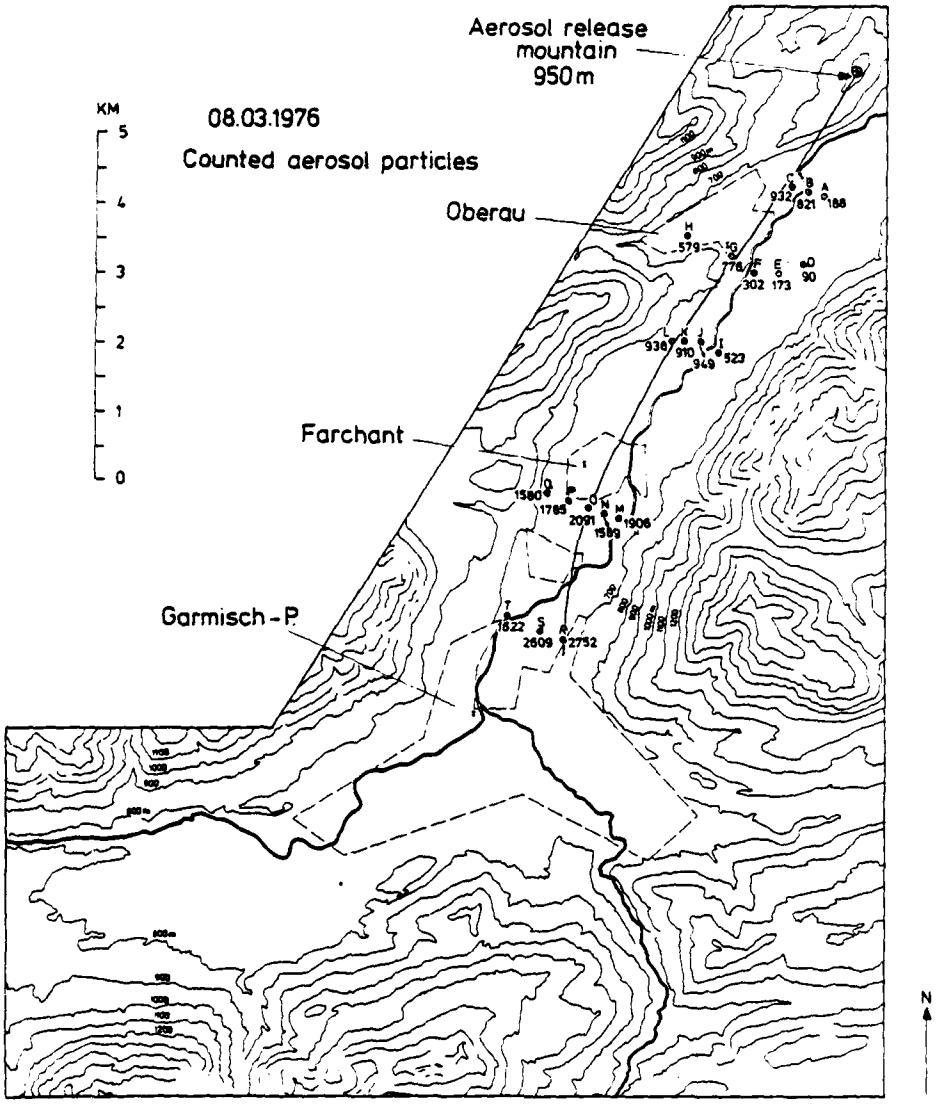


Fig. 8: Particle counts and plume centerline for Experiment No. 11 (8 March 1976)

absolute concentrations of all experiments were observed, and also from this point of view a more detailed discussion seems to be appropriate.

Fig. 8 shows the particle counts at the valley floor together with the plume centerline. The distribution appears remarkably well organized. Note that the location of the maximum exposure follows a fairly regular path. The highest counts are observed at the outlet of the northern part of the valley or at the entrance to the Garmisch basin, respectively.

The meteorological conditions may be seen from Figs. A1 - A3 in the appendix A. Fig. A1 shows the wind speed profiles (obtained by pibal tracking at Farchant), Fig. A2 shows both the trajectories and the time-height curves of the balloon flights (the ascents B, C, D were made during the release from 11.30 to 12.30 CET, see Table 4). It is to be seen that the up-valley wind was well developed during the time of the experiment and that a mean wind speed of $U \approx 5$ m/s is a reasonable approximation to the layer between the valley floor and the source. The temperature structure (Fig. A3) is characterized by an elevated temperature inversion with its base between 300 and 400 m above the valley floor (ascent B, D), i.e., the inversion barrier is present immediately above the source. With overcast conditions a D-stability class was indicated.

The results are summarized in Fig. 9, which shows the ground-level normalized concentration SU/Q as a function of distance. The theoretical curves are centerline values. The basic model input parameters are listed in the legend of Fig. 9. Case a is the "normal" Gaussian plume model with total reflection at the ground; case b assumes total reflection at the inversion lid. Case c describes the reflection from both the ground and the inversion, i.e. the trapping of the tracers within this layer; case d considers also the reflection from the walls (diffusion in the channel of width B and height h). Since the valley width B = 2000 m is relatively large and the plume width $\sigma_y$ keeps relatively small under D-stability conditions, there is practically no difference between the curves d and c.

The best approximation to the measured concentration pattern is curve b, assuming perfect reflection from the inversion, but none from the ground. This does not mean, however, that the diffusion really took place in this way. It was pointed out by Fosberg et al. [4] that the dispersion may not only be restricted to small scale turbulence but is also due to organized divergence fields occurring within the mesoscale valley wind circulation. The authors propose a 'divergence correction' to be applied to the Gaussian plume model; for realistic estimates of the 'toposcale' divergences it was shown that this term would reduce the concentration maximum by a factor of more than 2. This is the order of magnitude observed in our field experiment. Another difficulty stems from the fact, that the tracer material was not

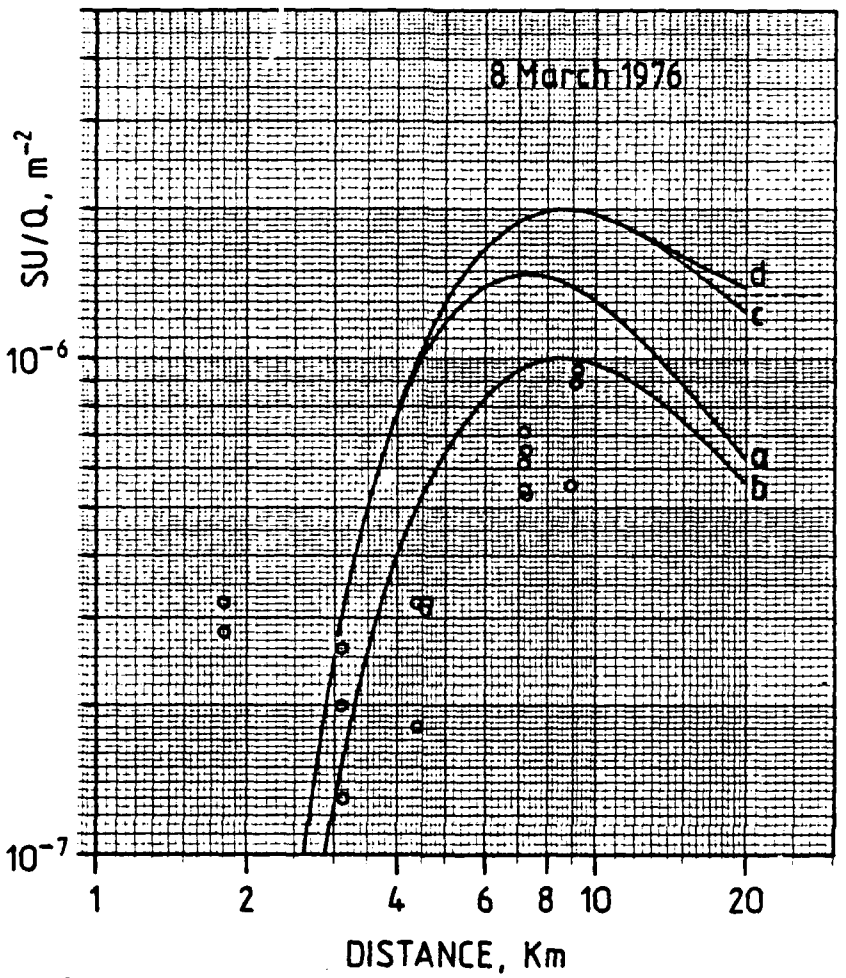


Fig. 9:
Wind-speed-normalized relative concentration SU/Q as a function of distance X. Theoretical curves (axial values) within the frame of the extended Gaussian plume model. Model input parameters: h = 375 m, B = 2000 m, H = 300 m, $Z_o$ = 0.40m, a = b = 1000 m, D stability.

| | α | β | γ | SU/Q = $S_y S_z$ | | Comments |
|---|---|---|---|---|---|---|
| (a) | 1 | 0 | 0 | Eqn. (7a) | | Total reflection at the ground (Gaussian plume) |
| (b) | 0 | 1 | 0 | Eqn. (6) | | Total reflection at the inversion lid |
| | α | β | γ | $S_y\sqrt{2\pi}\,\sigma_y$ | $S_z\sqrt{2\pi}\,\sigma_z$ | - |
| (c) | 1 | 1 | 0 | 1 | Eqn.(2a) | Trapping between the ground and the lid |
| (d) | 1 | 1 | 1 | Eqn.(2b) | Eqn.(2a) | Propagation in the channel |

released from a stack but from the top of a hill (acting like an obstacle to the valley wind). Thus, near the source wake effects - with particle loss - may occur, the relatively high concentration at x = 1,8 km is presumably caused by this effect. Due to the distortion of the windfield by the 'release mountain' the effective height H is not well defined too; therefore, the assumption H = 300 m (i.e. the equalizing of the effective source height with the height of the hill) is certainly only a first (crude) approximation.

The main facts are, that the observed concentration field shows an increase with distance as to be expected under D-stability conditions for the considered distance range, and that the maximum concentration is within a factor of 2 in agreement with the simple Gaussian plume model.

### 5.5.2. Unstable Lapse-rate Conditions

Most experiments were conducted during unstable lapse-rate conditions with no inversion structures being present in the lower layers. Fig. 10 shows the normalized centerline concentration as a function of downwind distance for the cases with strong insolation and with well developed up-valley winds (see also Table 4). The measured values are in good agreement with the Gaussian absorption model (curves for the B- and C-stabilities). Compared to the Gaussian plume model with total reflection from the ground the agreement is again within a factor of 2.

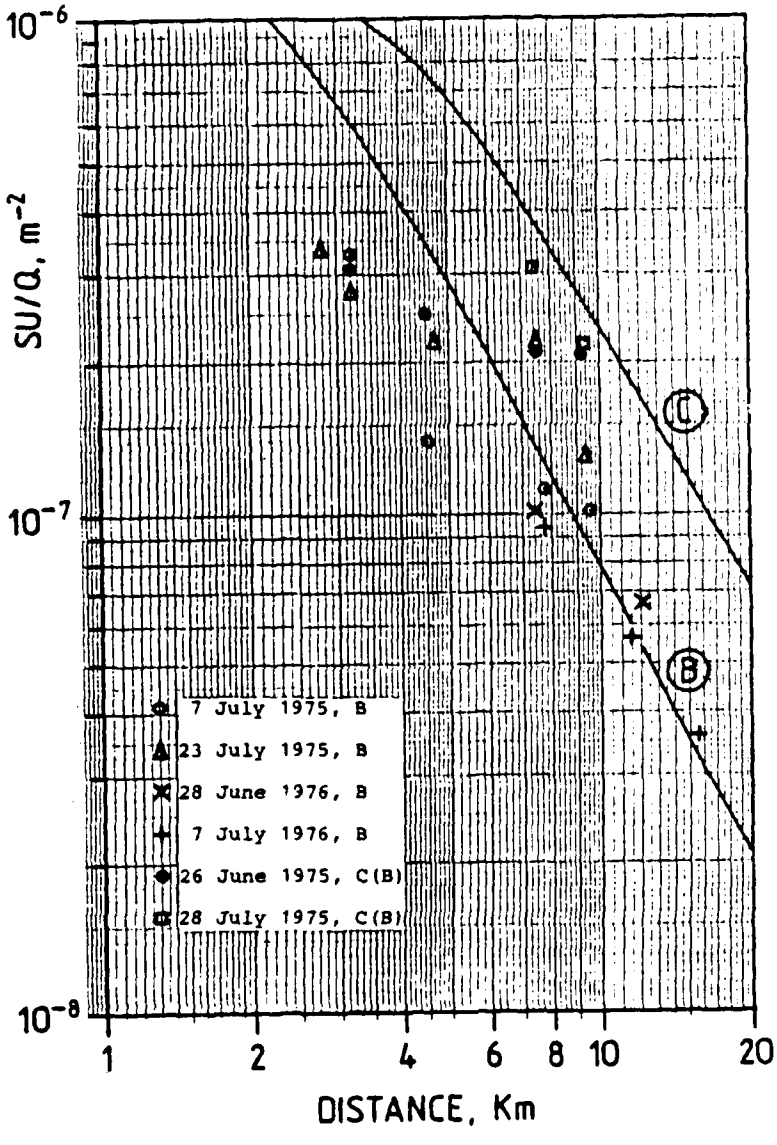


Fig. 10: Centerline ground-level normalized concentration versus downwind distance for experiments with strong insolation and well developed up-valley wind. Curves (for B- and C-stabilities) according to the Gaussian absorption formula (Eqn.7b).

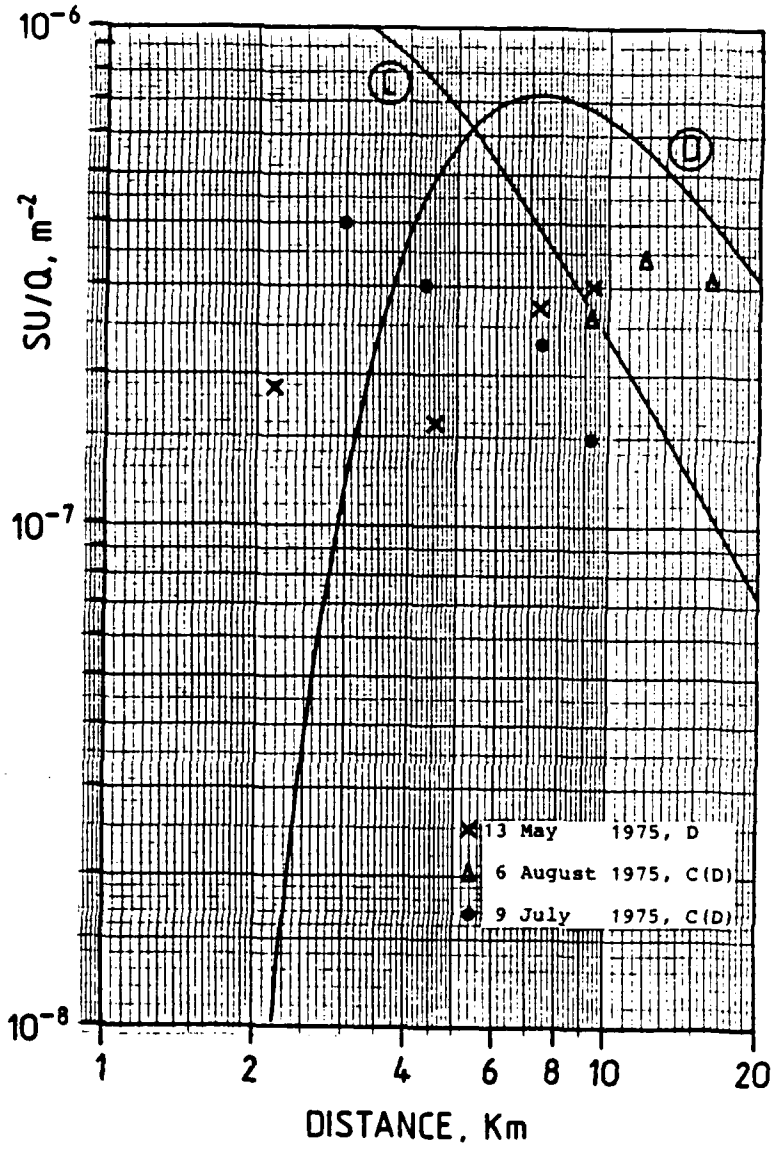


Fig. 11: Centerline ground-level normalized concentration versus downwind distance for experiments with C- and D-stabilities. Curves according to the Gaussian absorption formula (Eqn. 7b).

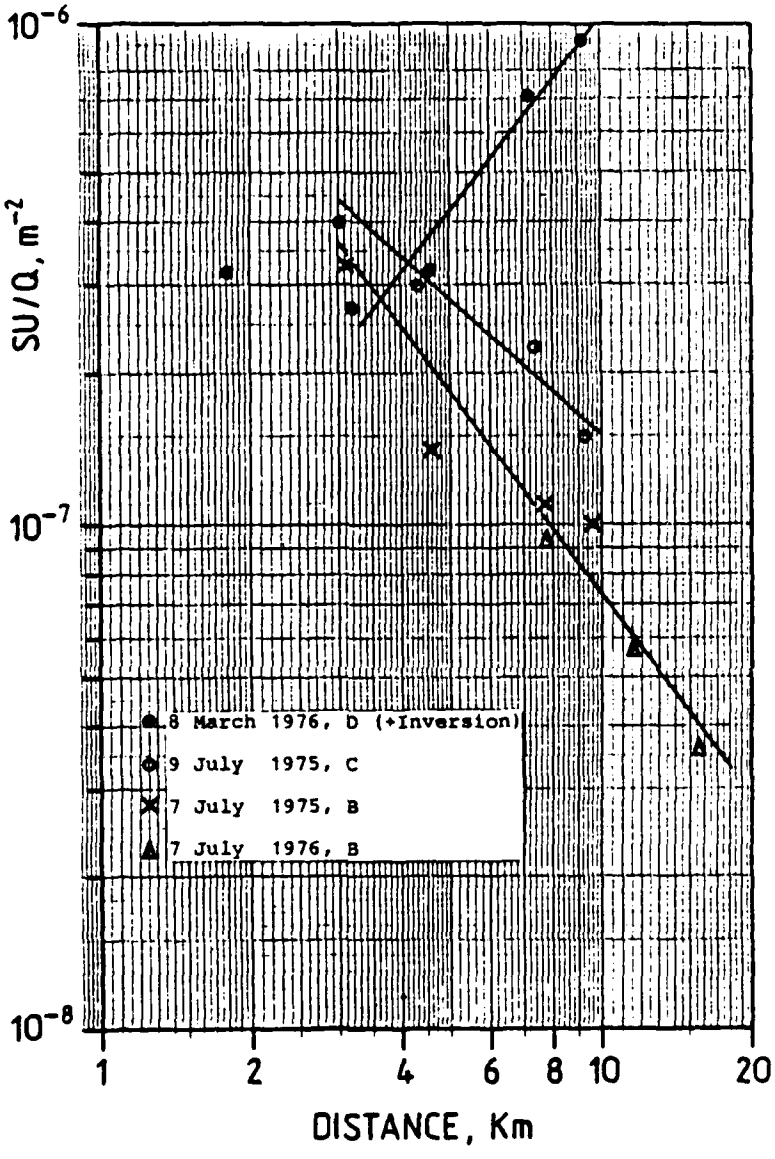


Fig. 12: Measured ground-level normalized concentration as a function of downwind distance for different stability conditions.

Fig. 11 shows the results of three experiments whose stability conditions were ranked between C and D. For comparison the Gaussian absorption model curves are also shown for both stability classes. There is no obvious agreement with the theory, but the tendency of the functional behaviour is evident: in 2 cases there is an increase of SU/Q with distance (May and August experiments), and in the remaining case there is a definite decrease with distance (as to be expected for C-stability conditions).

The range of the observed normalized centerline concentrations for different stability conditions is to be seen from Fig. 12. As already mentioned the highest SU/Q values were observed under D-stability conditions with an inversion layer aloft. At the distance of 9 km (i.e. at the entrance to the Garmisch basin) a value of $SU/Q \approx 10^{-6}\ m^{-2}$ was measured, exceeding those of the B-stability cases by an order of magnitude.

### 5.5.3. Special Aspects

#### 5.5.3.1. Source Above a Lifted Ground Based Inversion

A very interesting experiment (No. 10) took place on 16 December 1975. In this case the aerosol source was located above a persistent lifted ground based inversion with a temperature increase of about $10^{\circ}C$ between 100 and 300 m (Fig. 13).

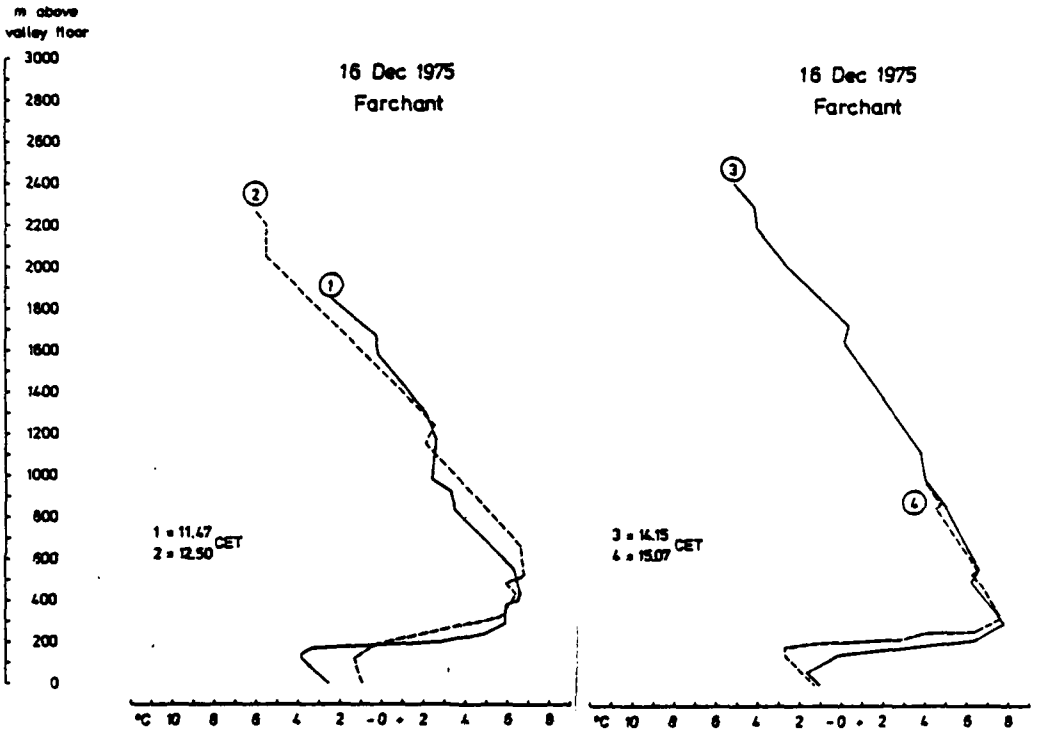


Fig. 13: Temperatur profiles on 16 December 1975 (Experiment No. 10).

In the first 100 m a weak wind with northern (up-valley) directions was prevailing; above this shallow cold layer a warm foehn current was blowing into the opposite direction (see Fig. A4 - ascents B, E, F - in the appendix A). It is remarkable that even then tracers could be counted in the up-valley area (Fig. 14). Obviously, a small fraction of the particles was able to penetrate the strong inversion layer and could reach the up-valley flow in the bottom cold layer.

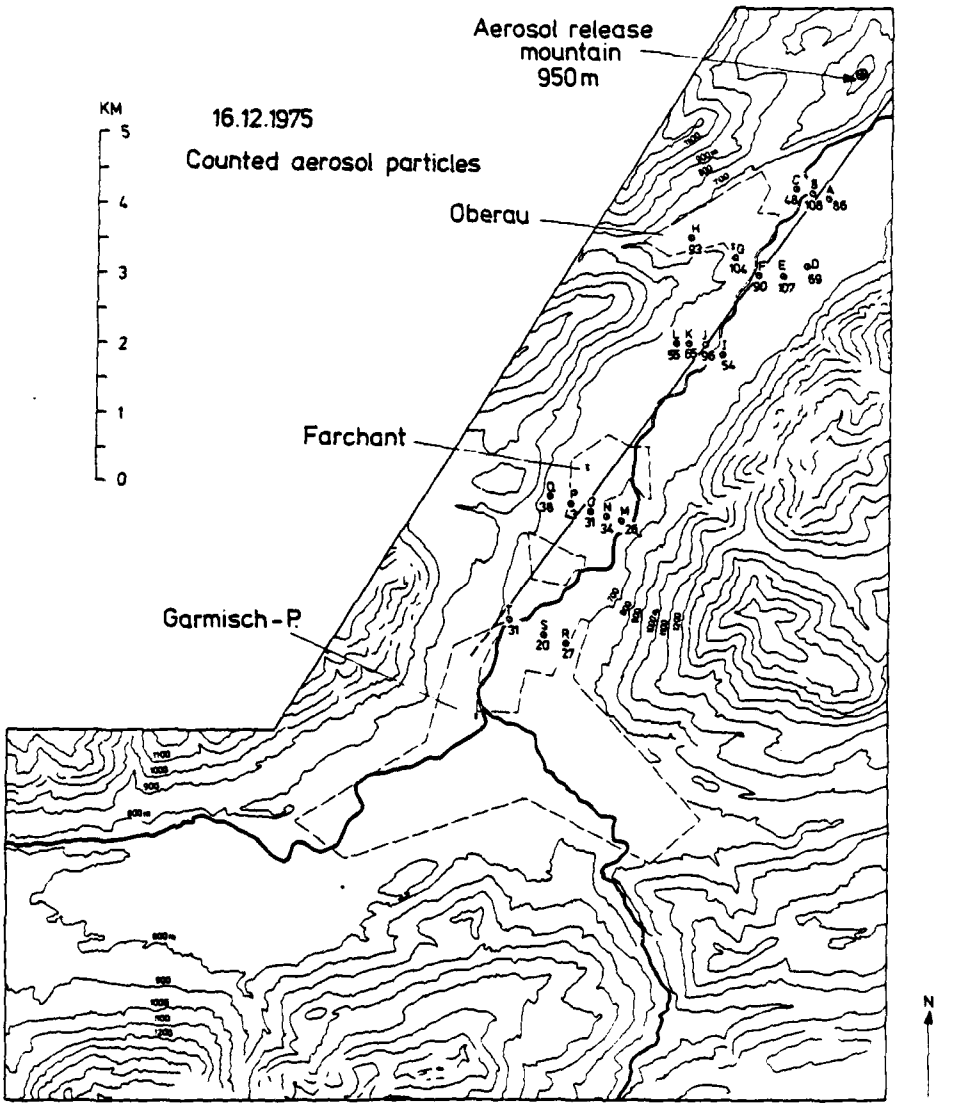


Fig. 14: Particle counts and plume centerline for Experiment No. 10 (16 December 1975)

5.5.3.2. Path of the Plume Centerline

It was shown in section 5.5.2. that similar meteorological conditions (well developed up-valley wind, strong insolation, B-stability) lead to comparable normalized ground-level centerline concentrations along the valley. This statement is, however, not valid for the whole cross-section of the valley, since the path of the centerline may very well differ from one experiment to the other.

This is clearly to be seen from a comparison of the particle counts on 28 June 1976 (Fig. 15) and on 7 July 1976 (Fig. 16). An inspection of the counts at the Farchant cross-section indicates that in both cases the plume centerline was not constrained to the center of the valley: in case of the June experiment it was found at the Kramer valley side and in the other case at the Wank valley side. Note that at the same time the particle counts were almost identical.

The different courses of the particle cloud could also be identified in the Garmisch basin, the respective "homologous" distribution of the counts is evident from Figs. 15 and 16.

Note that in both cases the up-valley wind was similarly well developed and that no obvious differences in the flow behaviour could be stated. Nevertheless, the different paths of the particle cloud hint at a mesoscale meandering of the mean flow, but for the manifestation of the meandering more elaborate measuring techniques are required.

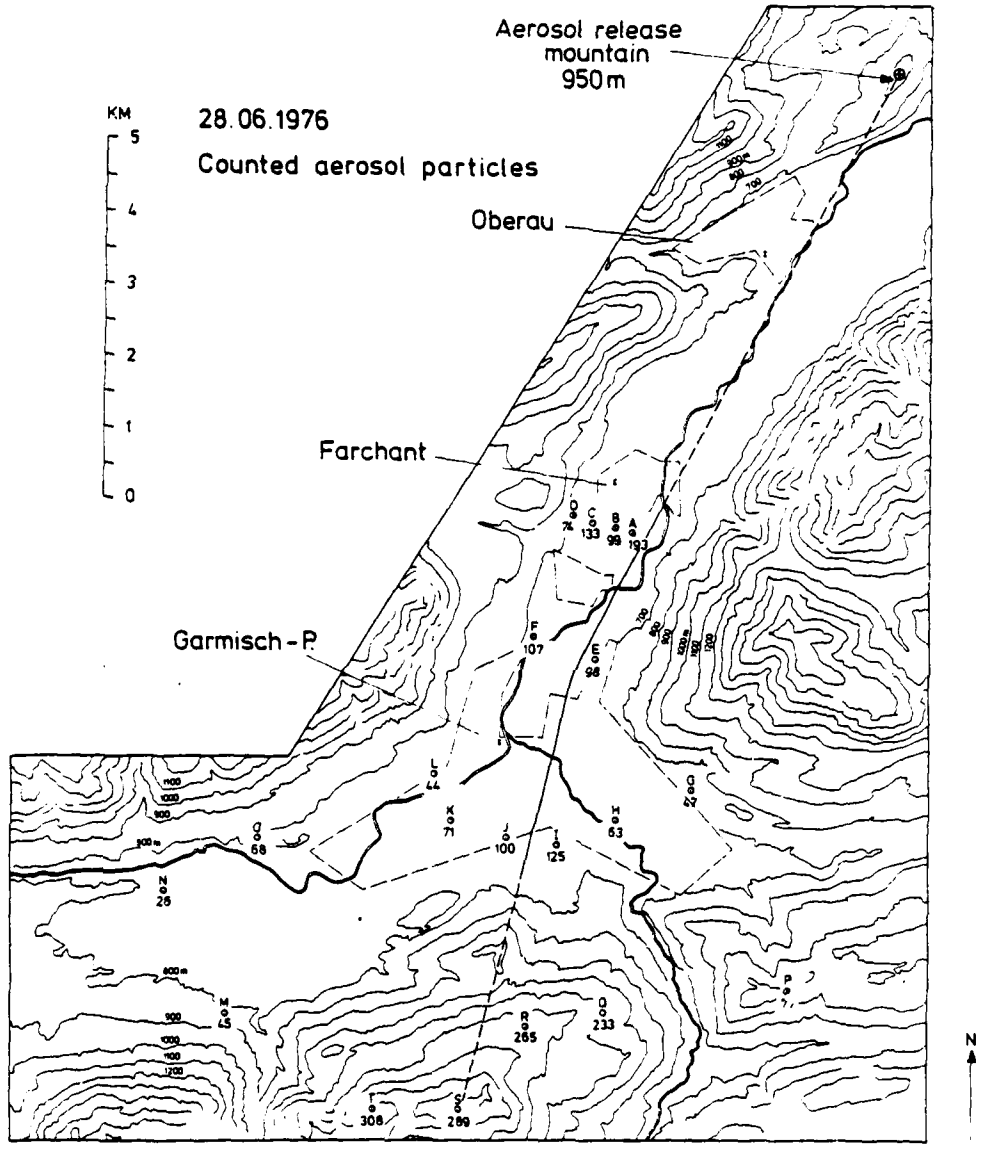


Fig. 15: Particle counts and plume centerline for Experiment No. 13 (28 June 1976)

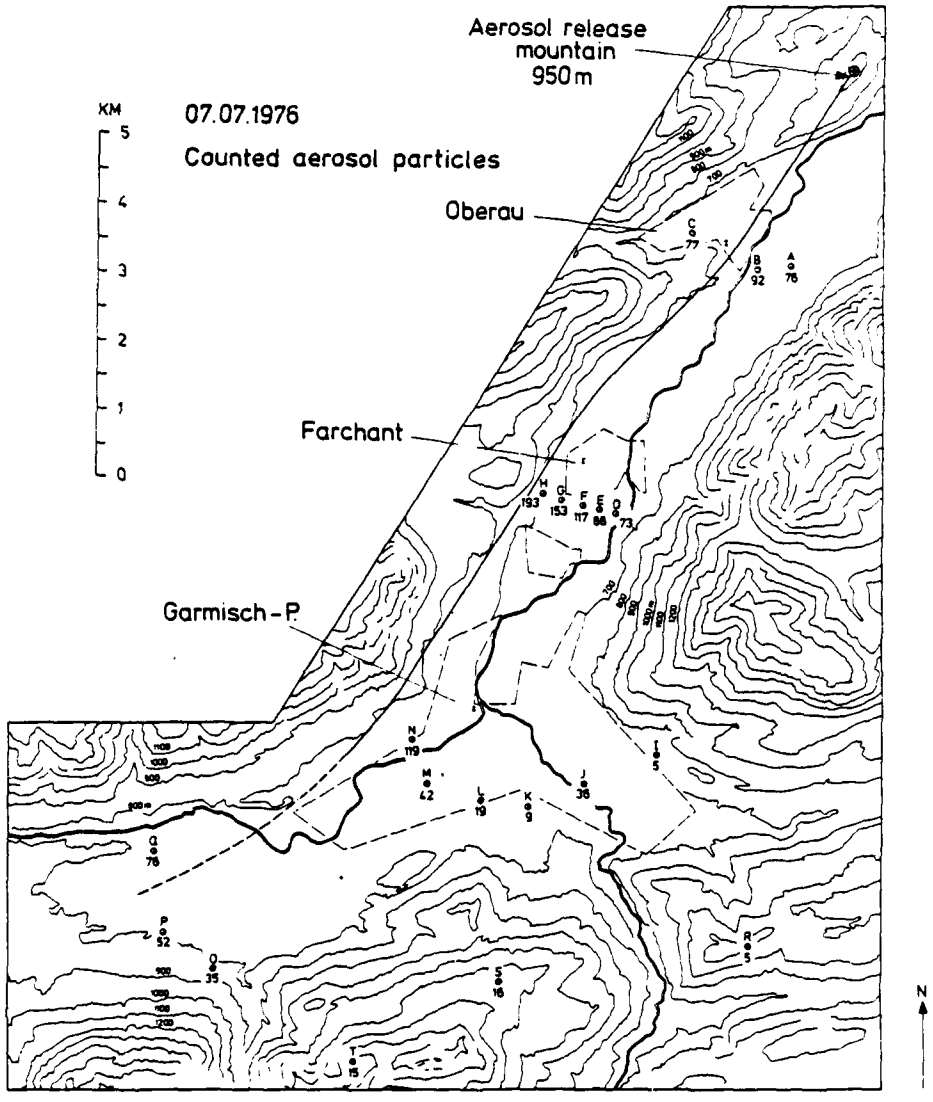


Fig. 16: Particle counts and plume centerline for Experiment No. 14 (7 July 1976)

5.5.3.3. Particle Concentrations at the Mountain Stations

Another important aspect follows from a comparison of the particle counts at the mountain stations for different synoptic (gradient) flow conditions.

On 28 June 1976 (Fig. 15) relatively high particle counts were observed at the Kreuzeck area, these were even higher than those at the Garmisch basin (the ratio of the counts for the plume centerline amounts to $R \simeq 300/100 = 3$). In this case the gradient wind was blowing from the eastern sector and, therefore, was not opposed to the up-valley (NE) wind channelled in the valley (see ascent E in Fig. A6). It can be seen from the trajectories of the pilot balloons near the entrance to the Garmisch basin (Fig. A5) that the flow in the considered height range was heading directly towards the Kreuzeck mountain chain, and this fact is thought to be the main reason for the observed high particle concentrations.

On 7 July 1976, however, practically no particles could reach the mountain samplers (Fig. 16). In this case the gradient wind was blowing from the western sector and, therefore, had a component opposite to the up-valley wind direction (see ascent B in Fig. A8). The reversal to westerly directions took place in the height range of the mountain stations (see also the pilot balloon trajectories in Fig. A7), and this change of direction - connected with low wind speeds - seems to be responsible for the absence of the particles.

The concentration pattern at the Kreuzeck area obviously depends to a high degree on the inlet of the valley wind into the Garmisch basin, and this inlet may be influenced at upper levels by the superimposed synoptic flow. This comparison confirms also the well-known fact that the valley wind system at low levels is often completely decoupled from the upper winds.

## 6. CONCLUSIONS AND FINAL REMARKS

The analysis of the tracer experiments described here illustrates the complexity of pollutant transport in a mountain valley but also demonstrates the difficulties in separating the different effective dispersal processes. The transport is governed to a high degree by valley and slope wind circulations with specific flow structures, by enhanced turbulence over rugged terrain and by along-valley channelling effects. Since the interaction of these processes is nonlinear, the measured concentration patterns are difficult to relate to model conceptions.

Most experiments were conducted with well-developed up-valley wind and unstable lapse-rate conditions (B- and C-stabilities). It is found that the normalized axial concentration of the tracer along the valley (SU/Q) is in good agreement with the Gaussian formula without reflection from the surface (Eqn. 7b) and with a sigma scheme applying to flat terrain conditions. On the other hand, compared to the classical Gaussian plume model (where the ground is assumed to be a perfect reflector

of the tracers, Eqn. 7a) the agreement is within a factor of 2. Dispersion by bulk fluid motion may be partly responsible for this difference. Indeed, Fosberg et al. [4] have shown that "mass divergence influences on plume dispersion may modify classic Gaussian calculations by as much as a factor of two". It must be mentioned, however, that in our experiments the tracers were released from the top of an isolated hill. Due to distortions of the windfield by the hill the effective source height is not well defined. Also, wake effects - with particle losses - are to be expected near the source. Both effects could cause reductions of ground-level concentration at greater downwind distances.

The highest centerline concentrations of SU/Q (which exceed those of the B-stability cases by an order of magnitude) were observed under D-stability conditions with an inversion layer immediately above the source. In this case, a distinct increase of the concentration with downwind distance was found; this indicates that, as expected, the inversion restricted the vertical dispersion of the tracer. The measured concentration pattern is in good agreement with a Gaussian plume model assuming perfect reflection from the inversion, but none from the ground (Eqn. 6).

The complexity of the aerosol transport becomes most evident in those cases when atmospheric conditions were such that none of the Gaussian plume models referred to above could be applied. For example, the tracers were able to partly penetrate a very strong inversion layer

and vertical wind shear enhanced this penetration. Secondly, the location of the centerline differed from one experiment to another; mesoscale meandering of the basic flow is thought to be responsible for this. Finally, in one case, at least, the concentrations at the mountain stations were considerably higher than those in the valley. This occurrence appears to be dependent on the manner in which the valley wind enters the Garmisch basin at upper levels and this, in turn, depends upon the synoptic flow pattern.

More tracer experiments in the Loisach river valley area are planned for the near future. With the tracer source at ground level, the main interest will be in the aerosol transport in nighttime diabatic mountain winds. The "straight channel" model reviewed in the first part of this report will provide a theorotical basis for interpretation of the new experimental data.

## 7. REFERENCES

[1] Archuleta, J., Barr, S., Clements, W.E., Gedayloo, T., and Wilson, S.K., 1978: Some atmospheric tracer experiments in complex terrain at LASL. Experimental design and data;
Los Alamos Scientific Laboratory of the University of California, Los Alamos, New Mexico, LA-7198-MS, Vol.I.

[2] Barr, S., Luna, R.E., Clements, W.E., and Church, H.W., Eds., 1977: Workshop on research needs for atmospheric transport and diffusion in complex terrain;
Energy Research and Development Administration Conference 7609160, Albuquerque, NM, September 28-30, 1976

[3] Csanady, G.T., 1973: Turbulent diffusion in the environment;
Geophysics and Astrophysics Monographs, Vol. 3, D. Reidel Publishing Company, Dordrecht/Boston.

[4] Fosberg, M.A., Fox, D.G., Howard, E.A., and Cohen, J.D., 1976: Nonturbulent dispersion processes in complex terrain;
Atmos. Environ., 10, 1053-1055.

[5] Gifford, F.A., 1976a: Turbulent diffusion-typing schemes: A review;
Environmental Research Laboratories, Atmospheric Turbulence and Diffusion Laboratory (ATDL), Oak Ridge, Tennessee, September 1976, 1975 Annual Report, 25-43.

[6] Gifford, F.A., 1976b: Atmospheric dispersion models for environmental pollution applications;
Environmental Research Laboratories, Atmospheric Turbulence and Diffusion Laboratory (ATDL), Oak Ridge, Tennessee, September 1976, 1975 Annual Report, 312-335.

[7] Gotaas, Y., 1972: A model of diffusion in a valley from a continuous point source;
Arch. Met. Geoph. Biokl., A, 21, 13-26.

[8] Grinnell, S.W., Webster, F.X., and Brown, T.S., 1965: Studies on the performance of the rotorod FP sampler;
Memorandum Report, No. 21 (R)-3, Aerosol Laboratory, Metronics Associates, Inc., Stanford Industrial Park, Palo Alto, Calif.

[9] Hovind, E.L., Spangler, T.C., and Anderson, A.J., 1974: The influence of rough mountainous terrain upon plume dispersion from an elevated source;
Symposium on Atmospheric Diffusion and Air Pollution, AMS, Santa Barbara, Calif., September 9-13, 1974, 214-217.

[10] Irwin, J.S., 1983: Estimating plume dispersion. A comparison of several sigma schemes;
J. Climate and Appl. Meteor., 22, 92-114.

[11] Kao, S.K., Lee, H.N., and Smidy, K.I., 1974: A preliminary analysis of the effect of mountain-valley terrains on turbulence and diffusion;
Symposium on Atmospheric Diffusion and Air Pollution, AMS, Santa Barbara, Calif., September 9-13, 1974, 59-63.

[12] Leighton, P.A., Perkins, W.A., Grinnell, S.W., and Webster, F.X., 1965: The fluorescent particle atmospheric tracer;
J. Appl. Meteor., 4, 334-348.

[13] Nowicki, M., 1976: Ein Beitrag zur Bestimmung universeller Diffusionskoeffizienten;
Arch. Met. Geophys. Biokl., A, 25, 31-45.

[14] Pasquill, F., 1961: The estimation of the dispersion of windborne material;
Meteor. Mag., 90, 33-49.

[15] Reid, J.D., 1979: Studies of pollutant transport and turbulent dispersion over rugged mountainous terrain near Climax, Colorado;
Atmos. Environ., 13, 23-28.

[16] Reiter, R., 1965: Luftverunreinigung und Kleinionendichte in Abhängigkeit von Windströmung und Austausch;
Arch. Met. Geoph. Biokl., B, 14, 53-80.

[17] Reiter, R., Müller, H., Sladkovic, R., 1981: Atmospheric dust and aerosol study - Data Report; prepared for USARDSG, Grant Number DAERO-77-G-035.

[18] Reiter, R., Müller, H., Sladkovic, R., Munzert, K., 1983: Aerological soundings of the mountain-valley wind system with special emphasis on the flow cross-sections through the valley (in german); Meteorol. Rdsch., 36, 225-242.

[19] Sivertsen, B., Lamb, B., and Grønskei, K.E., 1983: A tracer study of pollutant transport in a deep fjord valley; Atmos. Environ., 17, 1915-1922.

[20] Start, G.E., Dickson, C.R., and Wendell, L.L., 1975: Diffusion in a canyon within rough mountainous terrain; J. Appl. Meteor., 14, 333-346.

[21] Stern, A.C., Wohlers, H.C., Boubel, R.W., Lowry, W.P., 1973: Fundamentals of air pollution; Academic Press, New York and London (1973), p.277.

[22] Turner, D.B., 1961: Relationships between 24-hour mean air quality measurements and meteorological factors in Nashville, Tennessee; J. Air. Pollut. Control Assoc., 11, 483-489.

[23] Turner, D.B., 1970: Workbook of atmospheric dispersion estimates; Office of Air Programs Publ. No. AP-26 (Revised 1970), United States Environmental Protection Agency, Research Triangle Park, North Carolina.

# A P P E N D I X A

Figures A1 - A8

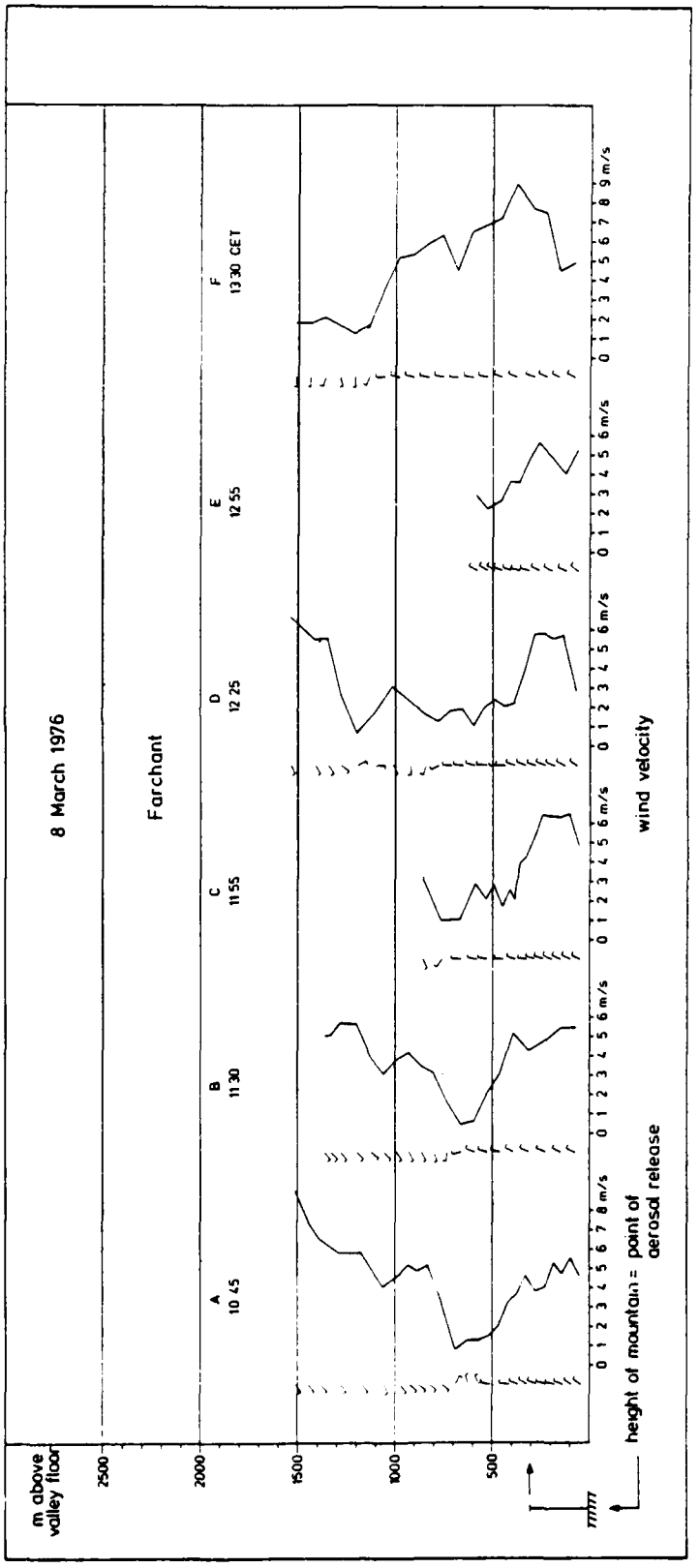


Fig. A1: Wind speed profiles on 8 March 1976 (Experiment No. 12)

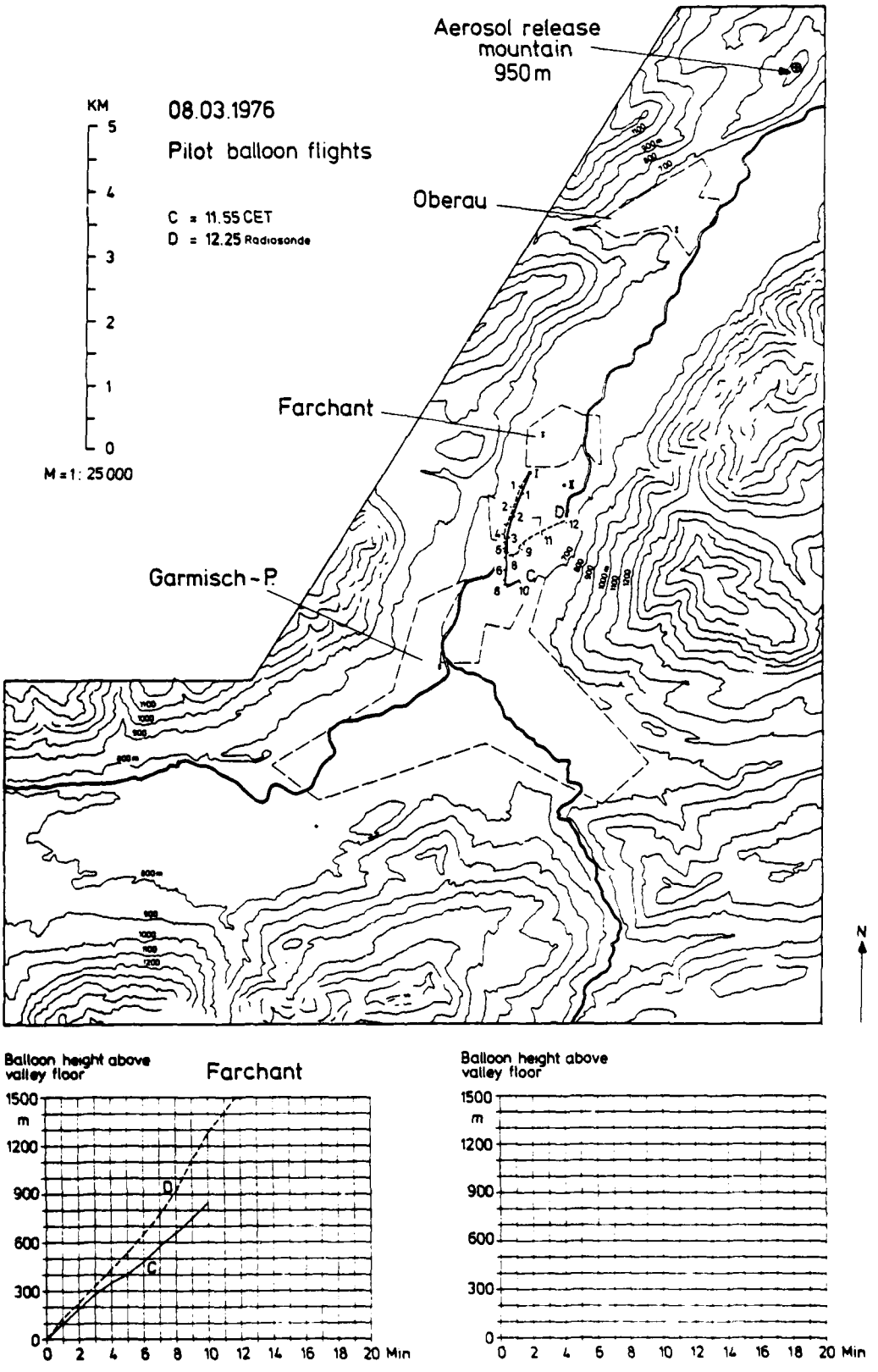


Fig. A2: Trajectories and time-height curves on 8 March 1976 (Experiment No. 12)

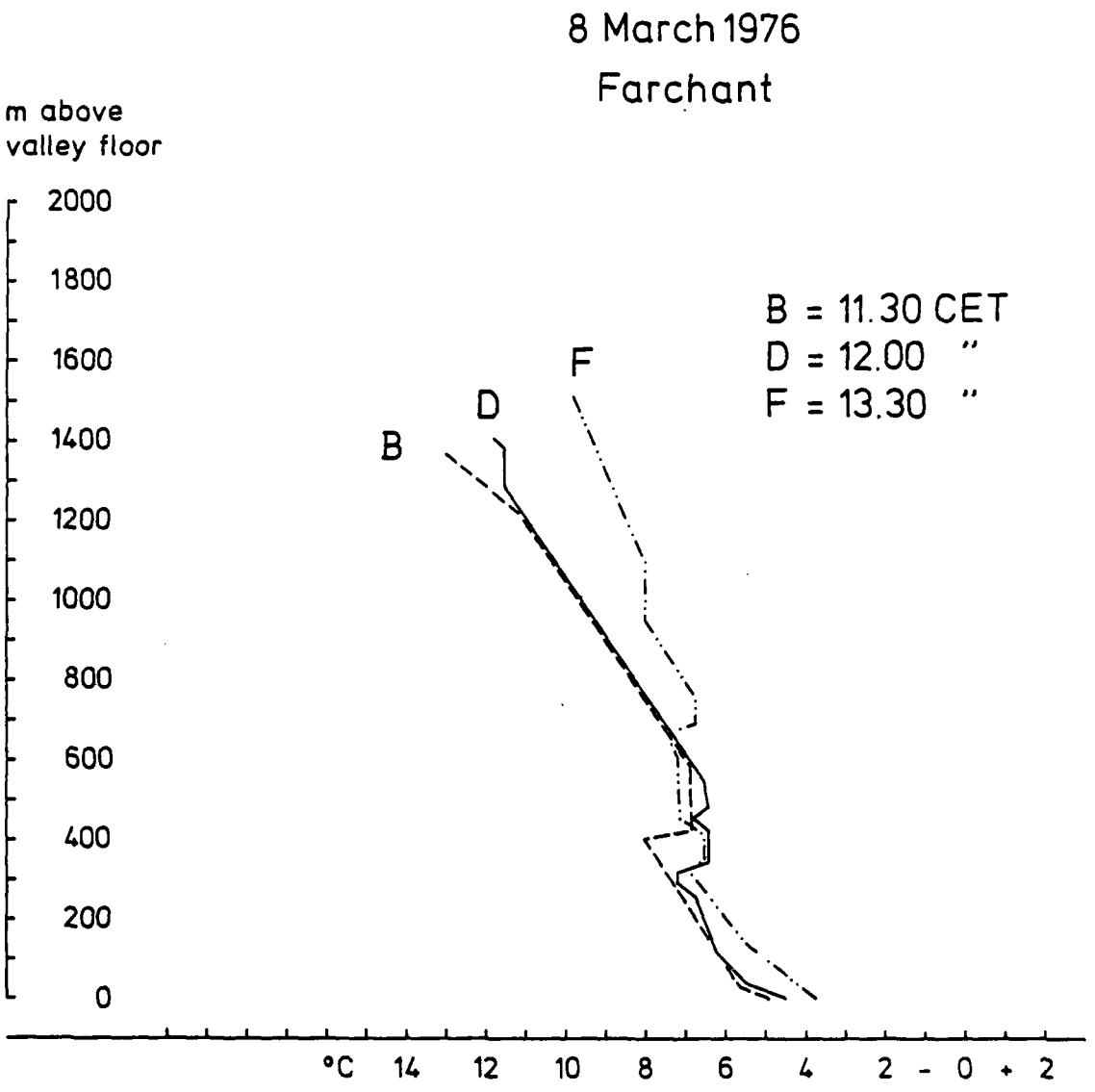


Fig. A3: Temperature profiles on 8 March 1976
(Experiment No. 12)

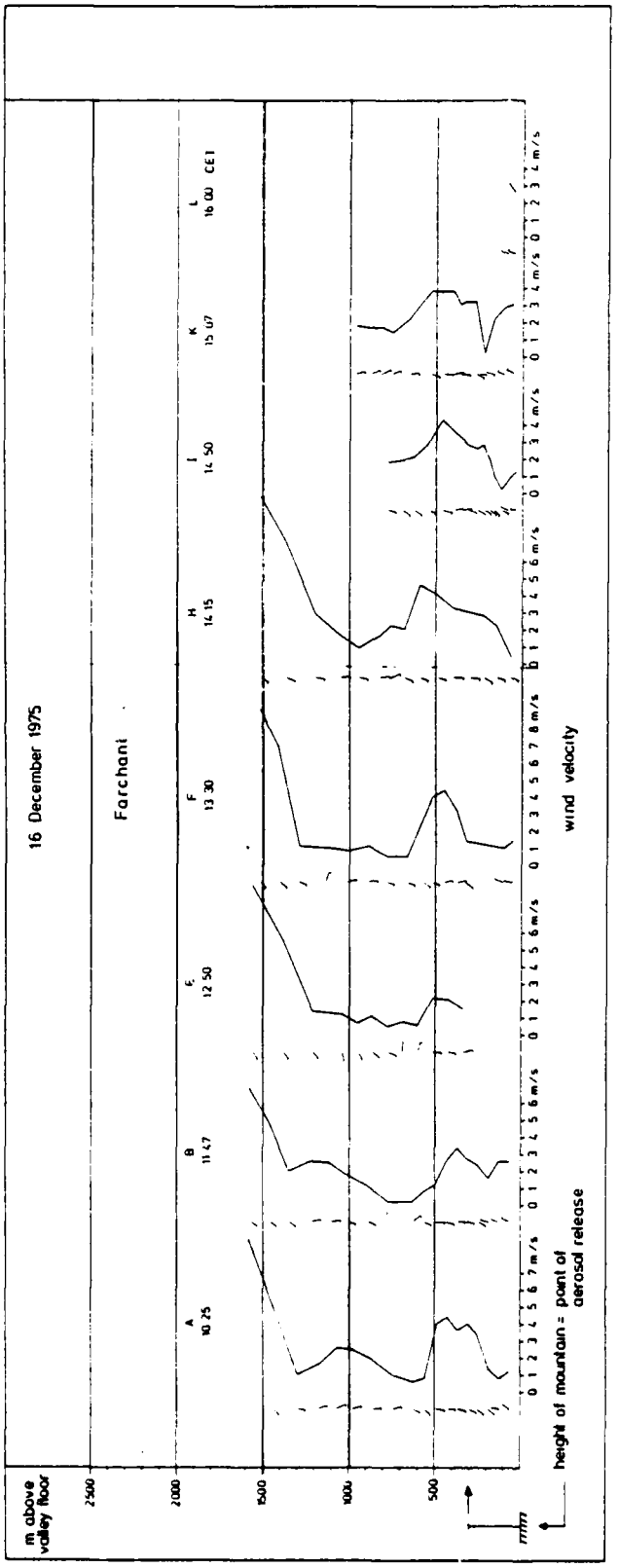


Fig. A4: Wind speed profiles on 16 December 1975 (Experiment No. 10)

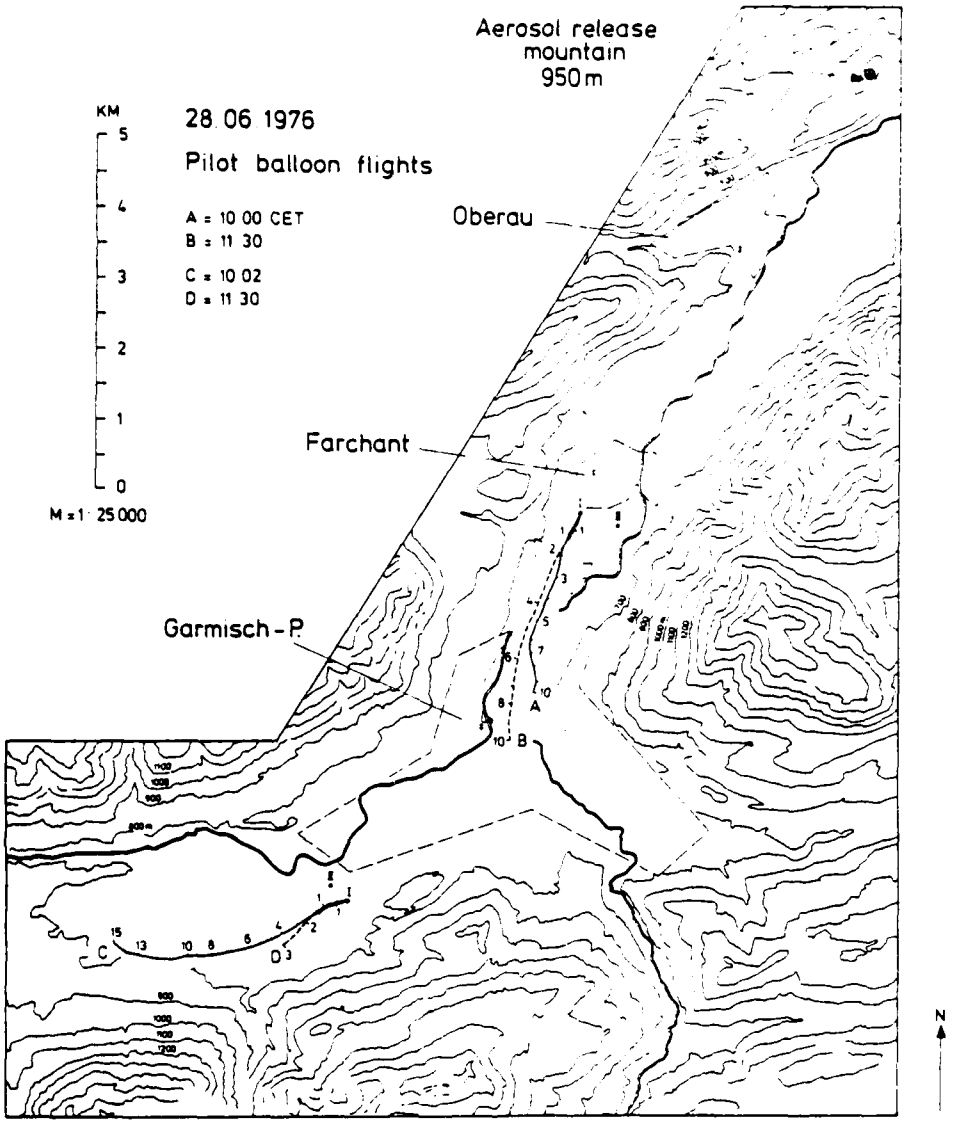


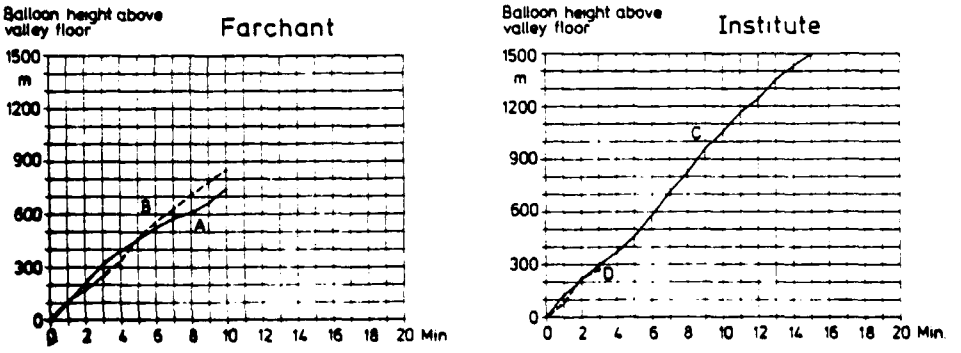


Fig. A5: Trajectories and time-height curves on 28 June 1976 (Experiment No. 13)

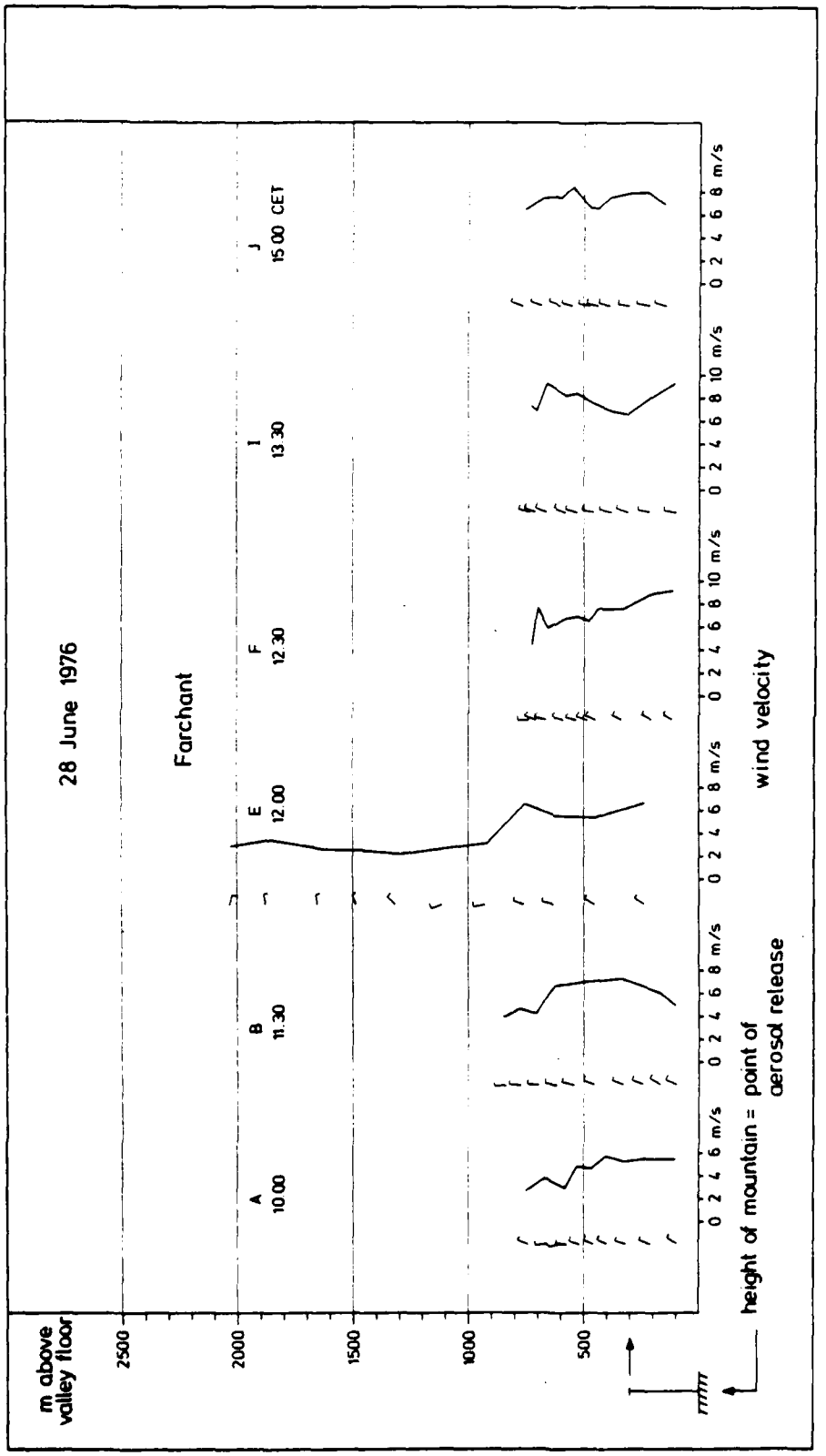


Fig. A6: Wind speed profiles on 28 June 1976 (Experiment No. 13)

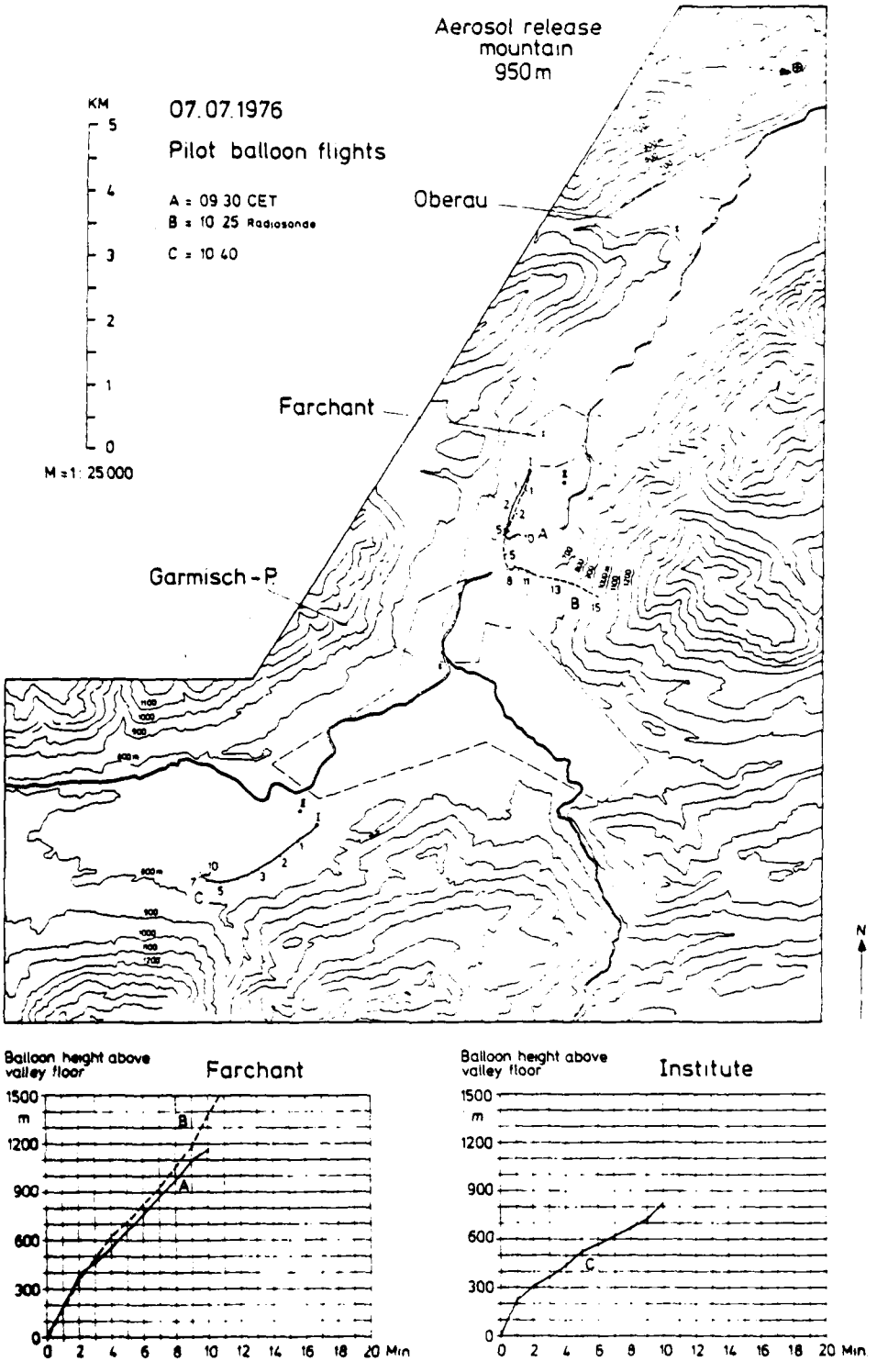


Fig. A7: Trajectories and time-height curves on 7 July 1976 (Experiment No. 14)

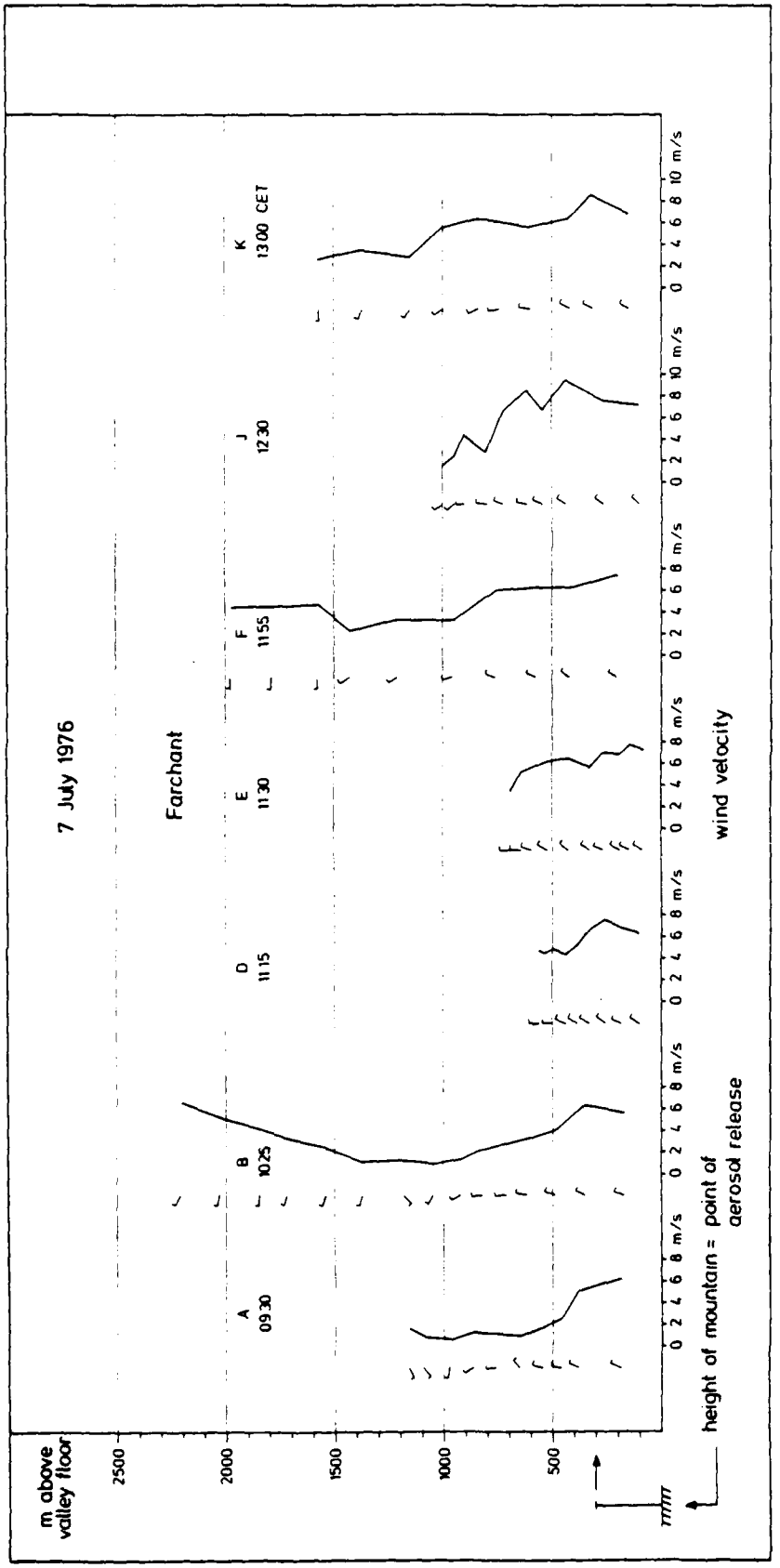


Fig. A8: Wind speed profiles on 7 July 1976 (Experiment No. 14)

# A P P E N D I X B

Table B1: Diffusive function $F^*(\sigma^*, l^*, \zeta^*)$ according to Eqn. (18).

$$S/S_{Lim} = F^*(\sigma_y^*, y^*, a^*) \cdot F^*(\sigma_z^*, z^*, H^*).$$

ZETA* = 0.0 ( L* UPPER SCALE ), ZETA* = 1.0 ( L* LOWER SCALE )

| SIGMA* \ L* | 0.0<br>1.0 | 0.1<br>0.9 | 0.2<br>0.8 | 0.3<br>0.7 | 0.4<br>0.6 | 0.5<br>0.5 | 0.6<br>0.4 | 0.7<br>0.3 | 0.8<br>0.2 | 0.9<br>0.1 | 1.0<br>0.0 |
|---|---|---|---|---|---|---|---|---|---|---|---|
| 0.01 | 79.79 | 0.00 | 0.00 | 0.00 | 0.00 | 0.00 | 0.00 | 0.00 | 0.00 | 0.00 | 0.00 |
| 0.02 | 39.89 | 0.00 | 0.00 | 0.00 | 0.00 | 0.00 | 0.00 | 0.00 | 0.00 | 0.00 | 0.00 |
| 0.03 | 26.60 | 0.10 | 0.00 | 0.00 | 0.00 | 0.00 | 0.00 | 0.00 | 0.00 | 0.00 | 0.00 |
| 0.04 | 19.95 | 0.88 | 0.00 | 0.00 | 0.00 | 0.00 | 0.00 | 0.00 | 0.00 | 0.00 | 0.00 |
| 0.05 | 15.96 | 2.16 | 0.01 | 0.00 | 0.00 | 0.00 | 0.00 | 0.00 | 0.00 | 0.00 | 0.00 |
| 0.06 | 13.30 | 3.32 | 0.05 | 0.00 | 0.00 | 0.00 | 0.00 | 0.00 | 0.00 | 0.00 | 0.00 |
| 0.07 | 11.40 | 4.11 | 0.19 | 0.00 | 0.00 | 0.00 | 0.00 | 0.00 | 0.00 | 0.00 | 0.00 |
| 0.08 | 9.97 | 4.57 | 0.44 | 0.01 | 0.00 | 0.00 | 0.00 | 0.00 | 0.00 | 0.00 | 0.00 |
| 0.09 | 8.87 | 4.78 | 0.75 | 0.03 | 0.00 | 0.00 | 0.00 | 0.00 | 0.00 | 0.00 | 0.00 |
| 0.10 | 7.98 | 4.84 | 1.08 | 0.09 | 0.00 | 0.00 | 0.00 | 0.00 | 0.00 | 0.00 | 0.00 |
| 0.11 | 7.25 | 4.80 | 1.39 | 0.18 | 0.01 | 0.00 | 0.00 | 0.00 | 0.00 | 0.00 | 0.00 |
| 0.12 | 6.65 | 4.70 | 1.66 | 0.29 | 0.03 | 0.00 | 0.00 | 0.00 | 0.00 | 0.00 | 0.00 |
| 0.13 | 6.14 | 4.57 | 1.88 | 0.43 | 0.05 | 0.00 | 0.00 | 0.00 | 0.00 | 0.00 | 0.00 |
| 0.14 | 5.70 | 4.42 | 2.05 | 0.57 | 0.10 | 0.01 | 0.00 | 0.00 | 0.00 | 0.00 | 0.00 |
| 0.15 | 5.32 | 4.26 | 2.19 | 0.72 | 0.15 | 0.02 | 0.00 | 0.00 | 0.00 | 0.00 | 0.00 |
| 0.16 | 4.99 | 4.10 | 2.28 | 0.86 | 0.22 | 0.04 | 0.00 | 0.00 | 0.00 | 0.00 | 0.00 |
| 0.17 | 4.69 | 3.95 | 2.35 | 0.99 | 0.29 | 0.06 | 0.01 | 0.00 | 0.00 | 0.00 | 0.00 |
| 0.18 | 4.43 | 3.80 | 2.39 | 1.11 | 0.38 | 0.09 | 0.02 | 0.00 | 0.00 | 0.00 | 0.00 |
| 0.19 | 4.20 | 3.66 | 2.41 | 1.21 | 0.46 | 0.13 | 0.03 | 0.00 | 0.00 | 0.00 | 0.00 |
| 0.20 | 3.99 | 3.52 | 2.42 | 1.30 | 0.54 | 0.18 | 0.04 | 0.01 | 0.00 | 0.00 | 0.00 |
| 0.21 | 3.80 | 3.39 | 2.41 | 1.37 | 0.62 | 0.22 | 0.06 | 0.01 | 0.00 | 0.00 | 0.00 |
| 0.22 | 3.63 | 3.27 | 2.40 | 1.43 | 0.69 | 0.27 | 0.09 | 0.02 | 0.00 | 0.00 | 0.00 |
| 0.23 | 3.47 | 3.16 | 2.38 | 1.48 | 0.76 | 0.33 | 0.12 | 0.03 | 0.01 | 0.00 | 0.00 |
| 0.24 | 3.32 | 3.05 | 2.35 | 1.52 | 0.83 | 0.38 | 0.15 | 0.05 | 0.01 | 0.00 | 0.00 |
| 0.25 | 3.19 | 2.95 | 2.32 | 1.55 | 0.89 | 0.43 | 0.18 | 0.06 | 0.02 | 0.01 | 0.00 |
| 0.26 | 3.07 | 2.85 | 2.28 | 1.58 | 0.94 | 0.48 | 0.21 | 0.08 | 0.03 | 0.01 | 0.00 |
| 0.27 | 2.96 | 2.76 | 2.25 | 1.59 | 0.99 | 0.53 | 0.25 | 0.10 | 0.04 | 0.01 | 0.01 |
| 0.28 | 2.85 | 2.67 | 2.21 | 1.61 | 1.03 | 0.58 | 0.29 | 0.13 | 0.05 | 0.02 | 0.01 |
| 0.29 | 2.75 | 2.59 | 2.17 | 1.61 | 1.06 | 0.62 | 0.32 | 0.15 | 0.06 | 0.02 | 0.01 |
| 0.30 | 2.66 | 2.52 | 2.13 | 1.61 | 1.09 | 0.66 | 0.36 | 0.18 | 0.08 | 0.03 | 0.02 |
| 0.31 | 2.57 | 2.44 | 2.09 | 1.61 | 1.12 | 0.70 | 0.40 | 0.20 | 0.09 | 0.04 | 0.03 |
| 0.32 | 2.49 | 2.37 | 2.05 | 1.61 | 1.14 | 0.74 | 0.43 | 0.23 | 0.11 | 0.05 | 0.04 |
| 0.33 | 2.42 | 2.31 | 2.01 | 1.60 | 1.16 | 0.77 | 0.46 | 0.26 | 0.13 | 0.07 | 0.05 |
| 0.34 | 2.35 | 2.25 | 1.97 | 1.59 | 1.17 | 0.80 | 0.50 | 0.28 | 0.15 | 0.08 | 0.06 |
| 0.35 | 2.28 | 2.19 | 1.94 | 1.58 | 1.19 | 0.82 | 0.53 | 0.31 | 0.17 | 0.10 | 0.08 |
| 0.36 | 2.22 | 2.13 | 1.90 | 1.57 | 1.20 | 0.85 | 0.55 | 0.34 | 0.20 | 0.12 | 0.09 |
| 0.37 | 2.16 | 2.08 | 1.86 | 1.55 | 1.20 | 0.87 | 0.58 | 0.36 | 0.22 | 0.14 | 0.11 |
| 0.38 | 2.10 | 2.03 | 1.83 | 1.54 | 1.21 | 0.88 | 0.61 | 0.39 | 0.24 | 0.16 | 0.13 |
| 0.39 | 2.05 | 1.98 | 1.79 | 1.52 | 1.21 | 0.90 | 0.63 | 0.42 | 0.27 | 0.18 | 0.15 |
| 0.40 | 1.99 | 1.93 | 1.76 | 1.51 | 1.21 | 0.92 | 0.65 | 0.44 | 0.29 | 0.20 | 0.18 |
| 0.41 | 1.95 | 1.89 | 1.73 | 1.49 | 1.21 | 0.93 | 0.67 | 0.47 | 0.32 | 0.23 | 0.20 |
| 0.42 | 1.90 | 1.85 | 1.70 | 1.47 | 1.21 | 0.94 | 0.69 | 0.49 | 0.34 | 0.25 | 0.22 |
| 0.43 | 1.86 | 1.81 | 1.67 | 1.46 | 1.21 | 0.95 | 0.71 | 0.51 | 0.37 | 0.28 | 0.25 |
| 0.44 | 1.81 | 1.77 | 1.64 | 1.44 | 1.20 | 0.96 | 0.73 | 0.53 | 0.39 | 0.30 | 0.27 |
| 0.45 | 1.77 | 1.73 | 1.61 | 1.42 | 1.20 | 0.96 | 0.74 | 0.56 | 0.42 | 0.33 | 0.30 |
| 0.46 | 1.73 | 1.69 | 1.58 | 1.40 | 1.19 | 0.97 | 0.76 | 0.58 | 0.44 | 0.36 | 0.33 |
| 0.47 | 1.70 | 1.66 | 1.55 | 1.39 | 1.19 | 0.97 | 0.77 | 0.60 | 0.46 | 0.38 | 0.35 |
| 0.48 | 1.66 | 1.63 | 1.53 | 1.37 | 1.18 | 0.98 | 0.78 | 0.62 | 0.49 | 0.41 | 0.38 |
| 0.49 | 1.63 | 1.60 | 1.50 | 1.35 | 1.17 | 0.98 | 0.80 | 0.64 | 0.51 | 0.43 | 0.41 |
| 0.50 | 1.60 | 1.57 | 1.48 | 1.34 | 1.17 | 0.99 | 0.81 | 0.65 | 0.53 | 0.46 | 0.43 |
| 0.52 | 1.54 | 1.51 | 1.43 | 1.31 | 1.15 | 0.99 | 0.83 | 0.69 | 0.58 | 0.51 | 0.48 |
| 0.54 | 1.48 | 1.46 | 1.39 | 1.28 | 1.14 | 0.99 | 0.85 | 0.72 | 0.62 | 0.55 | 0.53 |
| 0.56 | 1.43 | 1.41 | 1.35 | 1.25 | 1.13 | 1.00 | 0.87 | 0.75 | 0.66 | 0.60 | 0.58 |
| 0.58 | 1.38 | 1.36 | 1.31 | 1.22 | 1.12 | 1.00 | 0.88 | 0.78 | 0.69 | 0.64 | 0.62 |
| 0.60 | 1.34 | 1.32 | 1.27 | 1.20 | 1.10 | 1.00 | 0.89 | 0.80 | 0.73 | 0.68 | 0.66 |
| 0.62 | 1.30 | 1.29 | 1.24 | 1.18 | 1.09 | 1.00 | 0.91 | 0.82 | 0.76 | 0.72 | 0.70 |
| 0.64 | 1.27 | 1.25 | 1.21 | 1.16 | 1.08 | 1.00 | 0.92 | 0.84 | 0.79 | 0.75 | 0.74 |
| 0.66 | 1.23 | 1.22 | 1.19 | 1.14 | 1.07 | 1.00 | 0.93 | 0.86 | 0.81 | 0.78 | 0.77 |
| 0.68 | 1.20 | 1.19 | 1.17 | 1.12 | 1.06 | 1.00 | 0.94 | 0.88 | 0.83 | 0.81 | 0.80 |
| 0.70 | 1.18 | 1.17 | 1.14 | 1.10 | 1.05 | 1.00 | 0.94 | 0.90 | 0.86 | 0.83 | 0.82 |
| 0.72 | 1.15 | 1.15 | 1.13 | 1.09 | 1.05 | 1.00 | 0.95 | 0.91 | 0.87 | 0.85 | 0.85 |
| 0.74 | 1.13 | 1.13 | 1.11 | 1.08 | 1.04 | 1.00 | 0.96 | 0.92 | 0.89 | 0.87 | 0.87 |
| 0.76 | 1.12 | 1.11 | 1.09 | 1.07 | 1.04 | 1.00 | 0.96 | 0.93 | 0.91 | 0.89 | 0.88 |
| 0.78 | 1.10 | 1.09 | 1.08 | 1.06 | 1.03 | 1.00 | 0.97 | 0.94 | 0.92 | 0.91 | 0.90 |
| 0.80 | 1.09 | 1.08 | 1.07 | 1.05 | 1.03 | 1.00 | 0.97 | 0.95 | 0.93 | 0.92 | 0.92 |
| 0.82 | 1.07 | 1.07 | 1.06 | 1.04 | 1.02 | 1.00 | 0.98 | 0.96 | 0.94 | 0.93 | 0.93 |
| 0.84 | 1.06 | 1.06 | 1.05 | 1.04 | 1.02 | 1.00 | 0.98 | 0.96 | 0.95 | 0.94 | 0.94 |
| 0.86 | 1.05 | 1.05 | 1.04 | 1.03 | 1.02 | 1.00 | 0.98 | 0.97 | 0.96 | 0.95 | 0.95 |
| 0.88 | 1.04 | 1.04 | 1.04 | 1.03 | 1.01 | 1.00 | 0.99 | 0.97 | 0.96 | 0.96 | 0.96 |
| 0.90 | 1.04 | 1.03 | 1.03 | 1.02 | 1.01 | 1.00 | 0.99 | 0.98 | 0.97 | 0.97 | 0.96 |
| 0.92 | 1.03 | 1.03 | 1.02 | 1.02 | 1.01 | 1.00 | 0.99 | 0.98 | 0.98 | 0.97 | 0.97 |
| 0.94 | 1.03 | 1.02 | 1.02 | 1.02 | 1.01 | 1.00 | 0.99 | 0.98 | 0.98 | 0.98 | 0.97 |
| 0.96 | 1.02 | 1.02 | 1.02 | 1.01 | 1.01 | 1.00 | 0.99 | 0.99 | 0.98 | 0.98 | 0.98 |
| 0.98 | 1.02 | 1.02 | 1.01 | 1.01 | 1.01 | 1.00 | 0.99 | 0.99 | 0.99 | 0.98 | 0.98 |
| 1.00 | 1.01 | 1.01 | 1.01 | 1.01 | 1.00 | 1.00 | 1.00 | 0.99 | 0.99 | 0.99 | 0.99 |

ZETA* = 0.1 ( L* UPPER SCALE ), ZETA* = 0.9 ( L* LOWER SCALE )

| SIGMA* \ L* | 0.0<br>1.0 | 0.1<br>0.9 | 0.2<br>0.8 | 0.3<br>0.7 | 0.4<br>0.6 | 0.5<br>0.5 | 0.6<br>0.4 | 0.7<br>0.3 | 0.8<br>0.2 | 0.9<br>0.1 | 1.0<br>0.0 |
|---|---|---|---|---|---|---|---|---|---|---|---|
| 0.01 | 0.00 | 39.89 | 0.00 | 0.00 | 0.00 | 0.00 | 0.00 | 0.00 | 0.00 | 0.00 | 0.00 |
| 0.02 | 0.00 | 19.95 | 0.00 | 0.00 | 0.00 | 0.00 | 0.00 | 0.00 | 0.00 | 0.00 | 0.00 |
| 0.03 | 0.10 | 13.30 | 0.05 | 0.00 | 0.00 | 0.00 | 0.00 | 0.00 | 0.00 | 0.00 | 0.00 |
| 0.04 | 0.88 | 9.97 | 0.44 | 0.00 | 0.00 | 0.00 | 0.00 | 0.00 | 0.00 | 0.00 | 0.00 |
| 0.05 | 2.16 | 7.98 | 1.08 | 0.00 | 0.00 | 0.00 | 0.00 | 0.00 | 0.00 | 0.00 | 0.00 |
| 0.06 | 3.32 | 6.67 | 1.66 | 0.03 | 0.00 | 0.00 | 0.00 | 0.00 | 0.00 | 0.00 | 0.00 |
| 0.07 | 4.11 | 5.80 | 2.05 | 0.10 | 0.00 | 0.00 | 0.00 | 0.00 | 0.00 | 0.00 | 0.00 |
| 0.08 | 4.57 | 5.21 | 2.29 | 0.22 | 0.00 | 0.00 | 0.00 | 0.00 | 0.00 | 0.00 | 0.00 |
| 0.09 | 4.78 | 4.81 | 2.41 | 0.38 | 0.02 | 0.00 | 0.00 | 0.00 | 0.00 | 0.00 | 0.00 |
| 0.10 | 4.84 | 4.53 | 2.46 | 0.54 | 0.04 | 0.00 | 0.00 | 0.00 | 0.00 | 0.00 | 0.00 |
| 0.11 | 4.80 | 4.32 | 2.49 | 0.70 | 0.09 | 0.00 | 0.00 | 0.00 | 0.00 | 0.00 | 0.00 |
| 0.12 | 4.70 | 4.15 | 2.50 | 0.84 | 0.15 | 0.01 | 0.00 | 0.00 | 0.00 | 0.00 | 0.00 |
| 0.13 | 4.57 | 4.01 | 2.50 | 0.97 | 0.22 | 0.03 | 0.00 | 0.00 | 0.00 | 0.00 | 0.00 |
| 0.14 | 4.42 | 3.88 | 2.49 | 1.08 | 0.29 | 0.05 | 0.00 | 0.00 | 0.00 | 0.00 | 0.00 |
| 0.15 | 4.26 | 3.75 | 2.49 | 1.17 | 0.37 | 0.08 | 0.01 | 0.00 | 0.00 | 0.00 | 0.00 |
| 0.16 | 4.10 | 3.63 | 2.48 | 1.25 | 0.45 | 0.11 | 0.02 | 0.00 | 0.00 | 0.00 | 0.00 |
| 0.17 | 3.95 | 3.52 | 2.47 | 1.32 | 0.53 | 0.15 | 0.03 | 0.00 | 0.00 | 0.00 | 0.00 |
| 0.18 | 3.80 | 3.41 | 2.45 | 1.38 | 0.60 | 0.20 | 0.05 | 0.01 | 0.00 | 0.00 | 0.00 |
| 0.19 | 3.66 | 3.31 | 2.43 | 1.44 | 0.67 | 0.24 | 0.07 | 0.01 | 0.00 | 0.00 | 0.00 |
| 0.20 | 3.52 | 3.20 | 2.41 | 1.48 | 0.74 | 0.29 | 0.09 | 0.02 | 0.00 | 0.00 | 0.00 |
| 0.21 | 3.39 | 3.11 | 2.38 | 1.52 | 0.80 | 0.34 | 0.12 | 0.03 | 0.01 | 0.00 | 0.00 |
| 0.22 | 3.27 | 3.01 | 2.35 | 1.55 | 0.85 | 0.39 | 0.15 | 0.05 | 0.01 | 0.00 | 0.00 |
| 0.23 | 3.16 | 2.92 | 2.32 | 1.57 | 0.90 | 0.44 | 0.18 | 0.06 | 0.02 | 0.00 | 0.00 |
| 0.24 | 3.05 | 2.84 | 2.29 | 1.59 | 0.95 | 0.49 | 0.21 | 0.08 | 0.03 | 0.01 | 0.00 |
| 0.25 | 2.95 | 2.75 | 2.25 | 1.60 | 0.99 | 0.53 | 0.25 | 0.10 | 0.03 | 0.01 | 0.01 |
| 0.26 | 2.85 | 2.68 | 2.21 | 1.61 | 1.03 | 0.58 | 0.28 | 0.12 | 0.04 | 0.02 | 0.01 |
| 0.27 | 2.76 | 2.60 | 2.18 | 1.62 | 1.06 | 0.62 | 0.32 | 0.14 | 0.06 | 0.02 | 0.01 |
| 0.28 | 2.67 | 2.53 | 2.14 | 1.62 | 1.09 | 0.66 | 0.35 | 0.17 | 0.07 | 0.03 | 0.02 |
| 0.29 | 2.59 | 2.46 | 2.10 | 1.62 | 1.12 | 0.69 | 0.39 | 0.19 | 0.09 | 0.04 | 0.02 |
| 0.30 | 2.52 | 2.39 | 2.06 | 1.61 | 1.14 | 0.73 | 0.42 | 0.22 | 0.10 | 0.05 | 0.03 |
| 0.31 | 2.44 | 2.33 | 2.03 | 1.60 | 1.16 | 0.76 | 0.45 | 0.24 | 0.12 | 0.06 | 0.04 |
| 0.32 | 2.37 | 2.27 | 1.99 | 1.60 | 1.17 | 0.79 | 0.48 | 0.27 | 0.14 | 0.07 | 0.05 |
| 0.33 | 2.31 | 2.22 | 1.95 | 1.59 | 1.18 | 0.81 | 0.51 | 0.30 | 0.16 | 0.09 | 0.07 |
| 0.34 | 2.25 | 2.16 | 1.92 | 1.57 | 1.19 | 0.83 | 0.54 | 0.32 | 0.18 | 0.11 | 0.08 |
| 0.35 | 2.19 | 2.11 | 1.88 | 1.56 | 1.20 | 0.86 | 0.57 | 0.35 | 0.21 | 0.13 | 0.10 |
| 0.36 | 2.13 | 2.06 | 1.85 | 1.55 | 1.21 | 0.87 | 0.59 | 0.38 | 0.23 | 0.14 | 0.12 |
| 0.37 | 2.08 | 2.01 | 1.82 | 1.53 | 1.21 | 0.89 | 0.62 | 0.40 | 0.25 | 0.17 | 0.14 |
| 0.38 | 2.03 | 1.96 | 1.78 | 1.52 | 1.21 | 0.91 | 0.64 | 0.42 | 0.27 | 0.19 | 0.16 |
| 0.39 | 1.98 | 1.92 | 1.75 | 1.50 | 1.21 | 0.92 | 0.66 | 0.45 | 0.30 | 0.21 | 0.18 |
| 0.40 | 1.93 | 1.88 | 1.72 | 1.49 | 1.21 | 0.93 | 0.68 | 0.47 | 0.32 | 0.23 | 0.20 |
| 0.41 | 1.89 | 1.84 | 1.69 | 1.47 | 1.21 | 0.94 | 0.70 | 0.49 | 0.35 | 0.26 | 0.23 |
| 0.42 | 1.85 | 1.80 | 1.66 | 1.45 | 1.21 | 0.95 | 0.71 | 0.52 | 0.37 | 0.28 | 0.25 |
| 0.43 | 1.81 | 1.76 | 1.63 | 1.44 | 1.20 | 0.96 | 0.73 | 0.54 | 0.40 | 0.31 | 0.28 |
| 0.44 | 1.77 | 1.72 | 1.60 | 1.42 | 1.20 | 0.96 | 0.75 | 0.56 | 0.42 | 0.33 | 0.30 |
| 0.45 | 1.73 | 1.69 | 1.58 | 1.40 | 1.19 | 0.97 | 0.76 | 0.58 | 0.44 | 0.36 | 0.33 |
| 0.46 | 1.69 | 1.66 | 1.55 | 1.39 | 1.19 | 0.98 | 0.77 | 0.60 | 0.47 | 0.38 | 0.36 |
| 0.47 | 1.66 | 1.62 | 1.52 | 1.37 | 1.18 | 0.98 | 0.79 | 0.62 | 0.49 | 0.41 | 0.38 |
| 0.48 | 1.63 | 1.59 | 1.50 | 1.35 | 1.17 | 0.98 | 0.80 | 0.64 | 0.51 | 0.43 | 0.41 |
| 0.49 | 1.60 | 1.56 | 1.47 | 1.34 | 1.17 | 0.99 | 0.81 | 0.65 | 0.53 | 0.46 | 0.43 |
| 0.50 | 1.57 | 1.54 | 1.45 | 1.32 | 1.16 | 0.99 | 0.82 | 0.67 | 0.56 | 0.48 | 0.46 |
| 0.52 | 1.51 | 1.48 | 1.41 | 1.29 | 1.15 | 0.99 | 0.84 | 0.70 | 0.60 | 0.53 | 0.51 |
| 0.54 | 1.46 | 1.43 | 1.37 | 1.26 | 1.14 | 0.99 | 0.86 | 0.73 | 0.64 | 0.58 | 0.55 |
| 0.56 | 1.41 | 1.39 | 1.33 | 1.24 | 1.12 | 1.00 | 0.87 | 0.76 | 0.67 | 0.62 | 0.60 |
| 0.58 | 1.36 | 1.35 | 1.29 | 1.21 | 1.11 | 1.00 | 0.89 | 0.79 | 0.71 | 0.66 | 0.64 |
| 0.60 | 1.32 | 1.31 | 1.26 | 1.19 | 1.10 | 1.00 | 0.90 | 0.81 | 0.74 | 0.69 | 0.68 |
| 0.62 | 1.29 | 1.27 | 1.23 | 1.17 | 1.09 | 1.00 | 0.91 | 0.83 | 0.77 | 0.73 | 0.72 |
| 0.64 | 1.25 | 1.24 | 1.20 | 1.15 | 1.08 | 1.00 | 0.92 | 0.85 | 0.80 | 0.76 | 0.75 |
| 0.66 | 1.22 | 1.21 | 1.18 | 1.13 | 1.07 | 1.00 | 0.93 | 0.87 | 0.82 | 0.79 | 0.78 |
| 0.68 | 1.19 | 1.18 | 1.16 | 1.11 | 1.06 | 1.00 | 0.94 | 0.89 | 0.84 | 0.82 | 0.81 |
| 0.70 | 1.17 | 1.16 | 1.14 | 1.10 | 1.05 | 1.00 | 0.95 | 0.90 | 0.86 | 0.84 | 0.83 |
| 0.72 | 1.15 | 1.14 | 1.12 | 1.09 | 1.05 | 1.00 | 0.95 | 0.91 | 0.88 | 0.86 | 0.85 |
| 0.74 | 1.13 | 1.12 | 1.10 | 1.07 | 1.04 | 1.00 | 0.96 | 0.93 | 0.90 | 0.88 | 0.87 |
| 0.76 | 1.11 | 1.10 | 1.09 | 1.06 | 1.03 | 1.00 | 0.97 | 0.94 | 0.91 | 0.90 | 0.89 |
| 0.78 | 1.09 | 1.09 | 1.08 | 1.06 | 1.03 | 1.00 | 0.97 | 0.94 | 0.92 | 0.91 | 0.91 |
| 0.80 | 1.08 | 1.08 | 1.07 | 1.05 | 1.02 | 1.00 | 0.98 | 0.95 | 0.93 | 0.92 | 0.92 |
| 0.82 | 1.07 | 1.07 | 1.06 | 1.04 | 1.02 | 1.00 | 0.98 | 0.96 | 0.94 | 0.93 | 0.93 |
| 0.84 | 1.06 | 1.06 | 1.05 | 1.03 | 1.02 | 1.00 | 0.98 | 0.97 | 0.95 | 0.94 | 0.94 |
| 0.86 | 1.05 | 1.05 | 1.04 | 1.03 | 1.02 | 1.00 | 0.98 | 0.97 | 0.96 | 0.95 | 0.95 |
| 0.88 | 1.04 | 1.04 | 1.03 | 1.02 | 1.01 | 1.00 | 0.99 | 0.98 | 0.97 | 0.96 | 0.96 |
| 0.90 | 1.03 | 1.03 | 1.03 | 1.02 | 1.01 | 1.00 | 0.99 | 0.98 | 0.97 | 0.97 | 0.97 |
| 0.92 | 1.03 | 1.03 | 1.02 | 1.02 | 1.01 | 1.00 | 0.99 | 0.98 | 0.98 | 0.97 | 0.97 |
| 0.94 | 1.02 | 1.02 | 1.02 | 1.01 | 1.01 | 1.00 | 0.99 | 0.99 | 0.98 | 0.98 | 0.98 |
| 0.96 | 1.02 | 1.02 | 1.02 | 1.01 | 1.01 | 1.00 | 0.99 | 0.99 | 0.98 | 0.98 | 0.98 |
| 0.98 | 1.02 | 1.02 | 1.01 | 1.01 | 1.01 | 1.00 | 0.99 | 0.99 | 0.99 | 0.98 | 0.98 |
| 1.00 | 1.01 | 1.01 | 1.01 | 1.01 | 1.00 | 1.00 | 1.00 | 0.99 | 0.99 | 0.99 | 0.99 |

ZETA* = 0.2 ( L* UPPER SCALE ), ZETA* = 0.8 ( L* LOWER SCALE )

| SIGMA* \ L* | 0.0 / 1.0 | 0.1 / 0.9 | 0.2 / 0.8 | 0.3 / 0.7 | 0.4 / 0.6 | 0.5 / 0.5 | 0.6 / 0.4 | 0.7 / 0.3 | 0.8 / 0.2 | 0.9 / 0.1 | 1.0 / 0.0 |
|---|---|---|---|---|---|---|---|---|---|---|---|
| 0.01 | 0.00 | 0.00 | 39.89 | 0.00 | 0.00 | 0.00 | 0.00 | 0.00 | 0.00 | 0.00 | 0.00 |
| 0.02 | 0.00 | 0.00 | 19.95 | 0.00 | 0.00 | 0.00 | 0.00 | 0.00 | 0.00 | 0.00 | 0.00 |
| 0.03 | 0.00 | 0.05 | 13.30 | 0.05 | 0.00 | 0.00 | 0.00 | 0.00 | 0.00 | 0.00 | 0.00 |
| 0.04 | 0.00 | 0.44 | 9.97 | 0.44 | 0.00 | 0.00 | 0.00 | 0.00 | 0.00 | 0.00 | 0.00 |
| 0.05 | 0.01 | 1.08 | 7.98 | 1.08 | 0.00 | 0.00 | 0.00 | 0.00 | 0.00 | 0.00 | 0.00 |
| 0.06 | 0.05 | 1.66 | 6.65 | 1.66 | 0.03 | 0.00 | 0.00 | 0.00 | 0.00 | 0.00 | 0.00 |
| 0.07 | 0.19 | 2.05 | 5.70 | 2.05 | 0.10 | 0.00 | 0.00 | 0.00 | 0.00 | 0.00 | 0.00 |
| 0.08 | 0.44 | 2.29 | 4.99 | 2.28 | 0.22 | 0.00 | 0.00 | 0.00 | 0.00 | 0.00 | 0.00 |
| 0.09 | 0.75 | 2.41 | 4.43 | 2.39 | 0.38 | 0.02 | 0.00 | 0.00 | 0.00 | 0.00 | 0.00 |
| 0.10 | 1.08 | 2.46 | 3.99 | 2.42 | 0.54 | 0.04 | 0.00 | 0.00 | 0.00 | 0.00 | 0.00 |
| 0.11 | 1.39 | 2.49 | 3.63 | 2.40 | 0.69 | 0.09 | 0.00 | 0.00 | 0.00 | 0.00 | 0.00 |
| 0.12 | 1.66 | 2.50 | 3.34 | 2.35 | 0.83 | 0.15 | 0.01 | 0.00 | 0.00 | 0.00 | 0.00 |
| 0.13 | 1.88 | 2.50 | 3.10 | 2.28 | 0.94 | 0.21 | 0.03 | 0.00 | 0.00 | 0.00 | 0.00 |
| 0.14 | 2.05 | 2.49 | 2.90 | 2.21 | 1.03 | 0.29 | 0.05 | 0.00 | 0.00 | 0.00 | 0.00 |
| 0.15 | 2.19 | 2.49 | 2.74 | 2.14 | 1.09 | 0.36 | 0.08 | 0.01 | 0.00 | 0.00 | 0.00 |
| 0.16 | 2.28 | 2.48 | 2.60 | 2.07 | 1.14 | 0.43 | 0.11 | 0.02 | 0.00 | 0.00 | 0.00 |
| 0.17 | 2.35 | 2.47 | 2.49 | 2.00 | 1.18 | 0.50 | 0.15 | 0.03 | 0.00 | 0.00 | 0.00 |
| 0.18 | 2.39 | 2.45 | 2.40 | 1.95 | 1.20 | 0.55 | 0.19 | 0.05 | 0.01 | 0.00 | 0.00 |
| 0.19 | 2.41 | 2.43 | 2.33 | 1.89 | 1.22 | 0.61 | 0.23 | 0.07 | 0.01 | 0.00 | 0.00 |
| 0.20 | 2.42 | 2.41 | 2.26 | 1.85 | 1.23 | 0.65 | 0.27 | 0.09 | 0.02 | 0.00 | 0.00 |
| 0.21 | 2.41 | 2.38 | 2.21 | 1.81 | 1.24 | 0.69 | 0.31 | 0.11 | 0.03 | 0.01 | 0.00 |
| 0.22 | 2.40 | 2.35 | 2.16 | 1.77 | 1.24 | 0.73 | 0.35 | 0.14 | 0.04 | 0.01 | 0.00 |
| 0.23 | 2.38 | 2.32 | 2.12 | 1.74 | 1.25 | 0.76 | 0.39 | 0.16 | 0.06 | 0.02 | 0.01 |
| 0.24 | 2.35 | 2.29 | 2.08 | 1.71 | 1.25 | 0.78 | 0.42 | 0.19 | 0.07 | 0.03 | 0.01 |
| 0.25 | 2.32 | 2.25 | 2.04 | 1.69 | 1.25 | 0.81 | 0.45 | 0.22 | 0.09 | 0.03 | 0.02 |
| 0.26 | 2.28 | 2.21 | 2.00 | 1.67 | 1.25 | 0.83 | 0.48 | 0.25 | 0.11 | 0.04 | 0.03 |
| 0.27 | 2.25 | 2.18 | 1.97 | 1.65 | 1.25 | 0.85 | 0.51 | 0.27 | 0.13 | 0.06 | 0.04 |
| 0.28 | 2.21 | 2.14 | 1.94 | 1.63 | 1.25 | 0.87 | 0.54 | 0.30 | 0.15 | 0.07 | 0.05 |
| 0.29 | 2.17 | 2.10 | 1.91 | 1.61 | 1.25 | 0.88 | 0.56 | 0.32 | 0.17 | 0.09 | 0.06 |
| 0.30 | 2.13 | 2.06 | 1.88 | 1.59 | 1.24 | 0.89 | 0.59 | 0.35 | 0.19 | 0.10 | 0.08 |
| 0.31 | 2.09 | 2.03 | 1.85 | 1.57 | 1.24 | 0.91 | 0.61 | 0.37 | 0.21 | 0.12 | 0.09 |
| 0.32 | 2.05 | 1.99 | 1.82 | 1.56 | 1.24 | 0.92 | 0.63 | 0.40 | 0.23 | 0.14 | 0.11 |
| 0.33 | 2.01 | 1.95 | 1.79 | 1.54 | 1.24 | 0.93 | 0.65 | 0.42 | 0.26 | 0.16 | 0.13 |
| 0.34 | 1.97 | 1.92 | 1.76 | 1.52 | 1.23 | 0.94 | 0.66 | 0.44 | 0.28 | 0.18 | 0.15 |
| 0.35 | 1.94 | 1.88 | 1.73 | 1.51 | 1.23 | 0.94 | 0.68 | 0.46 | 0.30 | 0.21 | 0.17 |
| 0.36 | 1.90 | 1.85 | 1.71 | 1.49 | 1.23 | 0.95 | 0.70 | 0.48 | 0.32 | 0.23 | 0.20 |
| 0.37 | 1.86 | 1.82 | 1.68 | 1.47 | 1.22 | 0.96 | 0.71 | 0.50 | 0.35 | 0.25 | 0.22 |
| 0.38 | 1.83 | 1.78 | 1.65 | 1.46 | 1.22 | 0.96 | 0.73 | 0.52 | 0.37 | 0.27 | 0.24 |
| 0.39 | 1.79 | 1.75 | 1.63 | 1.44 | 1.21 | 0.97 | 0.74 | 0.54 | 0.39 | 0.30 | 0.27 |
| 0.40 | 1.76 | 1.72 | 1.60 | 1.42 | 1.21 | 0.97 | 0.75 | 0.56 | 0.41 | 0.32 | 0.29 |
| 0.41 | 1.73 | 1.69 | 1.58 | 1.41 | 1.20 | 0.98 | 0.76 | 0.58 | 0.44 | 0.35 | 0.32 |
| 0.42 | 1.70 | 1.66 | 1.55 | 1.39 | 1.19 | 0.98 | 0.78 | 0.60 | 0.46 | 0.37 | 0.34 |
| 0.43 | 1.67 | 1.63 | 1.53 | 1.38 | 1.19 | 0.98 | 0.79 | 0.61 | 0.48 | 0.40 | 0.37 |
| 0.44 | 1.64 | 1.60 | 1.51 | 1.36 | 1.18 | 0.99 | 0.80 | 0.63 | 0.50 | 0.42 | 0.39 |
| 0.45 | 1.61 | 1.58 | 1.49 | 1.35 | 1.17 | 0.99 | 0.81 | 0.65 | 0.52 | 0.44 | 0.42 |
| 0.46 | 1.58 | 1.55 | 1.46 | 1.33 | 1.17 | 0.99 | 0.82 | 0.66 | 0.54 | 0.47 | 0.44 |
| 0.47 | 1.55 | 1.52 | 1.44 | 1.32 | 1.16 | 0.99 | 0.83 | 0.68 | 0.56 | 0.49 | 0.46 |
| 0.48 | 1.53 | 1.50 | 1.42 | 1.30 | 1.16 | 0.99 | 0.83 | 0.69 | 0.58 | 0.51 | 0.49 |
| 0.49 | 1.50 | 1.47 | 1.40 | 1.29 | 1.15 | 0.99 | 0.84 | 0.71 | 0.60 | 0.53 | 0.51 |
| 0.50 | 1.48 | 1.45 | 1.38 | 1.28 | 1.14 | 1.00 | 0.85 | 0.72 | 0.62 | 0.56 | 0.53 |
| 0.52 | 1.43 | 1.41 | 1.35 | 1.25 | 1.13 | 1.00 | 0.87 | 0.75 | 0.66 | 0.60 | 0.58 |
| 0.54 | 1.39 | 1.37 | 1.31 | 1.22 | 1.12 | 1.00 | 0.88 | 0.77 | 0.69 | 0.64 | 0.62 |
| 0.56 | 1.35 | 1.33 | 1.28 | 1.20 | 1.11 | 1.00 | 0.89 | 0.80 | 0.72 | 0.67 | 0.66 |
| 0.58 | 1.31 | 1.29 | 1.25 | 1.18 | 1.09 | 1.00 | 0.90 | 0.82 | 0.75 | 0.71 | 0.69 |
| 0.60 | 1.27 | 1.26 | 1.22 | 1.16 | 1.08 | 1.00 | 0.91 | 0.84 | 0.78 | 0.74 | 0.73 |
| 0.62 | 1.24 | 1.23 | 1.20 | 1.14 | 1.07 | 1.00 | 0.92 | 0.86 | 0.80 | 0.77 | 0.76 |
| 0.64 | 1.21 | 1.20 | 1.17 | 1.13 | 1.07 | 1.00 | 0.93 | 0.87 | 0.83 | 0.80 | 0.79 |
| 0.66 | 1.19 | 1.18 | 1.15 | 1.11 | 1.06 | 1.00 | 0.94 | 0.89 | 0.85 | 0.82 | 0.81 |
| 0.68 | 1.17 | 1.16 | 1.13 | 1.10 | 1.05 | 1.00 | 0.95 | 0.90 | 0.87 | 0.84 | 0.83 |
| 0.70 | 1.14 | 1.14 | 1.12 | 1.08 | 1.04 | 1.00 | 0.96 | 0.92 | 0.88 | 0.86 | 0.86 |
| 0.72 | 1.13 | 1.12 | 1.10 | 1.07 | 1.04 | 1.00 | 0.96 | 0.93 | 0.90 | 0.88 | 0.87 |
| 0.74 | 1.11 | 1.10 | 1.09 | 1.06 | 1.03 | 1.00 | 0.97 | 0.94 | 0.91 | 0.90 | 0.89 |
| 0.76 | 1.09 | 1.09 | 1.08 | 1.05 | 1.03 | 1.00 | 0.97 | 0.95 | 0.92 | 0.91 | 0.91 |
| 0.78 | 1.08 | 1.08 | 1.07 | 1.05 | 1.02 | 1.00 | 0.98 | 0.95 | 0.93 | 0.92 | 0.92 |
| 0.80 | 1.07 | 1.07 | 1.06 | 1.04 | 1.02 | 1.00 | 0.98 | 0.96 | 0.94 | 0.93 | 0.93 |
| 0.82 | 1.06 | 1.06 | 1.05 | 1.03 | 1.02 | 1.00 | 0.98 | 0.97 | 0.95 | 0.94 | 0.94 |
| 0.84 | 1.05 | 1.05 | 1.04 | 1.03 | 1.02 | 1.00 | 0.98 | 0.97 | 0.96 | 0.95 | 0.95 |
| 0.86 | 1.04 | 1.04 | 1.03 | 1.02 | 1.01 | 1.00 | 0.99 | 0.98 | 0.97 | 0.96 | 0.96 |
| 0.88 | 1.04 | 1.03 | 1.03 | 1.02 | 1.01 | 1.00 | 0.99 | 0.98 | 0.97 | 0.97 | 0.96 |
| 0.90 | 1.03 | 1.03 | 1.02 | 1.02 | 1.01 | 1.00 | 0.99 | 0.98 | 0.98 | 0.97 | 0.97 |
| 0.92 | 1.02 | 1.02 | 1.02 | 1.01 | 1.01 | 1.00 | 0.99 | 0.99 | 0.98 | 0.98 | 0.98 |
| 0.94 | 1.02 | 1.02 | 1.02 | 1.01 | 1.01 | 1.00 | 0.99 | 0.99 | 0.98 | 0.98 | 0.98 |
| 0.96 | 1.02 | 1.02 | 1.01 | 1.01 | 1.01 | 1.00 | 0.99 | 0.99 | 0.99 | 0.98 | 0.98 |
| 0.98 | 1.01 | 1.01 | 1.01 | 1.01 | 1.00 | 1.00 | 1.00 | 0.99 | 0.99 | 0.99 | 0.99 |
| 1.00 | 1.01 | 1.01 | 1.01 | 1.01 | 1.00 | 1.00 | 1.00 | 0.99 | 0.99 | 0.99 | 0.99 |

ZETA* = 0.3 ( L* UPPER SCALE ), ZETA* = 0.7 ( L* LOWER SCALE )

| SIGMA* \ L* | 0.0 / 1.0 | 0.1 / 0.9 | 0.2 / 0.8 | 0.3 / 0.7 | 0.4 / 0.6 | 0.5 / 0.5 | 0.6 / 0.4 | 0.7 / 0.3 | 0.8 / 0.2 | 0.9 / 0.1 | 1.0 / 0.0 |
|---|---|---|---|---|---|---|---|---|---|---|---|
| 0.01 | 0.00 | 0.00 | 0.00 | 39.89 | 0.00 | 0.00 | 0.00 | 0.00 | 0.00 | 0.00 | 0.00 |
| 0.02 | 0.00 | 0.00 | 0.00 | 19.95 | 0.00 | 0.00 | 0.00 | 0.00 | 0.00 | 0.00 | 0.00 |
| 0.03 | 0.00 | 0.00 | 0.05 | 13.30 | 0.05 | 0.00 | 0.00 | 0.00 | 0.00 | 0.00 | 0.00 |
| 0.04 | 0.00 | 0.00 | 0.44 | 9.97 | 0.44 | 0.00 | 0.00 | 0.00 | 0.00 | 0.00 | 0.00 |
| 0.05 | 0.00 | 0.00 | 1.08 | 7.98 | 1.08 | 0.00 | 0.00 | 0.00 | 0.00 | 0.00 | 0.00 |
| 0.06 | 0.00 | 0.03 | 1.66 | 6.65 | 1.66 | 0.03 | 0.00 | 0.00 | 0.00 | 0.00 | 0.00 |
| 0.07 | 0.00 | 0.10 | 2.05 | 5.70 | 2.05 | 0.10 | 0.00 | 0.00 | 0.00 | 0.00 | 0.00 |
| 0.08 | 0.01 | 0.22 | 2.28 | 4.99 | 2.28 | 0.22 | 0.00 | 0.00 | 0.00 | 0.00 | 0.00 |
| 0.09 | 0.03 | 0.38 | 2.39 | 4.43 | 2.39 | 0.38 | 0.02 | 0.00 | 0.00 | 0.00 | 0.00 |
| 0.10 | 0.09 | 0.54 | 2.42 | 3.99 | 2.42 | 0.54 | 0.04 | 0.00 | 0.00 | 0.00 | 0.00 |
| 0.11 | 0.18 | 0.70 | 2.40 | 3.63 | 2.40 | 0.69 | 0.09 | 0.00 | 0.00 | 0.00 | 0.00 |
| 0.12 | 0.29 | 0.84 | 2.35 | 3.32 | 2.35 | 0.83 | 0.15 | 0.01 | 0.00 | 0.00 | 0.00 |
| 0.13 | 0.43 | 0.97 | 2.28 | 3.07 | 2.28 | 0.94 | 0.21 | 0.03 | 0.00 | 0.00 | 0.00 |
| 0.14 | 0.57 | 1.08 | 2.21 | 2.85 | 2.21 | 1.03 | 0.29 | 0.05 | 0.00 | 0.00 | 0.00 |
| 0.15 | 0.72 | 1.17 | 2.14 | 2.66 | 2.13 | 1.09 | 0.36 | 0.08 | 0.01 | 0.00 | 0.00 |
| 0.16 | 0.86 | 1.25 | 2.07 | 2.50 | 2.05 | 1.14 | 0.43 | 0.11 | 0.02 | 0.00 | 0.00 |
| 0.17 | 0.99 | 1.32 | 2.00 | 2.35 | 1.97 | 1.17 | 0.49 | 0.15 | 0.03 | 0.00 | 0.00 |
| 0.18 | 1.11 | 1.38 | 1.95 | 2.22 | 1.90 | 1.20 | 0.55 | 0.19 | 0.05 | 0.01 | 0.00 |
| 0.19 | 1.21 | 1.44 | 1.89 | 2.11 | 1.83 | 1.21 | 0.60 | 0.23 | 0.07 | 0.01 | 0.00 |
| 0.20 | 1.30 | 1.48 | 1.85 | 2.02 | 1.76 | 1.21 | 0.65 | 0.27 | 0.09 | 0.02 | 0.01 |
| 0.21 | 1.37 | 1.52 | 1.81 | 1.93 | 1.70 | 1.21 | 0.68 | 0.31 | 0.11 | 0.03 | 0.01 |
| 0.22 | 1.43 | 1.55 | 1.77 | 1.86 | 1.65 | 1.20 | 0.72 | 0.35 | 0.14 | 0.05 | 0.02 |
| 0.23 | 1.48 | 1.57 | 1.74 | 1.79 | 1.59 | 1.19 | 0.74 | 0.38 | 0.16 | 0.06 | 0.03 |
| 0.24 | 1.52 | 1.59 | 1.71 | 1.74 | 1.55 | 1.18 | 0.76 | 0.42 | 0.19 | 0.08 | 0.05 |
| 0.25 | 1.55 | 1.60 | 1.69 | 1.69 | 1.50 | 1.17 | 0.78 | 0.44 | 0.22 | 0.10 | 0.06 |
| 0.26 | 1.58 | 1.61 | 1.67 | 1.64 | 1.47 | 1.15 | 0.79 | 0.47 | 0.25 | 0.12 | 0.08 |
| 0.27 | 1.59 | 1.62 | 1.65 | 1.60 | 1.43 | 1.14 | 0.80 | 0.50 | 0.27 | 0.14 | 0.10 |
| 0.28 | 1.61 | 1.62 | 1.63 | 1.57 | 1.40 | 1.13 | 0.81 | 0.52 | 0.30 | 0.17 | 0.13 |
| 0.29 | 1.61 | 1.62 | 1.61 | 1.54 | 1.37 | 1.12 | 0.82 | 0.54 | 0.32 | 0.19 | 0.15 |
| 0.30 | 1.61 | 1.61 | 1.59 | 1.51 | 1.35 | 1.10 | 0.82 | 0.56 | 0.35 | 0.22 | 0.18 |
| 0.31 | 1.61 | 1.60 | 1.57 | 1.48 | 1.32 | 1.09 | 0.83 | 0.57 | 0.37 | 0.24 | 0.20 |
| 0.32 | 1.61 | 1.60 | 1.56 | 1.46 | 1.30 | 1.08 | 0.83 | 0.59 | 0.40 | 0.27 | 0.23 |
| 0.33 | 1.60 | 1.59 | 1.54 | 1.44 | 1.28 | 1.07 | 0.83 | 0.60 | 0.42 | 0.30 | 0.26 |
| 0.34 | 1.59 | 1.57 | 1.52 | 1.42 | 1.27 | 1.06 | 0.84 | 0.62 | 0.44 | 0.32 | 0.28 |
| 0.35 | 1.58 | 1.56 | 1.51 | 1.40 | 1.25 | 1.05 | 0.84 | 0.63 | 0.46 | 0.35 | 0.31 |
| 0.36 | 1.57 | 1.55 | 1.49 | 1.39 | 1.24 | 1.05 | 0.84 | 0.64 | 0.48 | 0.38 | 0.34 |
| 0.37 | 1.55 | 1.53 | 1.47 | 1.37 | 1.22 | 1.04 | 0.85 | 0.66 | 0.50 | 0.40 | 0.36 |
| 0.38 | 1.54 | 1.52 | 1.46 | 1.35 | 1.21 | 1.04 | 0.85 | 0.67 | 0.52 | 0.42 | 0.39 |
| 0.39 | 1.52 | 1.50 | 1.44 | 1.34 | 1.20 | 1.03 | 0.85 | 0.68 | 0.54 | 0.45 | 0.42 |
| 0.40 | 1.51 | 1.49 | 1.42 | 1.32 | 1.19 | 1.03 | 0.86 | 0.69 | 0.56 | 0.47 | 0.44 |
| 0.41 | 1.49 | 1.47 | 1.41 | 1.31 | 1.18 | 1.02 | 0.86 | 0.70 | 0.58 | 0.49 | 0.47 |
| 0.42 | 1.47 | 1.45 | 1.39 | 1.30 | 1.17 | 1.02 | 0.86 | 0.72 | 0.60 | 0.52 | 0.49 |
| 0.43 | 1.46 | 1.44 | 1.38 | 1.28 | 1.16 | 1.02 | 0.87 | 0.73 | 0.61 | 0.54 | 0.51 |
| 0.44 | 1.44 | 1.42 | 1.36 | 1.27 | 1.15 | 1.01 | 0.87 | 0.74 | 0.63 | 0.56 | 0.53 |
| 0.45 | 1.42 | 1.40 | 1.35 | 1.26 | 1.14 | 1.01 | 0.88 | 0.75 | 0.65 | 0.58 | 0.56 |
| 0.46 | 1.40 | 1.39 | 1.33 | 1.25 | 1.14 | 1.01 | 0.88 | 0.76 | 0.66 | 0.60 | 0.58 |
| 0.47 | 1.39 | 1.37 | 1.32 | 1.23 | 1.13 | 1.01 | 0.88 | 0.77 | 0.68 | 0.62 | 0.60 |
| 0.48 | 1.37 | 1.35 | 1.30 | 1.22 | 1.12 | 1.01 | 0.89 | 0.78 | 0.69 | 0.64 | 0.62 |
| 0.49 | 1.35 | 1.34 | 1.29 | 1.21 | 1.12 | 1.01 | 0.89 | 0.79 | 0.71 | 0.65 | 0.64 |
| 0.50 | 1.34 | 1.32 | 1.28 | 1.20 | 1.11 | 1.00 | 0.90 | 0.80 | 0.72 | 0.67 | 0.65 |
| 0.52 | 1.31 | 1.29 | 1.25 | 1.18 | 1.10 | 1.00 | 0.91 | 0.82 | 0.75 | 0.70 | 0.69 |
| 0.54 | 1.28 | 1.26 | 1.22 | 1.16 | 1.09 | 1.00 | 0.92 | 0.84 | 0.77 | 0.73 | 0.72 |
| 0.56 | 1.25 | 1.24 | 1.20 | 1.15 | 1.08 | 1.00 | 0.92 | 0.85 | 0.80 | 0.76 | 0.75 |
| 0.58 | 1.22 | 1.21 | 1.18 | 1.13 | 1.07 | 1.00 | 0.93 | 0.87 | 0.82 | 0.79 | 0.78 |
| 0.60 | 1.20 | 1.19 | 1.16 | 1.12 | 1.06 | 1.00 | 0.94 | 0.88 | 0.84 | 0.81 | 0.80 |
| 0.62 | 1.18 | 1.17 | 1.14 | 1.10 | 1.05 | 1.00 | 0.95 | 0.90 | 0.86 | 0.83 | 0.82 |
| 0.64 | 1.16 | 1.15 | 1.13 | 1.09 | 1.05 | 1.00 | 0.95 | 0.91 | 0.87 | 0.85 | 0.84 |
| 0.66 | 1.14 | 1.13 | 1.11 | 1.08 | 1.04 | 1.00 | 0.96 | 0.92 | 0.89 | 0.87 | 0.86 |
| 0.68 | 1.12 | 1.11 | 1.10 | 1.07 | 1.04 | 1.00 | 0.96 | 0.93 | 0.90 | 0.89 | 0.88 |
| 0.70 | 1.10 | 1.10 | 1.08 | 1.06 | 1.03 | 1.00 | 0.97 | 0.94 | 0.92 | 0.90 | 0.90 |
| 0.72 | 1.09 | 1.09 | 1.07 | 1.05 | 1.03 | 1.00 | 0.97 | 0.95 | 0.93 | 0.91 | 0.91 |
| 0.74 | 1.08 | 1.07 | 1.06 | 1.05 | 1.02 | 1.00 | 0.98 | 0.95 | 0.94 | 0.93 | 0.92 |
| 0.76 | 1.07 | 1.06 | 1.05 | 1.04 | 1.02 | 1.00 | 0.98 | 0.96 | 0.95 | 0.94 | 0.93 |
| 0.78 | 1.06 | 1.06 | 1.05 | 1.03 | 1.02 | 1.00 | 0.98 | 0.97 | 0.95 | 0.94 | 0.94 |
| 0.80 | 1.05 | 1.05 | 1.04 | 1.03 | 1.02 | 1.00 | 0.98 | 0.97 | 0.96 | 0.95 | 0.95 |
| 0.82 | 1.04 | 1.04 | 1.03 | 1.03 | 1.01 | 1.00 | 0.99 | 0.97 | 0.97 | 0.96 | 0.96 |
| 0.84 | 1.04 | 1.03 | 1.03 | 1.02 | 1.01 | 1.00 | 0.99 | 0.98 | 0.97 | 0.97 | 0.96 |
| 0.86 | 1.03 | 1.03 | 1.02 | 1.02 | 1.01 | 1.00 | 0.99 | 0.98 | 0.98 | 0.97 | 0.97 |
| 0.88 | 1.03 | 1.02 | 1.02 | 1.02 | 1.01 | 1.00 | 0.99 | 0.98 | 0.98 | 0.98 | 0.97 |
| 0.90 | 1.02 | 1.02 | 1.02 | 1.01 | 1.01 | 1.00 | 0.99 | 0.99 | 0.98 | 0.98 | 0.98 |
| 0.92 | 1.02 | 1.02 | 1.01 | 1.01 | 1.01 | 1.00 | 0.99 | 0.99 | 0.99 | 0.98 | 0.98 |
| 0.94 | 1.02 | 1.01 | 1.01 | 1.01 | 1.00 | 1.00 | 1.00 | 0.99 | 0.99 | 0.99 | 0.98 |
| 0.96 | 1.01 | 1.01 | 1.01 | 1.01 | 1.00 | 1.00 | 1.00 | 0.99 | 0.99 | 0.99 | 0.99 |
| 0.98 | 1.01 | 1.01 | 1.01 | 1.01 | 1.00 | 1.00 | 1.00 | 0.99 | 0.99 | 0.99 | 0.99 |
| 1.00 | 1.01 | 1.01 | 1.01 | 1.00 | 1.00 | 1.00 | 1.00 | 1.00 | 0.99 | 0.99 | 0.99 |

ZETA* = 0.4 ( L* UPPER SCALE ), ZETA* = 0.6 ( L* LOWER SCALE )

| SIGMA* \ L* | 0.0 / 1.0 | 0.1 / 0.9 | 0.2 / 0.8 | 0.3 / 0.7 | 0.4 / 0.6 | 0.5 / 0.5 | 0.6 / 0.4 | 0.7 / 0.3 | 0.8 / 0.2 | 0.9 / 0.1 | 1.0 / 0.0 |
|---|---|---|---|---|---|---|---|---|---|---|---|
| 0.01 | 0.00 | 0.00 | 0.00 | 0.00 | 39.89 | 0.00 | 0.00 | 0.00 | 0.00 | 0.00 | 0.00 |
| 0.02 | 0.00 | 0.00 | 0.00 | 0.00 | 19.95 | 0.00 | 0.00 | 0.00 | 0.00 | 0.00 | 0.00 |
| 0.03 | 0.00 | 0.00 | 0.00 | 0.05 | 13.30 | 0.05 | 0.00 | 0.00 | 0.00 | 0.00 | 0.00 |
| 0.04 | 0.00 | 0.00 | 0.00 | 0.44 | 9.97 | 0.44 | 0.00 | 0.00 | 0.00 | 0.00 | 0.00 |
| 0.05 | 0.00 | 0.00 | 0.00 | 1.08 | 7.98 | 1.08 | 0.00 | 0.00 | 0.00 | 0.00 | 0.00 |
| 0.06 | 0.00 | 0.00 | 0.03 | 1.66 | 6.65 | 1.66 | 0.03 | 0.00 | 0.00 | 0.00 | 0.00 |
| 0.07 | 0.00 | 0.00 | 0.10 | 2.05 | 5.70 | 2.05 | 0.10 | 0.00 | 0.00 | 0.00 | 0.00 |
| 0.08 | 0.00 | 0.00 | 0.22 | 2.28 | 4.99 | 2.28 | 0.22 | 0.00 | 0.00 | 0.00 | 0.00 |
| 0.09 | 0.00 | 0.02 | 0.38 | 2.39 | 4.43 | 2.39 | 0.38 | 0.02 | 0.00 | 0.00 | 0.00 |
| 0.10 | 0.00 | 0.04 | 0.54 | 2.42 | 3.99 | 2.42 | 0.54 | 0.04 | 0.00 | 0.00 | 0.00 |
| 0.11 | 0.01 | 0.09 | 0.69 | 2.40 | 3.63 | 2.40 | 0.69 | 0.09 | 0.00 | 0.00 | 0.00 |
| 0.12 | 0.03 | 0.15 | 0.83 | 2.35 | 3.32 | 2.35 | 0.83 | 0.15 | 0.01 | 0.00 | 0.00 |
| 0.13 | 0.05 | 0.22 | 0.94 | 2.28 | 3.07 | 2.28 | 0.94 | 0.21 | 0.03 | 0.00 | 0.00 |
| 0.14 | 0.10 | 0.29 | 1.03 | 2.21 | 2.85 | 2.21 | 1.03 | 0.29 | 0.05 | 0.00 | 0.00 |
| 0.15 | 0.15 | 0.37 | 1.09 | 2.13 | 2.66 | 2.13 | 1.09 | 0.36 | 0.08 | 0.01 | 0.00 |
| 0.16 | 0.22 | 0.45 | 1.14 | 2.05 | 2.49 | 2.05 | 1.14 | 0.43 | 0.11 | 0.02 | 0.00 |
| 0.17 | 0.29 | 0.53 | 1.18 | 1.97 | 2.35 | 1.97 | 1.17 | 0.49 | 0.15 | 0.03 | 0.01 |
| 0.18 | 0.38 | 0.60 | 1.20 | 1.90 | 2.22 | 1.90 | 1.20 | 0.55 | 0.19 | 0.05 | 0.02 |
| 0.19 | 0.46 | 0.67 | 1.22 | 1.83 | 2.10 | 1.83 | 1.21 | 0.60 | 0.23 | 0.07 | 0.03 |
| 0.20 | 0.54 | 0.74 | 1.23 | 1.76 | 2.00 | 1.76 | 1.21 | 0.65 | 0.27 | 0.09 | 0.04 |
| 0.21 | 0.62 | 0.80 | 1.24 | 1.70 | 1.90 | 1.70 | 1.21 | 0.68 | 0.31 | 0.12 | 0.06 |
| 0.22 | 0.69 | 0.85 | 1.24 | 1.65 | 1.82 | 1.64 | 1.20 | 0.72 | 0.35 | 0.15 | 0.09 |
| 0.23 | 0.76 | 0.90 | 1.25 | 1.59 | 1.74 | 1.58 | 1.19 | 0.74 | 0.39 | 0.18 | 0.12 |
| 0.24 | 0.83 | 0.95 | 1.25 | 1.55 | 1.67 | 1.53 | 1.18 | 0.76 | 0.42 | 0.21 | 0.15 |
| 0.25 | 0.89 | 0.99 | 1.25 | 1.50 | 1.61 | 1.48 | 1.16 | 0.78 | 0.45 | 0.25 | 0.18 |
| 0.26 | 0.94 | 1.03 | 1.25 | 1.47 | 1.55 | 1.43 | 1.14 | 0.79 | 0.48 | 0.28 | 0.21 |
| 0.27 | 0.99 | 1.06 | 1.25 | 1.43 | 1.50 | 1.39 | 1.13 | 0.80 | 0.51 | 0.32 | 0.25 |
| 0.28 | 1.03 | 1.09 | 1.25 | 1.40 | 1.45 | 1.35 | 1.11 | 0.81 | 0.54 | 0.35 | 0.29 |
| 0.29 | 1.06 | 1.12 | 1.25 | 1.37 | 1.41 | 1.31 | 1.09 | 0.82 | 0.56 | 0.39 | 0.32 |
| 0.30 | 1.09 | 1.14 | 1.24 | 1.35 | 1.37 | 1.27 | 1.08 | 0.82 | 0.59 | 0.42 | 0.36 |
| 0.31 | 1.12 | 1.16 | 1.24 | 1.32 | 1.33 | 1.24 | 1.06 | 0.83 | 0.61 | 0.45 | 0.40 |
| 0.32 | 1.14 | 1.17 | 1.24 | 1.30 | 1.30 | 1.21 | 1.04 | 0.83 | 0.63 | 0.48 | 0.43 |
| 0.33 | 1.16 | 1.18 | 1.24 | 1.28 | 1.27 | 1.19 | 1.03 | 0.83 | 0.65 | 0.51 | 0.46 |
| 0.34 | 1.17 | 1.19 | 1.23 | 1.27 | 1.25 | 1.17 | 1.02 | 0.84 | 0.66 | 0.54 | 0.50 |
| 0.35 | 1.19 | 1.20 | 1.23 | 1.25 | 1.23 | 1.14 | 1.01 | 0.84 | 0.68 | 0.57 | 0.53 |
| 0.36 | 1.20 | 1.21 | 1.23 | 1.24 | 1.21 | 1.13 | 1.00 | 0.84 | 0.70 | 0.59 | 0.55 |
| 0.37 | 1.20 | 1.21 | 1.22 | 1.22 | 1.19 | 1.11 | 0.99 | 0.85 | 0.71 | 0.62 | 0.58 |
| 0.38 | 1.21 | 1.21 | 1.22 | 1.21 | 1.17 | 1.09 | 0.98 | 0.85 | 0.73 | 0.64 | 0.61 |
| 0.39 | 1.21 | 1.21 | 1.21 | 1.20 | 1.16 | 1.08 | 0.97 | 0.85 | 0.74 | 0.66 | 0.63 |
| 0.40 | 1.21 | 1.21 | 1.21 | 1.19 | 1.14 | 1.07 | 0.97 | 0.86 | 0.75 | 0.68 | 0.65 |
| 0.41 | 1.21 | 1.21 | 1.20 | 1.18 | 1.13 | 1.06 | 0.96 | 0.86 | 0.76 | 0.70 | 0.67 |
| 0.42 | 1.21 | 1.21 | 1.19 | 1.17 | 1.12 | 1.05 | 0.96 | 0.86 | 0.78 | 0.71 | 0.69 |
| 0.43 | 1.21 | 1.20 | 1.19 | 1.16 | 1.11 | 1.04 | 0.96 | 0.87 | 0.79 | 0.73 | 0.71 |
| 0.44 | 1.20 | 1.20 | 1.18 | 1.15 | 1.10 | 1.04 | 0.95 | 0.87 | 0.80 | 0.75 | 0.73 |
| 0.45 | 1.20 | 1.19 | 1.17 | 1.14 | 1.09 | 1.03 | 0.95 | 0.88 | 0.81 | 0.76 | 0.74 |
| 0.46 | 1.19 | 1.19 | 1.17 | 1.14 | 1.09 | 1.02 | 0.95 | 0.88 | 0.82 | 0.77 | 0.76 |
| 0.47 | 1.19 | 1.18 | 1.16 | 1.13 | 1.08 | 1.02 | 0.95 | 0.88 | 0.83 | 0.79 | 0.77 |
| 0.48 | 1.18 | 1.17 | 1.16 | 1.12 | 1.08 | 1.02 | 0.95 | 0.89 | 0.83 | 0.80 | 0.78 |
| 0.49 | 1.17 | 1.17 | 1.15 | 1.12 | 1.07 | 1.01 | 0.95 | 0.89 | 0.84 | 0.81 | 0.80 |
| 0.50 | 1.17 | 1.16 | 1.14 | 1.11 | 1.07 | 1.01 | 0.95 | 0.90 | 0.85 | 0.82 | 0.81 |
| 0.52 | 1.15 | 1.15 | 1.13 | 1.10 | 1.06 | 1.01 | 0.96 | 0.91 | 0.87 | 0.84 | 0.83 |
| 0.54 | 1.14 | 1.14 | 1.12 | 1.09 | 1.05 | 1.01 | 0.96 | 0.92 | 0.88 | 0.86 | 0.85 |
| 0.56 | 1.13 | 1.12 | 1.11 | 1.08 | 1.04 | 1.00 | 0.96 | 0.92 | 0.89 | 0.87 | 0.87 |
| 0.58 | 1.12 | 1.11 | 1.09 | 1.07 | 1.04 | 1.00 | 0.97 | 0.93 | 0.90 | 0.89 | 0.88 |
| 0.60 | 1.10 | 1.10 | 1.08 | 1.06 | 1.03 | 1.00 | 0.97 | 0.94 | 0.91 | 0.90 | 0.89 |
| 0.62 | 1.09 | 1.09 | 1.07 | 1.05 | 1.03 | 1.00 | 0.97 | 0.95 | 0.92 | 0.91 | 0.91 |
| 0.64 | 1.08 | 1.08 | 1.07 | 1.05 | 1.03 | 1.00 | 0.98 | 0.95 | 0.93 | 0.92 | 0.92 |
| 0.66 | 1.07 | 1.07 | 1.06 | 1.04 | 1.02 | 1.00 | 0.98 | 0.96 | 0.94 | 0.93 | 0.93 |
| 0.68 | 1.06 | 1.06 | 1.05 | 1.04 | 1.02 | 1.00 | 0.98 | 0.96 | 0.95 | 0.94 | 0.94 |
| 0.70 | 1.05 | 1.05 | 1.04 | 1.03 | 1.02 | 1.00 | 0.98 | 0.97 | 0.96 | 0.95 | 0.94 |
| 0.72 | 1.05 | 1.05 | 1.04 | 1.03 | 1.01 | 1.00 | 0.99 | 0.97 | 0.96 | 0.95 | 0.95 |
| 0.74 | 1.04 | 1.04 | 1.03 | 1.02 | 1.01 | 1.00 | 0.99 | 0.98 | 0.97 | 0.96 | 0.96 |
| 0.76 | 1.04 | 1.03 | 1.03 | 1.02 | 1.01 | 1.00 | 0.99 | 0.98 | 0.97 | 0.97 | 0.96 |
| 0.78 | 1.03 | 1.03 | 1.02 | 1.02 | 1.01 | 1.00 | 0.99 | 0.98 | 0.98 | 0.97 | 0.97 |
| 0.80 | 1.03 | 1.02 | 1.02 | 1.02 | 1.01 | 1.00 | 0.99 | 0.98 | 0.98 | 0.98 | 0.97 |
| 0.82 | 1.02 | 1.02 | 1.02 | 1.01 | 1.01 | 1.00 | 0.99 | 0.99 | 0.98 | 0.98 | 0.98 |
| 0.84 | 1.02 | 1.02 | 1.02 | 1.01 | 1.01 | 1.00 | 0.99 | 0.99 | 0.98 | 0.98 | 0.98 |
| 0.86 | 1.02 | 1.02 | 1.01 | 1.01 | 1.00 | 1.00 | 1.00 | 0.99 | 0.99 | 0.98 | 0.98 |
| 0.88 | 1.01 | 1.01 | 1.01 | 1.01 | 1.00 | 1.00 | 1.00 | 0.99 | 0.99 | 0.99 | 0.99 |
| 0.90 | 1.01 | 1.01 | 1.01 | 1.01 | 1.00 | 1.00 | 1.00 | 0.99 | 0.99 | 0.99 | 0.99 |
| 0.92 | 1.01 | 1.01 | 1.01 | 1.01 | 1.00 | 1.00 | 1.00 | 0.99 | 0.99 | 0.99 | 0.99 |
| 0.94 | 1.01 | 1.01 | 1.01 | 1.00 | 1.00 | 1.00 | 1.00 | 1.00 | 0.99 | 0.99 | 0.99 |
| 0.96 | 1.01 | 1.01 | 1.01 | 1.00 | 1.00 | 1.00 | 1.00 | 1.00 | 0.99 | 0.99 | 0.99 |
| 0.98 | 1.01 | 1.01 | 1.00 | 1.00 | 1.00 | 1.00 | 1.00 | 1.00 | 1.00 | 0.99 | 0.99 |
| 1.00 | 1.00 | 1.00 | 1.00 | 1.00 | 1.00 | 1.00 | 1.00 | 1.00 | 1.00 | 1.00 | 1.00 |

ZETA* = 0.5 ( L* UPPER SCALE ),  ZETA* = 0.5 ( L* LOWER SCALE )

| SIGMA* \ L* | 0.0<br>1.0 | 0.1<br>0.9 | 0.2<br>0.8 | 0.3<br>0.7 | 0.4<br>0.6 | 0.5<br>0.5 | 0.6<br>0.4 | 0.7<br>0.3 | 0.8<br>0.2 | 0.9<br>0.1 | 1.0<br>0.0 |
|---|---|---|---|---|---|---|---|---|---|---|---|
| 0.01 | 0.00 | 0.00 | 0.00 | 0.00 | 0.00 | 39.89 | 0.00 | 0.00 | 0.00 | 0.00 | 0.00 |
| 0.02 | 0.00 | 0.00 | 0.00 | 0.00 | 0.00 | 19.95 | 0.00 | 0.00 | 0.00 | 0.00 | 0.00 |
| 0.03 | 0.00 | 0.00 | 0.00 | 0.00 | 0.05 | 13.30 | 0.05 | 0.00 | 0.00 | 0.00 | 0.00 |
| 0.04 | 0.00 | 0.00 | 0.00 | 0.00 | 0.44 | 9.97 | 0.44 | 0.00 | 0.00 | 0.00 | 0.00 |
| 0.05 | 0.00 | 0.00 | 0.00 | 0.00 | 1.08 | 7.98 | 1.08 | 0.00 | 0.00 | 0.00 | 0.00 |
| 0.06 | 0.00 | 0.00 | 0.00 | 0.03 | 1.66 | 6.65 | 1.66 | 0.03 | 0.00 | 0.00 | 0.00 |
| 0.07 | 0.00 | 0.00 | 0.00 | 0.10 | 2.05 | 5.70 | 2.05 | 0.10 | 0.00 | 0.00 | 0.00 |
| 0.08 | 0.00 | 0.00 | 0.00 | 0.22 | 2.28 | 4.99 | 2.28 | 0.22 | 0.00 | 0.00 | 0.00 |
| 0.09 | 0.00 | 0.00 | 0.02 | 0.38 | 2.39 | 4.43 | 2.39 | 0.38 | 0.02 | 0.00 | 0.00 |
| 0.10 | 0.00 | 0.00 | 0.04 | 0.54 | 2.42 | 3.99 | 2.42 | 0.54 | 0.04 | 0.00 | 0.00 |
| 0.11 | 0.00 | 0.00 | 0.09 | 0.69 | 2.40 | 3.63 | 2.40 | 0.69 | 0.09 | 0.00 | 0.00 |
| 0.12 | 0.00 | 0.01 | 0.15 | 0.83 | 2.35 | 3.32 | 2.35 | 0.83 | 0.15 | 0.01 | 0.00 |
| 0.13 | 0.00 | 0.03 | 0.21 | 0.94 | 2.28 | 3.07 | 2.28 | 0.94 | 0.21 | 0.03 | 0.00 |
| 0.14 | 0.01 | 0.05 | 0.29 | 1.03 | 2.21 | 2.85 | 2.21 | 1.03 | 0.29 | 0.05 | 0.01 |
| 0.15 | 0.02 | 0.08 | 0.36 | 1.09 | 2.13 | 2.66 | 2.13 | 1.09 | 0.36 | 0.08 | 0.02 |
| 0.16 | 0.04 | 0.11 | 0.43 | 1.14 | 2.05 | 2.49 | 2.05 | 1.14 | 0.43 | 0.11 | 0.04 |
| 0.17 | 0.06 | 0.15 | 0.50 | 1.17 | 1.97 | 2.35 | 1.97 | 1.17 | 0.50 | 0.15 | 0.06 |
| 0.18 | 0.09 | 0.20 | 0.55 | 1.20 | 1.90 | 2.22 | 1.90 | 1.20 | 0.55 | 0.20 | 0.09 |
| 0.19 | 0.13 | 0.24 | 0.61 | 1.21 | 1.83 | 2.10 | 1.83 | 1.21 | 0.61 | 0.24 | 0.13 |
| 0.20 | 0.18 | 0.29 | 0.65 | 1.21 | 1.76 | 1.99 | 1.76 | 1.21 | 0.65 | 0.29 | 0.18 |
| 0.21 | 0.22 | 0.34 | 0.69 | 1.21 | 1.70 | 1.90 | 1.70 | 1.21 | 0.69 | 0.34 | 0.22 |
| 0.22 | 0.27 | 0.39 | 0.73 | 1.20 | 1.64 | 1.81 | 1.64 | 1.20 | 0.73 | 0.39 | 0.27 |
| 0.23 | 0.33 | 0.44 | 0.76 | 1.19 | 1.58 | 1.73 | 1.58 | 1.19 | 0.76 | 0.44 | 0.33 |
| 0.24 | 0.38 | 0.49 | 0.78 | 1.18 | 1.53 | 1.66 | 1.53 | 1.18 | 0.78 | 0.49 | 0.38 |
| 0.25 | 0.43 | 0.53 | 0.81 | 1.17 | 1.48 | 1.60 | 1.48 | 1.17 | 0.81 | 0.53 | 0.43 |
| 0.26 | 0.48 | 0.58 | 0.83 | 1.15 | 1.43 | 1.54 | 1.43 | 1.15 | 0.83 | 0.58 | 0.48 |
| 0.27 | 0.53 | 0.62 | 0.85 | 1.14 | 1.39 | 1.48 | 1.39 | 1.14 | 0.85 | 0.62 | 0.53 |
| 0.28 | 0.58 | 0.66 | 0.87 | 1.13 | 1.35 | 1.43 | 1.35 | 1.13 | 0.87 | 0.66 | 0.58 |
| 0.29 | 0.62 | 0.69 | 0.88 | 1.12 | 1.31 | 1.38 | 1.31 | 1.12 | 0.88 | 0.69 | 0.62 |
| 0.30 | 0.66 | 0.73 | 0.89 | 1.10 | 1.27 | 1.34 | 1.27 | 1.10 | 0.89 | 0.73 | 0.66 |
| 0.31 | 0.70 | 0.76 | 0.91 | 1.09 | 1.24 | 1.30 | 1.24 | 1.09 | 0.91 | 0.76 | 0.70 |
| 0.32 | 0.74 | 0.79 | 0.92 | 1.08 | 1.21 | 1.27 | 1.21 | 1.08 | 0.92 | 0.79 | 0.74 |
| 0.33 | 0.77 | 0.81 | 0.93 | 1.07 | 1.19 | 1.23 | 1.19 | 1.07 | 0.93 | 0.81 | 0.77 |
| 0.34 | 0.80 | 0.83 | 0.94 | 1.06 | 1.17 | 1.20 | 1.17 | 1.06 | 0.94 | 0.83 | 0.80 |
| 0.35 | 0.82 | 0.86 | 0.94 | 1.05 | 1.14 | 1.18 | 1.14 | 1.05 | 0.94 | 0.86 | 0.82 |
| 0.36 | 0.85 | 0.87 | 0.95 | 1.05 | 1.13 | 1.15 | 1.13 | 1.05 | 0.95 | 0.87 | 0.85 |
| 0.37 | 0.87 | 0.89 | 0.96 | 1.04 | 1.11 | 1.13 | 1.11 | 1.04 | 0.96 | 0.89 | 0.87 |
| 0.38 | 0.88 | 0.91 | 0.96 | 1.04 | 1.09 | 1.12 | 1.09 | 1.04 | 0.96 | 0.91 | 0.88 |
| 0.39 | 0.90 | 0.92 | 0.97 | 1.03 | 1.08 | 1.10 | 1.08 | 1.03 | 0.97 | 0.92 | 0.90 |
| 0.40 | 0.92 | 0.93 | 0.97 | 1.03 | 1.07 | 1.09 | 1.07 | 1.03 | 0.97 | 0.93 | 0.92 |
| 0.41 | 0.93 | 0.94 | 0.98 | 1.02 | 1.06 | 1.07 | 1.06 | 1.02 | 0.98 | 0.94 | 0.93 |
| 0.42 | 0.94 | 0.95 | 0.98 | 1.02 | 1.05 | 1.06 | 1.05 | 1.02 | 0.98 | 0.95 | 0.94 |
| 0.43 | 0.95 | 0.96 | 0.98 | 1.02 | 1.04 | 1.05 | 1.04 | 1.02 | 0.98 | 0.96 | 0.95 |
| 0.44 | 0.96 | 0.96 | 0.99 | 1.01 | 1.04 | 1.04 | 1.04 | 1.01 | 0.99 | 0.96 | 0.96 |
| 0.45 | 0.96 | 0.97 | 0.99 | 1.01 | 1.03 | 1.04 | 1.03 | 1.01 | 0.99 | 0.97 | 0.96 |
| 0.46 | 0.97 | 0.98 | 0.99 | 1.01 | 1.02 | 1.03 | 1.02 | 1.01 | 0.99 | 0.98 | 0.97 |
| 0.47 | 0.97 | 0.98 | 0.99 | 1.01 | 1.02 | 1.03 | 1.02 | 1.01 | 0.99 | 0.98 | 0.97 |
| 0.48 | 0.98 | 0.98 | 0.99 | 1.01 | 1.02 | 1.02 | 1.02 | 1.01 | 0.99 | 0.98 | 0.98 |
| 0.49 | 0.98 | 0.99 | 0.99 | 1.01 | 1.01 | 1.02 | 1.01 | 1.01 | 0.99 | 0.99 | 0.98 |
| 0.50 | 0.99 | 0.99 | 1.00 | 1.00 | 1.01 | 1.01 | 1.01 | 1.00 | 1.00 | 0.99 | 0.99 |
| 0.52 | 0.99 | 0.99 | 1.00 | 1.00 | 1.01 | 1.01 | 1.01 | 1.00 | 1.00 | 0.99 | 0.99 |
| 0.54 | 0.99 | 0.99 | 1.00 | 1.00 | 1.01 | 1.01 | 1.01 | 1.00 | 1.00 | 0.99 | 0.99 |
| 0.56 | 1.00 | 1.00 | 1.00 | 1.00 | 1.00 | 1.00 | 1.00 | 1.00 | 1.00 | 1.00 | 1.00 |
| 0.58 | 1.00 | 1.00 | 1.00 | 1.00 | 1.00 | 1.00 | 1.00 | 1.00 | 1.00 | 1.00 | 1.00 |
| 0.60 | 1.00 | 1.00 | 1.00 | 1.00 | 1.00 | 1.00 | 1.00 | 1.00 | 1.00 | 1.00 | 1.00 |
| 0.62 | 1.00 | 1.00 | 1.00 | 1.00 | 1.00 | 1.00 | 1.00 | 1.00 | 1.00 | 1.00 | 1.00 |
| 0.64 | 1.00 | 1.00 | 1.00 | 1.00 | 1.00 | 1.00 | 1.00 | 1.00 | 1.00 | 1.00 | 1.00 |
| 0.66 | 1.00 | 1.00 | 1.00 | 1.00 | 1.00 | 1.00 | 1.00 | 1.00 | 1.00 | 1.00 | 1.00 |
| 0.68 | 1.00 | 1.00 | 1.00 | 1.00 | 1.00 | 1.00 | 1.00 | 1.00 | 1.00 | 1.00 | 1.00 |
| 0.70 | 1.00 | 1.00 | 1.00 | 1.00 | 1.00 | 1.00 | 1.00 | 1.00 | 1.00 | 1.00 | 1.00 |
| 0.72 | 1.00 | 1.00 | 1.00 | 1.00 | 1.00 | 1.00 | 1.00 | 1.00 | 1.00 | 1.00 | 1.00 |
| 0.74 | 1.00 | 1.00 | 1.00 | 1.00 | 1.00 | 1.00 | 1.00 | 1.00 | 1.00 | 1.00 | 1.00 |
| 0.76 | 1.00 | 1.00 | 1.00 | 1.00 | 1.00 | 1.00 | 1.00 | 1.00 | 1.00 | 1.00 | 1.00 |
| 0.78 | 1.00 | 1.00 | 1.00 | 1.00 | 1.00 | 1.00 | 1.00 | 1.00 | 1.00 | 1.00 | 1.00 |
| 0.80 | 1.00 | 1.00 | 1.00 | 1.00 | 1.00 | 1.00 | 1.00 | 1.00 | 1.00 | 1.00 | 1.00 |
| 0.82 | 1.00 | 1.00 | 1.00 | 1.00 | 1.00 | 1.00 | 1.00 | 1.00 | 1.00 | 1.00 | 1.00 |
| 0.84 | 1.00 | 1.00 | 1.00 | 1.00 | 1.00 | 1.00 | 1.00 | 1.00 | 1.00 | 1.00 | 1.00 |
| 0.86 | 1.00 | 1.00 | 1.00 | 1.00 | 1.00 | 1.00 | 1.00 | 1.00 | 1.00 | 1.00 | 1.00 |
| 0.88 | 1.00 | 1.00 | 1.00 | 1.00 | 1.00 | 1.00 | 1.00 | 1.00 | 1.00 | 1.00 | 1.00 |
| 0.90 | 1.00 | 1.00 | 1.00 | 1.00 | 1.00 | 1.00 | 1.00 | 1.00 | 1.00 | 1.00 | 1.00 |
| 0.92 | 1.00 | 1.00 | 1.00 | 1.00 | 1.00 | 1.00 | 1.00 | 1.00 | 1.00 | 1.00 | 1.00 |
| 0.94 | 1.00 | 1.00 | 1.00 | 1.00 | 1.00 | 1.00 | 1.00 | 1.00 | 1.00 | 1.00 | 1.00 |
| 0.96 | 1.00 | 1.00 | 1.00 | 1.00 | 1.00 | 1.00 | 1.00 | 1.00 | 1.00 | 1.00 | 1.00 |
| 0.98 | 1.00 | 1.00 | 1.00 | 1.00 | 1.00 | 1.00 | 1.00 | 1.00 | 1.00 | 1.00 | 1.00 |
| 1.00 | 1.00 | 1.00 | 1.00 | 1.00 | 1.00 | 1.00 | 1.00 | 1.00 | 1.00 | 1.00 | 1.00 |


DATE
IL ME